Analysis of the novel surface protein P159 and the ribosomal protein L7/L12 of *Mycoplasma hyopneumoniae*

A thesis submitted in fulfillment of the requirements for the award of the degree of

Doctor of Philosophy

From

The University of Wollongong

By

Tracey A. Burnett

Department of Biological Sciences

2005

Declaration

This thesis is submitted in accordance with the regulations of the University of Wollongong in fulfilment of the degree of Doctor of Philosophy. It does not include any material previously published by another person except where due reference is made in the text. The experimental work described in this thesis is original work and has not been submitted for a degree in any other University or Institution.

Tracey A. Burnett

July 2005

Acknowledgements

First of all I would like to acknowledge the supervision and guidance of Dr Steven Djordjevic (Elizabeth Macarthur Agricultural Institute) and Professor Mark Walker (University of Wollongong), I will always be indebted. I thank them for allowing me the opportunity to broaden my knowledge through the attendance and presentation of my results at both domestic and international conferences. The contributions of Professor Chris Minion (Iowa State University) and Professor Steven Geary (University of Connecticut) are greatly appreciated. The expert proteomic analysis conducted by Dr Stuart Cordwell and other members of the Australian Proteome Analysis Facility were also important to the success of this project. Mukesh Srivastava of EMAI and Dr Stephen Schibeci of the ICPMR at Westmead Hospital are also thanked for their contributions and expertise.

Part of this project was conducted using facilities at the German Research Centre for Biotechnology (GBF). I would like to thank all those members of Professor Chhatwal's group at GBF and especially Professor Gursharan Singh Chhatwal, Dr Katrin Dinkla and Dr Manfred Rohde for their expertise and guidance.

I thank everybody at the Elizabeth Macarthur Agricultural Institute and especially the Microbiology section for their hospitality throughout my research. I especially thank Linda Falconer, Alison Collins and Jody Gorman for their assistance and friendship. A special thank you is given to Renee Levings and Cheryl Jenkins for their relentless support, the ability to pick me up when I needed it most and most importantly their unwavering friendship. Cheryl is also gratefully acknowledged for proof-reading this thesis and for her expert opinion. I will always be indebted to my family for the continued

support and the joy they always (well most of the time) bring to my life. This is what gets us through the hard times. Lastly I thank my fiancé Michael Kuit for his undying support and commitment. We got there.

This research is a testament to the contribution and commitment of all of those above.

Abstract

Mycoplasma hyopneumoniae colonise swine ciliated respiratory epithelia, leading to the development of porcine enzootic pneumonia. Heparin and other glycosaminoglycans are known to block adherence of this pathogen to porcine tracheal cilia, however adhesins with heparin-binding capacity have not been identified. Previous studies have implicated a 97 kDa surface protein of *M. hyopneumoniae*, P97 that appeared to be involved in the interaction of *M. hyopneumoniae* with swine cilia. This study aimed at identifying other potential adhesins of *M. hyopneumoniae*.

In this study, immuno-electron microscopy and trypsin degradation analyses demonstrated that a 159 kDa protein (P159) resides on the surface of *M. hyopneumoniae*. Furthermore, proteomic analyses indicate that this molecule is post-translationally cleaved. *In vitro*, these proteins are found to be cleaved and highly expressed at all stages during the growth cycle of *M. hyopneumoniae*. This molecule was also shown to be immunogenic due to its reactivity with sera from pigs naturally infected with *M. hyopneumoniae*. Recombinant expression of P159 domains was undertaken (F1, F2, F3, and F4). Two of these domains (F3 and F4) were found to bind heparin in a dose-dependent, saturable and specific manner. The Kd for this interaction was 142.37 $\pm$ 22.01 nM for F3 and 75.37 $\pm$ 7.34 nM for F4. Some pathogenic bacteria have been shown to bind heparin which can then bind to further components on the surface of cells, thereby acting as a bridging molecule in adhesion to host cells. Non-labeled heparin was shown to competitively inhibit this interaction with an IC_{50} value of 52.92 $\pm$ 1.03 μg/ml for F3 and 66.63 $\pm$ 1.02 μg/ml for F4. Fucoidan was also shown to competitively inhibit the binding of heparin to F3 (IC_{50} 96.28 $\pm$ 1.19 μg/ml) and F4 (IC_{50} 36.23 $\pm$ 1.14 μg/ml). Fluorescent and electron microscopic studies employing latex beads coated with P159 domains

revealed that F2, F3 and F4 promoted adherence to the porcine epithelial-like cell line PK15. Additionally, F2 and F4 also mediated the uptake of the latex beads into PK15 cells. Collectively this data suggests that P159 is a good candidate for an adhesin of *M. hyopneumoniae* and thus may play a role in the colonization of the respiratory tract of swine.

Ribosomal protein L7/L12 has been shown to play a role in the pathogenesis of a number of bacterial pathogens *in vitro*, and has been found to be expressed on the cell surface of some pathogenic bacteria. While work in this study revealed that the L7/L12 molecule is cytoplasmically expressed in *M.hyopneumoniae,* an immunoreaction with convalescent pig serum indicated the protein has immunogenic properties. The immunogenicity of the *M. hyopneumoniae* L7/L12 protein may make it a potential target for vaccine development.

List of Figures

Figure		Page
	Chapter 1. Review of Literature	
1.1	A phylogenetic tree showing the taxonomy of the mycoplasmas and their relatedness to Gram-positive bacteria.	2
1.2	*M. pneumoniae* cell morphology and ultrastructure.	7
1.3	Colonization of tracheal ring epithelium by *M. hyopneumoniae.*	7
1.4	A scanning electron micrograph of trachea 2 weeks post infection with *M. hyopneumoniae*.	12
1.5	Map of the cilium adhesin of *M. hyopneumoniae*.	16
1.6	Schematic overview of the types of molecules that bind cells to each other and to the extracellular matrix.	20
1.7	Structure of various glycosaminoglycans.	23
1.8	Model of the basal lamina.	26
1.9	Structure of laminin.	27
1.10	Schematic representation of the domains of the fibronectin molecule.	29
	Chapter 3. P159 is an immunogenic surface antigen of *M. hyopneumoniae* that is proteolytically processed	
3.1	Diagram of the *p97/p102* gene families in *M. hyopneumoniae* strain 232.	45
3.2	TMpred output for P159.	62
3.3	Peptide mass fingerprint analysis of P159 from *M.hyopneumoniae*.	63
3.4	(A) Recombinant P159 expression products as they resolve on a 15% reducing SDS-PAGE gel. (B) Peptide matches from MALDI-TOF mass spectrometry of F4.	65
3.5	Immunoblot analyses with anti-P159 sera.	66
3.6	Whole cell preparations of *M. hyopneumoniae* strain 232 subjected to trypsin treatment.	68
3.7	Immunolocalization of P159 cleavage products on the surface of *M. hyopneumoniae* strain 232.	69

3.8 Eclustalw alignment of the P159 protein sequence from *M. hyopneumoniae* strains J and 232. 72

3.9 Whole cell extracts of *M. hyopneumoniae* strains J and 232 after western blotting with a pool of anti-P159 sera. 73

3.10 P159 expression products of *M. hyopneumoniae*. 75

Chapter 4. *M. hyopneumoniae* surface antigen P159 binds heparin and promotes adhesion to and internalization of eukaryotic (PK15) cells

4.1 Binding of P159 fragments to biotinylated heparin. 94

4.2 Effect of inhibitors on P159 fragments binding to biotinylated heparin. 95

4.3 Electron micrographs of *M. hyopneumoniae* J strain bacterial cells adhering to PK15 cells. 97

4.4 Double immunofluorescence analysis of the adherence of P159 F1-F4 coated latex beads to PK15 cells. 99

4.5 Electron microscopy of the interaction of P159 F2 and F4 coated latex beads with PK15 cells. 100

Chapter 5. Characterisation of *M. hyopneumoniae* ribosomal protein L7/L12

5.1 Secondary structure of the L7/L12 dimer. 107

5.2 Primers to amplify the entire *rpL7/L12* gene from *M. hyopneumoniae.* 111

5.3 Alignment of the complete amino acid sequences available for L7/L12 ribosomal proteins from 27 different bacterial species. 122

5.4 A phylogenetic tree of the relationship between rpL7/L12 proteins of various bacterial species. 123

5.5 The sequence of the *rpL7/L12* gene from *M. hyopneumoniae*. 124

5.6 A. The pQE-9 cloning vector and the rpL7/L12 gene inserted between the *Bam*H1 and *Hin*DIII sites. B. B*am*H1 and *Hin*DIII restriction digest of *M. hyopneumoniae* 232 rpL7/L12 pQE9 clones on an agarose gel. 125

5.7 SDS-PAGE and immunoblot analyses of rpL7/L12. 127

5.8 Peptide matches from mass-spectrometry analysis of the recombinant rpL7/L12 expression product from *E. coli*. 127

5.9 Western blot images of whole cell protein preparations of *M. hyopneumoniae* 232 and *M. hyopneumoniae* J reacted with anti-rpL7/L12 rabbit serum. 128

5.10 FACScan analysis with anti-rpL7/L12 rabbit serum and normal rabbit serum. 129

5.11 Reactivity of rpL7/L12 with 16 different convalescent pig sera. 132

Appendices

A1 Map of the prokaryotic expression vector pQE-9 (Qiagen) used to express rpL7/L12 and P159 proteins in this study. 168

A2 Map of the prokaryotic cloning vector pPCR-Script Amp SK(+) (Stratagene) used to clone *p159* in this study before being further cloned into the pQE-9 expression vector. 169

List of Tables

Table **Page**

Chapter 1. Review of Literature

1.1 Properties distinguishing mollicutes from other bacteria 3

1.2 Some examples of bacterial species capable of binding proteins of the ECM. 31

Chapter 3. P159 is an immunogenic surface antigen of *M. hyopneumoniae* that is proteolytically processed

3.1 First dimension electrophoresis protocol for 11 or 17 cm IPG strips. 47

3.2 Second dimension electrophoresis protocol. 48

3.3 Primer sequences used to amplify various fragments of the *p159* gene. 50

3.4 Reaction conditions of the various P159 primer combinations. 50

3.5 P159 reactivity with convalescent pig sera. 76

Chapter 5. Characterisation of *M. hyopneumoniae* ribosomal protein L7/L12

5.1 Reaction conditions for the rpL7/L12 PCR. 112

5.2 FACScan analysis of intact and saponin treated *M. hyopneumoniae* cells with anti-rpL7/L12 serum and normal rabbit serum. 130

5.3 *M. hyopneumoniae* (EMAI) ELISA ratios for each of the 16 pig sera used in the rpL7/L12 ELISA. 131

Abbreviations

ABTS	2,2'-azino-bis(3-ethylebenzthiazoline-6-sulfonic acid) diammonium salt
ANGIS	Australian National Genomic Information Service
ATCC	American Type Culture Collection
bp	base pairs
CPM	counts per minute
CSPD	disodium 3-(4-methoxyspiro{1,2-dioxetane-3,2'-(5'-chloro)tricyclo[3.3.1.1^{3,7}]decan}-4-yl)phenylphosphate
DAB	diaminobenzidine
DMEM	Dulbecco's modified Eagle medium
DNA	deoxyribonucleic acid
^{o}C	degrees celsius
1-DGE	one-dimensional gel electrophoresis
2-DGE	two-dimensional gel electrophoresis
ECM	extracellular matrix
EDTA	ethylenediamine tetra-acetic acid
ELISA	enzyme linked immunosorbent assay
EMAI	Elizabeth Macarthur Agricultural Institute
FCS	foetal calf serum
g	gram
g	g forces for centrifugation
GAGs	glycosaminoglycans
h	hour
IPTG	isopropyl-β-D-thiogalactopyranoside
Kb	kilobases
kDa	kilo daltons
l	litre
LB	Luria bertani
m	milli
M	molar
mA	milliamps
MALDI-TOF	matrix-assisted laser desorption ionization-time-of-flight
µ	micro
min	minute
ml	milliliter
MS	mass spectrometry
MSCRAMMs	microbial surface components recognizing adhesive matrix molecules
n	nano
NCBI	National Centre for Biotechnology Information
OD	optical density
ORF	open reading frame
PAGE	polyacrylamide gel electrophoresis
PBS	phosphate buffered saline
PBST	phosphate buffered saline with tween20
PCR	polymerase chain reaction
PEP	porcine enzootic pneumonia
pH	picohenry
PRDC	porcine respiratory disease complex

PVDF	polyvinylidene difluoride
rpm	revolutions per minute
RT	room temperature
SDS	sodium dodecyl sulfate
sec	second
TBE	tris-borate EDTA
TCA	tricarboxylic acid
V	volts
v/v	volume per volume
w/v	weight per volume

Table of Contents

Declaration i

Acknowledgements ii

Abstract iv

List of Figures vi

List of Tables ix

Abbreviations x

Table of Contents xii

Chapter 1. Review of Literature

1.1 General notes on Mycoplasmas 1

1.2 Mycoplasma adhesion to host cells 4

1.3 Internalisation by mycoplasmas 8

1.4 Mycoplasmas of swine 9

1.5 *M. hyopneumoniae* colonization of swine respiratory epithelia 11

1.6 Adhesins of *Mycoplasma hyopneumoniae* 14

1.7 Extracellular matrix components and bacterial interaction 18

1.7.1 *Host extracellular matrix (ECM)* 19

1.7.2 *ECM components and bacterial interaction* 19

1.7.3 *Proteoglycans* 22

1.7.3.1 Heparin and heparan sulfate 24

1.7.4 *Laminin* 25

1.7.5 *Fibronectin* 28

1.7.6 *Collagen* 30

1.7.7 *Interactions of bacteria with the ECM* 30

Chapter 2. General Methods

2.1 *M. hyopneumoniae in vitro* culture sample preparation 32

2.2 Cloning 33

2.2.1 *PCR amplification* 33

2.2.2 *Agarose gel electrophoresis* 33

2.2.3 *Restriction enzyme digestion* 33

2.2.4 *Ligation and transformation* 34
2.2.5 *DNA sequence analysis of* M. hyopneumoniae *genes* 34
2.2.6 *Plasmid mini-preparations* 35
2.2.7 *Plasmid DNA Extraction - Midi/Maxi Preparation* 36
2.3 Protein expression 37
2.4 Protein purification under denaturing conditions 37
2.5 Bradford assay to calculate protein concentration 38
2.6 Generation of polyclonal antiserum in rabbits 38
2.7 One-dimensional protein gel electrophoresis (SDS-PAGE) 39
2.8 Mass spectrometry analysis of proteins 39
2.9 Western transfer and ligand/western blot 40
2.10 ELISA 41

Chapter 3. P159 is an immunogenic surface antigen of *M. hyopneumoniae* that is proteolytically processed

3.1 Introduction 43
3.2 Methods 46
3.2.1 *Detection of transmembrane domains in protein P159* 46
3.2.2 *Proteomic analyses: 2-D gel electrophoresis* 46
3.2.3 *N-terminal sequencing of P159 cleavage products* 48
3.2.4 *PCR amplification of the* p159 *gene of* M. hyopneumoniae 48
3.2.5 *Construction of a pQE9-based expression plasmid system for* M. hyopneumoniae *P159 proteins* 51
3.2.5.1 Cloning into pPCR-Script plasmid 51
3.2.5.2 Cloning into pQE-9 plasmid 52
3.2.5.3 Colony blotting for screening of recombinants 52
3.2.5.4 DNA sequencing of the *M. hyopneumoniae p159* fragment gene inserts 54
3.2.6 *Expression of P159 protein fragments* 54
3.2.7 *Generation of polyclonal antiserum in rabbits* 55
3.2.8 *Growth time-course assay for detecting P159 expression* 55
3.2.9 *Determining cellular location of P159* 56
3.2.9.1 Trypsin treatment of *M. hyopneumoniae* 56
3.2.9.2 Immuno-electron microscopy of intact *M. hyopneumoniae* 57

3.2.10 Triton X-114 extraction of *M. hyopneumoniae* for 2-DGE 57
3.2.11 *Convalescent pig sera ELISA* 59
3.3 Results 60
3.3.1 *P159 possesses a transmembrane domain* 60
3.3.2 *Proteomic analysis of P159 expression in* M. hyopneumoniae 60
3.3.3 *Cloning and expression of different regions of P159 within* E. coli 61
3.3.4 *Cellular location of P159 fragments* 67
3.3.5 C*omparison of P159 from* M. hyopneumoniae *strains 232 and J* 70
3.3.5.1 Sequence comparison 70
3.3.5.2 Comparison of P159 expression products 70
3.3.6 *P159 reacts with convalescent pig sera* 76
3.4 Discussion 77

Chapter 4. *M. hyopneumoniae* surface antigen P159 binds heparin and promotes adhesion to and internalization of eukaryotic (PK15) cells

4.1 Introduction 83
4.2 Methods 85
4.2.1 *Ligand blots* 85
4.2.2 *Fibronectin and Fibrinogen ELISA* 85
4.2.3 *Radioactive pull-downs and western blots* 86
4.2.3.1 Radioactively labelling ECM proteins 86
4.2.3.2 Radioactivity pull-down experiments 87
4.2.3.3 Radioactivity western blots 88
4.2.4 *Heparin binding assays* 88
4.2.5 *Adherence/invasion assay of P159 fragments with PK15 cells* 89
4.2.5.1 Coating latex beads with F1-F4 and incubation with PK15 cells 89
4.2.5.2 Double immunofluorescence detection of F1-F4 beads 90
4.2.6 *Incubation of PK15 cells with* M. hyopneumoniae 91
4.3 Results 92
4.3.1 *Recombinant P159 proteins bind heparin* 92
4.3.2 Mycoplasma hyopnemoniae *adheres to porcine epithelial cells* 96
4.3.3 *P159 fragments adhere to porcine epithelial cells* 98
4.4 Discussion 101

Chapter 5. Characterisation of *M. hyopneumoniae* ribosomal protein L7/L12

5.1 Introduction 106

5.2 Methods 110

5.2.1 *Microbial* rpL7/L12 *gene similarity analysis* 110

5.2.2 *Genetic Techniques* 111

5.2.2.1 PCR amplification of the *M. hyopneumoniae* strain 232 *rpL7/L12* gene 111

5.2.2.2 Purification of the rpL7/L12 PCR product 112

5.2.3 *Expression of rpL7/L12 in pQE-9* 113

5.2.3.1 Plasmid DNA extraction 113

5.2.3.2 Restriction enzyme digestion and gel extraction 113

5.2.3.3 Ligation and transformation 114

5.2.3.4 Screening recombinant plasmids and plasmid DNA extraction 114

5.2.3.5 DNA sequence analysis of *M. hyopneumoniae rpL7/L12* genes 114

5.2.4 *Protein techniques* 115

5.2.4.1 RpL7/L12 protein expression 115

5.2.4.2 Sodium dodecyl sulphate polyacrylamide gel electrophoresis (SDS-PAGE) 116

5.2.5 *Generation of polyclonal antiserum to recombinant rpL7/L12* 116

5.2.6 *Mass spectrometry analysis of recombinant rpL7L12* 116

5.2.7 *Expression patterns of rpL7/L12 by* M. hyopneumoniae *J and 232* 117

5.2.8 *FACScan analysis of* M. hyopneumoniae *with anti-rpL7/L12 sera* 117

5.2.9 *Convalescent pig sera ELISA* 118

5.3 Results 120

5.3.1 *Sequence similarity of L7/L12 between bacterial species* 120

5.3.2 *Cloning and expression of rpL7/L12 in* Escherichia coli 124

5.3.3 *Verifying recombinant rpL7/L12 expression and the production of rabbit polyclonal antiserum* 126

5.3.4 *Expression pattern of* M. hyopneumoniae *rpL7/L12 in strains 232 and J* 126

5.3.5 *rpL7/L12 is expressed inside the* M. hyopneumoniae *cell* 128

5.3.6 *rpL7/L12 is recognized by convalescent pig serum* 130
5.4 Discussion 133

Chapter 6. General Discussion and Future Studies 136

References 141

Appendices

Appendix A. General buffers and reagents 158
Appendix B. Source of ECM compounds and their antibodies 165
Appendix C. Commercial kits used in this study 166
Appendix D. Cell lines used in this study 167
Appendix E. Vector maps 168
Appendix F. Presentation of results at conferences 170

Chapter 1: Review of Literature

1.1 General notes on Mycoplasmas

Mycoplasmas are distinguished phenotypically from other bacteria by their small size (0.15-0.30 μm) and lack of a cell wall. Taxonomically, the lack of a cell wall was used to separate mycoplasmas from other bacteria into the class *Mollicutes* (*mollis*, soft; *cutis*, skin). However, 16S rRNA analyses revealed that the Mycoplasmas are phylogenetically related to Gram-positive bacteria (Fig. 1.1) and evolved regressively (by genome reduction) from Gram-positive bacteria (Razin, 1992). As a result of regressive evolution, members of the *Mollicutes* possess small genomes (580 kb – 2,200 kb). The genome sizes of the mycoplasmas vary not only within the same Genus but even among strains of the same species (Carle *et al*., 1995; Humphery-Smith *et al*., 1997; Ladefoged and Christiansen, 1994; Robertson *et al*., 1990). One of the reasons for this variability is the frequent occurrence of repetitive elements and insertion sequences (Razin *et al*., 1998). It is also notable that the mycoplasma genome has a characteristically low G+C content. With a few exceptions, the G+C content is within the range of 24 to 33 mol%. Furthermore in mycoplasmas, the codon UGA encodes for a tryptophan codon whereas in most other bacteria UGA encodes a stop codon. A consequence of this phenomenon is the difficulty in expressing cloned mycoplasma genes in *E. coli*, as termination occurs at UGA codons resulting in truncated proteins. Table 1.1 highlights some of the most distinguishing features of the *Mollicutes*.

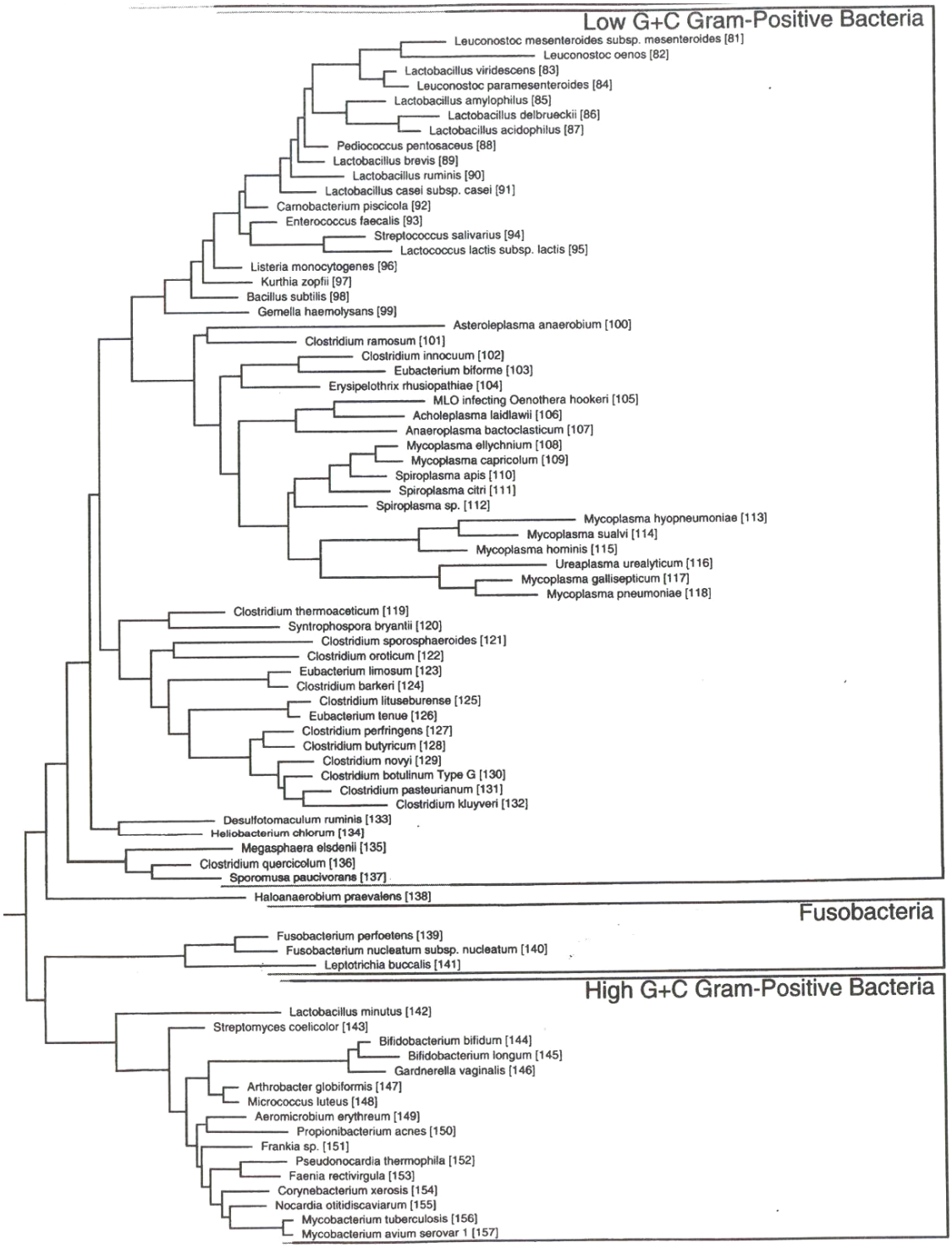

Fig. 1.1. A phylogenetic tree derived by maximum likelihood analysis of small-subunit rRNA sequences, showing the taxonomy of the mycoplasmas and their relatedness to Gram-positive bacteria. For the complete tree and list of organisms from which the sequences used in this figure were obtained see Olsen *et al.*, 1994.

Table 1.1. Properties distinguishing mollicutes from other bacteria [a]

Property	Mollicutes	Other bacteria
Cell wall	Absent	Present
Plasma membrane	Cholesterol present in most species	Cholesterol absent
Genome size	550-2,220 kb	1,050->10,000 kb
G+C content of genome	23-40 mol%	25-75 mol%
No. of rRNA operons	1 or 2 [b]	1-10
5S rRNA length	104-113 nucleotides	>114 nucleotides
No. of tRNA genes	30 (*M. capricolum*), 33 (*M. pneumoniae*)	84 (*B. subtilis*), 86 (*E. coli*)
UGA codon usage	Tryptophan codon in *Mycoplasma, Ureaplasma, Spiroplasma, Mesoplasma*	Stop codon
RNA polymerase	Rifampin resistant	Rifampin sensitive

[a] Taken from Razin *et al*., 1998.
[b] Three rRNA operons in *Mesoplasma lactucae* (Bove, 1993).

Mycoplasmas are widespread in nature as parasites of humans, mammals, reptiles, fish, arthropods, and plants (Razin, 1992). The list of hosts known to harbor mycoplasmas is continuously increasing, as is the number of established mycoplasma species. There are approximately 180 characterised mycoplasma species, but it is widely agreed that these constitute only a fraction of the number of mollicutes in nature (Razin *et al*., 1998). Mycoplasmas generally have a rather strict host, organ and tissue specificity, probably reflecting their nutritionally exacting nature and obligate parasitic mode of life. The primary habitats of human and animal mycoplasmas are the mucosal surfaces of the respiratory and urogenital tracts, the eyes, alimentary canal, mammary glands and joints. Recent mycoplasma genome projects have revealed a paucity of genes involved in biosynthetic pathways, and as a consequence, many field strains are difficult to culture *in vitro*. For example, both *M. genitalium* and *M. pneumoniae* lack genes involved in amino acid biosynthesis (Fraser *et al*., 1995; Himmelreich *et al*., 1996), making them totally dependent on exogenous sources of amino acids. Most mycoplasmas live as commensals. Infections with pathogenic mycoplasmas are rarely of the fulminant type but rather, follow a chronic course. It could be argued that mycoplasmas are close to the concept of

"ideal parasites", usually living in harmony with their host. The molecular basis of mycoplasma pathogenicity remains largely elusive.

Lacking a cell wall and intracytoplasmic membranes, the mollicutes have only one type of membrane, the plasma membrane. Proteins constitute over two-thirds of the mycoplasma membrane mass, with the rest being membrane lipids. The abundance of lipoproteins in mycoplasma membranes is in contrast to other bacteria which contain a limited number. Furthermore, membrane lipoproteins are among the most dominant antigens in mollicutes and a majority of the mycoplasma cell surface antigens known to undergo antigenic and size variation are lipoproteins (Razin *et al*., 1998). This unusually large number of lipoproteins may be attributed to the absence of a periplasmic space in the wall-less mollicutes. Virtually all mycoplasma lipids are located in the cell membrane and, as in other biological membranes, consist of phospholipids, glycolipids, and neutral lipids. However, the mycoplasmas are either partially or totally incapable of fatty acid synthesis and depend on the host or the culture medium for their supply. Due to the lack of a cell wall, the mycoplasma cell membrane is exposed to the environment and is in direct contact with the eukaryotic host cell. The fusion of the two membranes could enable the transfer or exchange of membrane components (Razin, 1978; Razin, 1985; Razin and Jacobs, 1992), possibly allowing mycoplasma proteins to enter host cells.

1.2 Mycoplasma adhesion to host cells

Most human and animal mycoplasmas adhere to the epithelial linings of the respiratory or urogenital tract and appear to rarely invade tissues. Adhesion of mycoplasmas to host cells is a prerequisite for colonisation and for infection. The loss of adhesion capacity by

mutation results in a loss of infectivity, and reversion to the cytadhering phenotype is accompanied by regaining infectivity and virulence (Razin *et al*., 1998).

Mycoplasma colonization results from the interaction between adhesin proteins on the mycoplasma surface and sulfated glycolipid or sialoglycoprotein molecules on the host cells. The attachment tip organelle is a polar structure (Fig. 1.2) that orients mycoplasma binding to host cells and functions in cell division and gliding motility (Krause and Balish, 2001). This organelle has been found in *M. pneumoniae, M. genitalium* (Razin *et al*., 1998), *M. gallisepticum* (Markham *et al*., 1994; pMGA), *M. pirum* (Tham *et al*., 1994) and *M. penetrans* (Lo *et al*., 1993). Although adhesins play a major role in cytadhesion, the process appears to be multifactorial, also involving a number of accessory proteins acting in concert with cytoskeletal elements to facilitate the lateral movement and concentration of the adhesin molecules at the attachment tip organelle. Panel B of Fig. 1.2 shows the cell structure of *M. pneumoniae*, with a terminal organelle, colonizing hamster tracheal ring in organ culture (Krause and Balish, 2004). Alternatively, Fig. 1.3 shows *M. hyopneumoniae* cells, which do not possess a terminal organelle, colonizing swine tracheal ring epithelium (DeBey and Ross, 1994). Therefore mycoplasma species not possessing a terminal organelle still have an adherent ability.

Several adhesins of mycoplasmas have been described, however the best understood are those of *M. pneumoniae*. The number of proteins associated with cytadherence in *M. pneumoniae* is large and include high molecular weight proteins 1-3 (HMW1-3), P30, P1, P65, B (P90) and C (P40), Fig. 1.2. Some of these proteins are structural elements of the attachment organelle (Krause and Balish, 2001). The structure and assembly of the terminal organelle of *M. pneumoniae* is very complex and is abbreviated below but is reviewed in Krause and Balish (2004). Strains that lack P1 or are not able to properly

position P1 at the surface of the tip organelle fail to attach to the respiratory epithelium (Baseman *et al*., 1982; Krause *et al*., 1982). However, the finding that P1 is usually not lost from non-adhering cells indicates that P1 alone is not sufficient for mediating cytadherence. It is known that cytadherence competence requires proper localization of P1, B, C and P30 to the terminal organelle. P65 is found at the surface of the terminal organelle, co-localizing with P30 (Jordan *et al*., 2001; Seto *et al*., 2001; Seto and Miyata, 2003) but its function is unknown. However, P30 is required for P65 to remain fully cell associated. P1 localization to the terminal organelle requires stable HMW1 and it is also known that P30 fails to localize to the terminal organelle without HMW3. HMW3 stabilizes the electron-dense core of the terminal organelle. No core is observed in the absence of HMW1 or HMW2 which appear to be required early in assembly of the terminal organelle (Krause and Balish, 2004).

The receptors on host cell membranes responsible for mycoplasma attachment, identified so far, are mostly sialoglycoconjugates and sulfated glycolipids (reviewed in Razin, 1985; Razin and Jacobs, 1992; Zhang *et al*., 1994a,b). It has been shown that there is more than one type of receptor for *M. pneumoniae*, and presumably other adhering mycoplasmas as well. This is not surprising considering that each mycoplasma may carry more than one adhesin type (Razin and Jacobs, 1992).

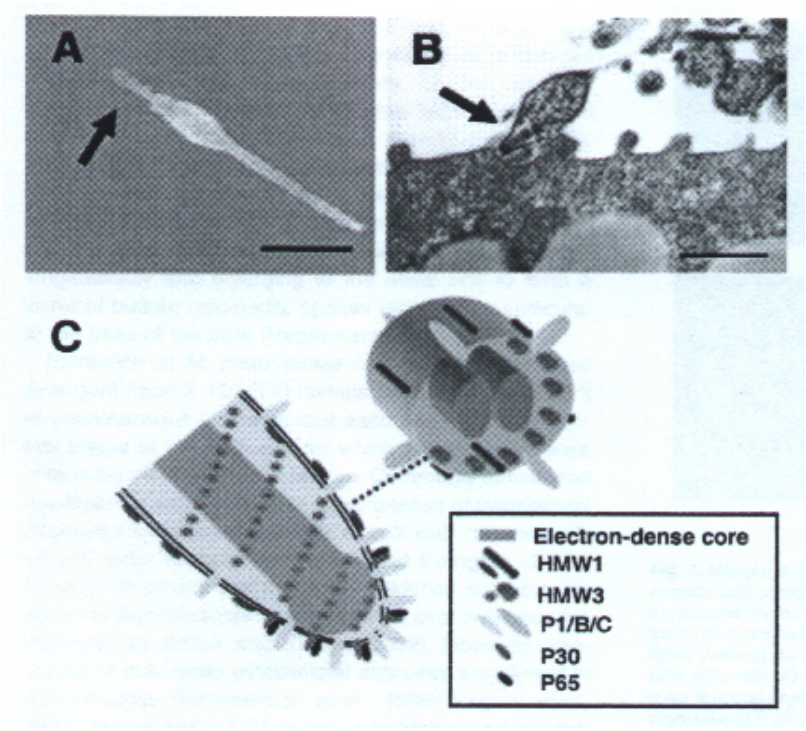

Fig. 1.2. *M. pneumoniae* cell morphology and ultrastructure. A. Scanning electron-micrograph of *M. pneumoniae* cells cultured on glass. Arrow denotes the terminal organelle. Bar, 0.5 μm (Courtesy S. Ross). B. Transmission electron micrograph of *M. pneumoniae* cells colonizing hamster tracheal ring in organ culture. Arrow indicates electron-dense core of terminal organelle. Bar, 0.5 μm. (Courtesy J. Jordan). C. Schematic illustration of protein localization in the terminal organelle of *M. pneumoniae* as depicted in longitudinal and cross-sections (left and right respectively). The number of proteins associated with cytadherence in *M. pneumoniae* is large and include high molecular weight proteins 1 and 3 (HMW1 and HMW3 [which stabilizes the electron-dense core]), P30, P65, P1, B (P90) and C (P40) (Krause and Balish, 2004).

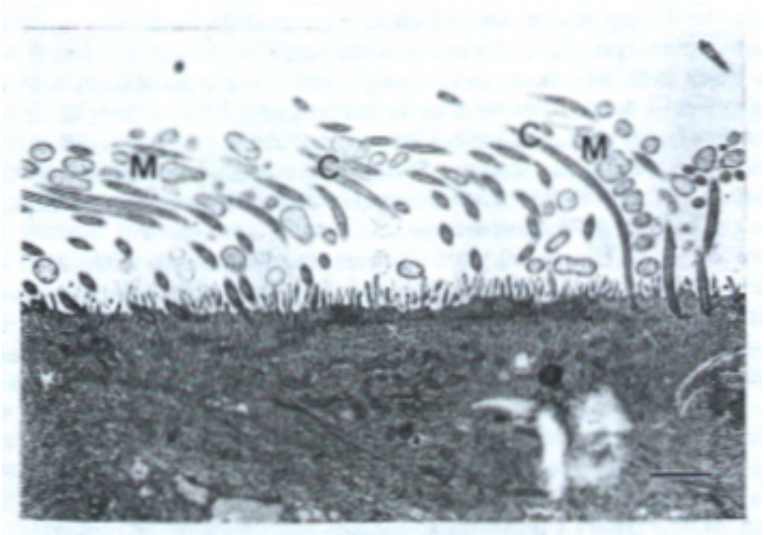

Fig. 1.3. Colonization of tracheal ring epithelium by *M. hyopneumoniae* (M) 5 days after inoculation. Mycoplasma cells are closely associated with cilia (C). Bar 0.83 μm. (DeBey and Ross, 1994).

1.3 Internalisation by mycoplasmas

While certain human and animal mycoplasmas are known to be taken up by polymorphonuclear leukocytes and macrophages (Marshall *et al*., 1995), the question of whether mycoplasmas can enter epithelial cells has not been easy to resolve. However, studies have shown that some species can invade the epithelia. Studies using confocal microscopy and flow cytometry of fluorochrome-labelled mycoplasmas, revealed that *M. penetrans*, *M. pneumoniae*, and *M. genitalium* entered the intracellular spaces and were located throughout the cytoplasm and perinuclear regions of cultured human cells (Baseman *et al*., 1995). The mechanism of entry of mycoplasmas is still unclear. While mycoplasmas such as *M. penetrans* and *M. genitalium* appear to enter the cells through the specialised tip structure (Jensen *et al*., 1994; Lo *et al*., 1993), other mycoplasmas which have been shown to internalise, such as *M. fermentans* and *M. hominis*, have no such tip structure (Taylor-Robinson *et al*., 1991).

Invasion of mycoplasmas into host cells may disrupt the cells integrity and function. Lo *et al*. (1993) stated that extensive invasion of cells by *M. penetrans* eventually results in cell disruption and necrosis. Furthermore, Mernaugh *et al*. (1993) showed by electron microscopy the complete lysis of human lung fibroblasts 96 h after infection of *M. genitalium*, accompanied by large numbers of mycoplasmas in the milieu. Internalisation of mycoplasmas, even if only for a brief period, may protect them against the effects of antimicrobials and the host immune system and may account to some extent for the difficulty of eradicating mycoplasmas from infected cell cultures (Razin *et al*., 1998). Thus, intracellular localisation may promote the establishment of latent or chronic infection states and circumvent bactericidal immune mechanisms and selective drug

therapies (Baseman and Tully, 1997). Cell invasion may also allow the systemic dissemination of the pathogen to other tissues within the host.

1.4 Mycoplasmas of swine

Many mycoplasma species are present in the respiratory tract of swine without being pathogenic. Such species include *M. flocculare, M. sualvi* and *M. hyopharyngis* (Ross, 1992). *M. hyorhinis* and *M. hyosynoviae* however are pathogenic and can cause polysterositis and arthritis (Kobisch and Friis, 1996). The most prevalent species of Mycoplasma found in the respiratory tract of swine and the species causing the greatest economic impact is *M. hyopneumoniae*.

Porcine enzootic pneumonia (PEP) is one of the most common and economically important diseases occurring in swine. *Mycoplasma hyopneumoniae* is the causative agent of PEP and is the focus of this study. *M. hyopneumoniae* has also been implicated in another swine respiratory syndrome, porcine respiratory disease complex (PRDC) which is prevalent in countries (Europe, U.S.A.) that harbour porcine reproductive and respiratory syndrome virus (PRRSV; Thacker *et al*., 2000). These diseases are responsible for retarded growth and poor weight gain in affected herds and together they have resulted in significant economic losses in major swine producing countries. Furthermore, infected swine may be predisposed to secondary bacterial pulmonary infections (Frey *et al*., 1994; Ross, 1992). A study conducted in 1991 estimated that economic losses to the pig industry are estimated at $20 million a year in Australia and up to $1 billion a year worldwide (Clarke *et al*., 1991). *M. hyopneumoniae* transmission occurs through direct contact, aerosol, sow-to-pig transmission and can be spread in litters, with increased

animal density influencing disease prevalence (Maes *et al*., 1996). Therefore control of PEP requires good management practices and effective vaccination regimes.

Antibiotics have been useful in treating the symptoms of PEP but do not eliminate *M. hyopneumoniae*. Eliminating the bacteria is required to prevent secondary infections and to avoid re-infection. Antibiotics that interfere with cell wall synthesis, such as penicillin and ampicillin, are ineffective as *M. hyopneumoniae* lacks a cell wall. Currently quinolines, which inhibit the activity of bacterial DNA gyrase which is essential for DNA replication, are the most effective antibiotics (Maes *et al*., 1996). It is believed that vaccines that effectively block adherence and colonisation will be the best way to prevent PEP. Currently the use of denatured *M. hyopneumoniae* membrane protein antigens as vaccine components have been investigated with the aim to identify essential antigens to be used in future vaccines (Djordjevic *et al*., 1997). Studies with bacterin *M. hyopneumoniae* vaccines show protection against experimental *M. hyopneumoniae* challenge, although pneumonia is often not completely eliminated and colonization is only marginally reduced (Thacker *et al*., 1998).

Under field conditions, grower pigs are the major source of infection with *M. hyopneumoniae*; however pigs of all ages can develop acute pneumonia and appear to be equally susceptible to the disease (Kobisch *et al*., 1993; Ross, 1992). Enzootic pneumonia is characterised by high morbidity and low mortality. Coughing is the principal clinical sign, observed over a few weeks or months, but is not constant. If the infection is complicated by other bacteria, particularly *Pasteurella multocida*, other symptoms such as laboured breathing and fever, and even death, may occur (Kobisch and Friis, 1996).

1.5 *M. hyopneumoniae* colonization of swine respiratory epithelia

Electron microscope studies show that colonisation of the epithelium is visible during the first or second week after challenge of a pig with *M. hyopneumoniae* (Kobisch and Friis, 1996). Two to eight weeks after inoculation, clumping and loss of cilia is evident, reflecting the colonization of the mucosal surface. Studies of the respiratory tract of infected swine show that *M. hyopneumoniae* cells predominantly adhere to trachea, bronchi, and bronchiolar epithelial cilia (Fig. 1.4), but were also seen in association with the epithelial microvilli and surfaces, and on leukocytes in the trachea (Blanchard *et al*., 1992; Mebus and Underdahl, 1977; Tajima and Yagihashi, 1982). Buttenschon and colleagues (1997) have also cultured *M. hyopneumoniae* from the pericardium, which is a double layer of serous membrane surrounding the heart, in Danish slaughter pigs. Thirty-three isolates of *M. hyopneumoniae* were cultured from 46 pigs showing fibrinous pericarditis. *M. hyopneumoniae* however, has not been shown to be able to invade the epithelial cells and it is not known how these bacteria were able to localize in the pericardium. A number of pig respiratory pathogens such as *Haemophilus parasuis*, *Actinobacillus pleuropneumoniae*, *Pasteurella multocida* and *Mycoplasma hyorhinis* are known to induce pleurisy (inflammation of the membrane surrounding the lungs, pleura) and pericarditis. When there is acute inflammation of the lungs and pleura, inflammatory exudate can flow into the thoracic cavity and spread the infection to the pericardium. Although *M. hyopneumoniae* is not known to induce pleurisy, in conjunction with other bacteria pleurisy may occur and allow *M. hyopneumoniae* to spread to the pericardium.

During *in vitro* studies, observation by electron microscopy shows that after infection the mucosal surface of the swine respiratory tract is less ciliated and mycoplasmas are associated with the remaining cilia. Organisms have also been observed to be attached to

cellular debris and to sloughed cilia (Zielinski and Ross, 1993). Mucopurulent exudate in small airways is a prominent feature of *M. hyopneumoniae* pneumonia in pigs and may be attributable to hypersecretion of mucus as well as ciliostatsis (DeBey *et al*., 1992) which are common in *M. hyopneumoniae* infections.

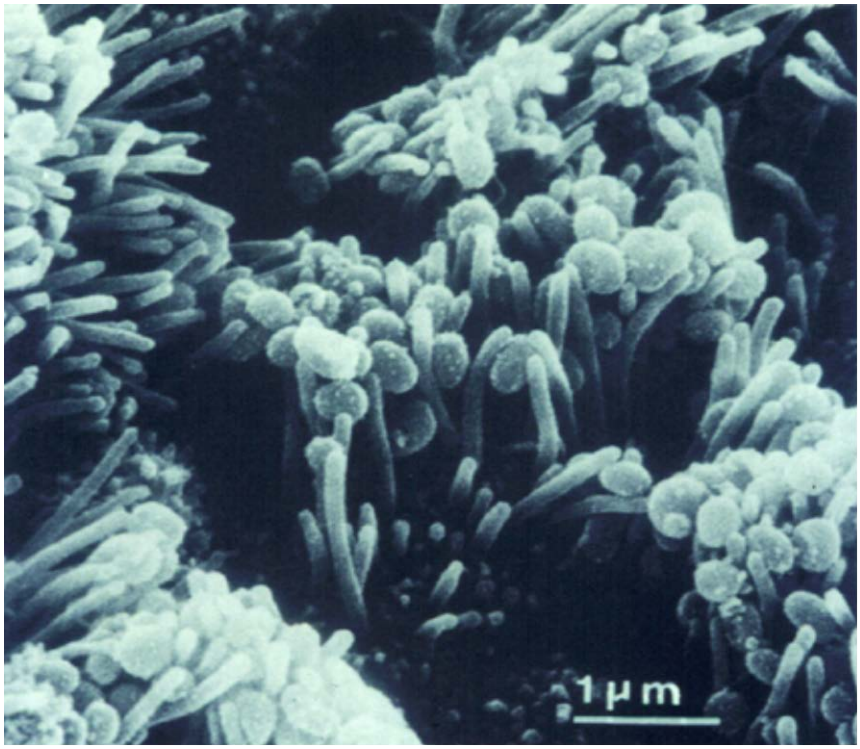

Fig. 1.4. A scanning electron micrograph of trachea 2 weeks post infection with *M. hyopneumoniae*. *M. hyopneumoniae* appear closely associated with the upper part of cilia, bar = 1 µm (Blanchard *et al*., 1992).

M. hyopneumoniae infection is associated with a marked infiltration of lymphocytes, macrophages, neutrophils and plasma cells to the lungs, trachea and bronchi, which are believed to be responsible for the lesions seen on these surfaces as early as two weeks after infection (Livingston *et al*., 1972). Throughout the disease progression ciliostasis, loss of cilia and epithelial cell death occurs (Blanchard *et al*., 1992). Excessive mucous production, in combination with cilial damage, decreases the function of the mucociliary escalator (DeBey and Ross, 1994), which is responsible for moving trapped bacteria up to

the back of the throat where they are swallowed. Loss of this function increases the risk of secondary respiratory infections.

For cilial damage to occur *M. hyopneumoniae* must attach to the swine respiratory epithelial cells. Non-pathogenic *M. hyopneumoniae* and excessively *in vitro* passaged *M. hyopneumoniae* are unable to adhere to ciliated cells (Zielinski and Ross, 1990), and are therefore unable to colonize the respiratory epithelium and establish infection, confirming that adherence is essential for the initiation of epithelial cell damage. This was also confirmed by DeBey and Ross (1994) where it was found that epithelial cell damage did not occur when *M. hyopneumoniae* was separated from ciliated epithelium with a 0.1-μm-pore-size membrane. Evidence that attachment is necessary for induction of ciliary damage occurring during *M. hyopneumoniae* infection *in vitro* further demonstrates the importance of identifying the adhesins associated with attachment of *M. hyopneumoniae in vivo* for production of vaccines that prevent infection in the pig (DeBey and Ross, 1994).

During a study of the mechanisms by which *M. pneumoniae* induces loss of cilia of respiratory epithelium, it was noted that an increase in the concentration of Ca^{2+} in the medium resulted in the loss of cilia (Zhang *et al*., 1994a,b). Park and colleagues (2002) later showed that *M. hyopneumoniae* activates receptors that are coupled to G_i or G_o, which in turn activates a phospholipase C pathway, thereby releasing Ca^{2+} from the endoplasmic reticulum. Thus, an increase in Ca^{2+} may serve as a signal for the pathogenesis of *M. hyopneumoniae* (Park *et al*., 2002).

1.6 Adhesins of *Mycoplasma hyopneumoniae*

M. hyopneumoniae lacks the specialised tip attachment organelle that *M. pneumoniae* and *M. genitalium* use to attach to host cells (Dybvig and Voelker, 1996; Krause, 1996; Razin *et al*., 1998). Nevertheless *M. hyopneumoniae* is capable of adhesion to ciliated epithelia. Pre-incubation of *M. hyopneumoniae* cells with periodate and trypsin abolished attachment of the bacteria to ciliated respiratory tract cells (Zielinski and Ross, 1993), indicating that adherence is mediated by proteins and carbohydrates on the surface of the organism.

A 97-kDa surface protein of *M. hyopneumoniae*, P97, has been implicated as playing a role in host cell adhesion. MAbs F1B6 and F2G5, which recognise P97 in immunoblots (Zhang *et al*., 1995) reduce adherence *in vitro* (by 67%) to purified cilia and to ciliated cells. DNA sequence analysis revealed an open reading frame coding for a 124.9-kDa protein in strain 232 (pathogenic strain; Hsu *et al*., 1997) and 123 kDa in strain J (laboratory adapted non-pathogenic strain; Wilton *et al*., 1998). In J strain the product is a 94kDa protein (P94) as opposed to P97 (Wilton *et al*., 1998). The only significant hydrophobic stretch representing a potential trans-membrane domain was found at the N-terminus. The N-terminal sequence of purified P97 and P94 mapped at amino acid 195 of the translated sequence, indicating that a significant processing event takes place removing the only potential trans-membrane domain in *M. hyopneumoniae* (Hsu *et al*., 1997). This processing results in the production of a 22-kDa protein, P22, which represents the N-terminal 195 amino acids of the cilium adhesin pre-protein, as well as P97 or P94. This observation suggests that *M. hyopneumoniae* secretes proteins destined for the cell surface very differently compared with models proposed for Gram-positive organisms, from which mycoplasmas evolved.

Using swine cilia adherence assays, binding of recombinant P97 to cilia was inhibited by the exogenous addition of heparin and fucoidan (Hsu *et al*., 1997). These substances were shown to prevent *M. hyopneumoniae* binding to swine cilia (Zhang *et al*., 1994b), supporting the hypothesis that P97 was involved in *M. hyopneumoniae* binding to cilia *in vivo*.

The cilium binding activity of P97 or P94 is localised at the carboxy-terminus of the protein and includes two repeat regions, R1 and R2 (Hsu *et al*., 1997). Studies show that the cilium binding site is located in the R1 repeat sequence (AAKPV(E)). In *M. hyopneumoniae* strain 232 there are 15 tandem copies of this sequence in the R1 region of P97 while in strain J there are 9 tandem copies in P94 (Hsu and Minion 1998a; Wilton *et al*., 1998) and it is this difference that largely accounts for the size variation between the homologous proteins. For functional binding to swine respiratory cilia Hsu and Minion (1998a) suggest that eight AAKPV(E) repeats are required. The adherence-blocking monoclonal antibody F1B6 also recognises this region but requires only three AAKPV(E) repeats for recognition. A comparison of the R1 regions of *M. hyopneumoniae* strains displaying variation in cilium adherence failed to identify changes that could account for the differences in adherence shown by the strains examined (Hsu and Minion, 1998a) as only eight AAKPV(E) repeats are required for cilium binding and both strains 232 and J contain this minimum number while strain 232 can adhere to cilia but strain J cannot. Thus, other proteins, in addition to P97 or P94, are likely to be involved in adherence, possibly in combination with P97 or P94. The R2 region is composed of four repeats of the 10-amino acid sequence GTPNQGKKAE in *M. hyopneumoniae* strain 232 and 5 repeats in strain J and does not appear to be directly involved in cilium binding (Hsu *et al*., 1997). The function of this repeat region remains unknown.

Recently, Djordjevic *et al*. (2004) demonstrated that the P97 cilium adhesin is proteolytically processed on the surface. Proteomic analysis of *M. hyopneumoniae* strain J and 232 identified cleavage products of 22, 28, 66 and 94 kDa in strain J and 22, 28, 70, and 97 kDa in strain 232, (Fig. 1.5). N-terminal sequencing showed that the 66- and 94-kDa proteins possessed identical N-termini and that the 66-kDa variant was generated by cleavage of an R2 containing 28-kDa fragment from the C-terminus. As stated earlier, the 22-kDa product represents the N-terminal 195 amino acids of the cilium adhesin pre-protein. Comparative studies with pathogenic *M. hyopneumoniae* strain 232 found that the major cleavage products are similar but differ slightly in size, although P22 and P28 appear to be further processed in 232. Immunoblotting studies demonstrated that the processing is complex and strain specific, with cleavage occurring with different frequencies at multiple sites. Immuno-gold electron microscopy of *M. hyopneumoniae* cells showed that protein fragments containing the cilium-binding site remain associated with the cell surface whereas cleavage products not containing the R1 element are located elsewhere (Djordjevic *et al*., 2004).

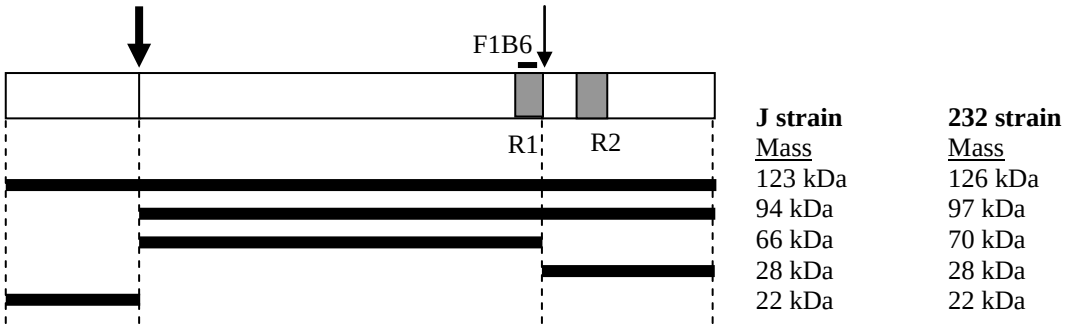

Fig. 1.5. Map of the cilium adhesin of *M. hyopneumoniae*. This map shows the antibody epitope location of F1B6 as a bar above the map. The major cleavage event at amino acid 195 (thick arrow) and another event at amino acid 891 (thin arrow) are shown. The locations of the R1 and R2 repeat regions are represented by grey-shaded boxes. The cleavage products of strains J and 232 are shown as bars below the map and their molecular masses are indicated on the right (adapted from Djordjevic *et al*., 2004).

Further analysis of the DNA sequences surrounding the P97 structural gene revealed that it is located in a two gene operon with an ORF coding for a 102.3 kDa protein (designated P102). Although Southern hybridisation data indicated that the P97 adhesin-encoding gene is present as a single copy in the *M. hyopneumoniae* chromosome, these studies indicated that P102 or P102-related sequences may exist in multiple copies in the genome of *M. hyopneumoniae* (Hsu *et al.*, 1997). Within the *M. hyopneumoniae* genome six paralogs of P97 and six of P102 were discovered. The P97 paralogs only show a small degree of homology to P97 at the DNA level and thus were unable to hybridise in Southern experiments but are more homologous at the amino acid level (>30% amino acid identity over 70% of their length; Minion *et al*., 2004). A database search of other bacterial genomes for genes homologous to *p102* revealed no significant match to any known sequence, including other bacterial adhesin genes. It was also found that P102 is expressed *in vivo* because convalescent swine sera recognised a clone containing only *P102* sequences (Hsu and Minion, 1998b). The function of P102 is not known, but the translated sequence shows a prominent transmembrane domain, suggesting that it may be a cell surface protein (Hsu and Minion, 1998b). A potential role for P102 in cilium adherence is speculative and requires further study, but accessory proteins are often found in multigene operons with adhesin structural genes in mycoplasmas (Hsu and Minion, 1998b) and other mycoplasma species have been shown to require more than one protein for adhesion, for example the terminal organelle of *M. pneumoniae*. Electron microscopy studies confirm P102 to be located exclusively on the surface of *M. hyopneumoniae* (Djordjevic *et al*., 2004).

Djordjevic *et al*. (2004) examined whether the protein, P102 like P97, undergoes proteolytic cleavage in *M. hyopneumoniae*. Results showed that cleavage of this molecule occurs at one or two sites generating a 42-kDa protein representing the C-terminal

cleavage fragment of P102. Further studies are required to confirm the identity of the remaining protein with a predicted molecular mass of 72-kDa.

1.7 Extracellular matrix components and bacterial interaction

The importance of microbial adhesion to epithelia in mucosa-associated infections has been recognised for many years. The discovery by Kuusela in 1978 that *Staphylococcus aureus* strains bind to the intricate network of macromolecules known as the extracellular matrix (ECM), and specifically the glycoprotein fibronectin launched a new and extensive field of research. Investigations have revealed how microorganisms (bacteria, parasites, fungi and viruses) interact with the ECM components and have highlighted the importance of these interactions in pathogenesis (Ljungh and Wadström, 1995).

Zhang and colleagues (Zhang *et al*., 1994b) established a microtiter plate adherence assay for *M. hyopneumoniae* using purified swine tracheal cilia. *M. hyopneumoniae* was found to bind specifically to plates coated with solubilized cilia. The ECM components and glycosaminoglycans dextran sulfate, heparin, chondroitin sulfate, laminin, mucin and fucoidan significantly inhibited the binding of the mycoplasmas in the assay and also disrupted the adherence of the mycoplasmas to intact ciliated cells. Pre-incubation with either mycoplasmas or cilia indicated that heparin, mucin, fucoidan and chondroitin sulfate interacted with the adhesive molecules on the surface of the mycoplasmas, while laminin blocked the receptors in cilia. The basis of the inhibition induced by dextran sulfate was unknown.

1.7.1 Host extracellular matrix (ECM)

Tissues are not solely made up of cells, a substantial part of the volume is extracellular space which is filled by the extracellular matrix (ECM). The ECM is composed of glycoproteins and glycosaminoglycans (GAGs) which form a network by means of a number of specific interactions between different ECM components. The composition of the ECM differs in various organs, but the dominating molecules are fibronectin, collagens type I to XV, laminin and GAGs such as, heparan sulfate, chondroitin sulfate and others (Kreis and Vale, 1993), see Fig. 1.6. Of these, type IV collagen, laminin and heparan sulfate are major constituents of basement membranes. Some constituents are found exclusively in the ECM, such as collagen and laminin. Others are part-time ECM molecules and also occur in soluble forms in body fluids, these include fibronectin, fibrinogen and vitronectin. The conformation of some ECM components, including fibronectin and vitronectin, differ significantly when the glycoprotein is immobilised in tissues or on surfaces, or appear in soluble form. Other ECM ligands such as heparan sulphate proteoglycans occur both in ECM forms and as intercalated cell membrane proteoglycans (Patti *et al*., 1994b). The ECM serves a structural function, but also profoundly affects eukaryotic cell adhesion, migration, differentiation and proliferation.

1.7.2 ECM components and bacterial interaction

Bacterial adherence requires bacterial surface components recognising and binding to host extracellular matrix and cell surface components. The cell surface adhesins of bacteria that specifically interact with extracellular matrix components can be designated as MSCRAMMs (microbial surface components recognizing adhesive matrix molecules) (Patti *et al*., 1994a).

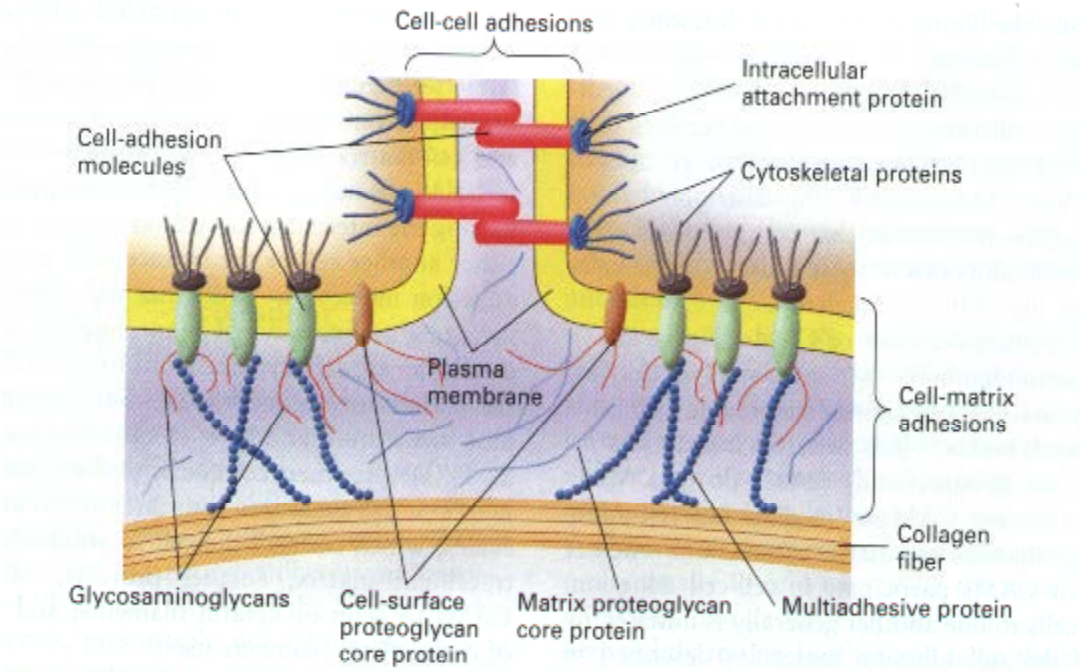

Fig. 1.6. Schematic overview of the types of molecules that bind cells to each other and to the extracellular matrix. Cell-adhesion molecules (CAMs) are integral membrane proteins. Some interact with similar molecules on other cells and, via intracellular attachment proteins, form anchors for cytoskeletal proteins. Other CAMs form connections with components of the extracellular matrix and also, via attachment proteins, with cytoskeletal proteins. Multiadhesive proteins bind to cell-surface receptor proteins and to other matrix components. Proteoglycans, consisting of a core protein, to which glycosaminoglycan chains are attached, also participate in adhesion of cells to one another and to the protein components of the matrix. Together, these interactions allow cells to adhere to one another, interconnect the cytoskeletons of adjacent cells, and give tissues their strength and resistance to shear forces (Lodish *et al*., 2000).

A single MSCRAMM can bind several ECM ligands. For example, the plasmid-encoded outer membrane protein YadA, which appears to be a collagen-binding MSCRAMM on enteropathogenic *Yersinia enterocolitica* and *Y. pseudotuberculosis* (Emödy *et al*., 1989), can also bind laminin and an isoform of fibronectin (Tertti *et al*., 1992). In addition, a microorganism can express several MSCRAMMs that recognize the same matrix molecule. For example, *Staphylococcus aureus* appears to express several fibrinogen-binding proteins (Bodén and Flock, 1989; McDevitt *et al*., 1994).

How does the ECM become exposed to bacteria? One obvious mechanism is trauma that would disrupt the skin or epithelial integrity. Also, viral and bacterial infections of mucosal surfaces cause exposure of the ECM through the action of proteolytic enzymes and toxins. The normal shedding of epithelia also exposes ECM components at the epithelial surface. Finally, pathogenic bacteria may gain access to various body fluids. Bacteria which are capable of binding ECM components may coat themselves with these components, thereby representing an important mechanism to evade the immune defence mechanisms (Höök *et al*., 1989).

Understanding the role of MSCRAMMs in pathogenesis and determining their potential as targets for antimicrobial therapy relies on knowledge of the ECM components with which they interact. The next part of this review focuses on some of the most important components of the ECM and some bacterial MSCRAMMs that interact with them.

1.7.3 Proteoglycans

The proteoglycans have a much higher ratio of polysaccharide to protein than do collagen, fibronectin, and similar glycoproteins in the ECM. The polysaccharide chains in proteoglycans are long repeating linear polymers of specific disaccharides called glycosaminoglycans (GAGs). Usually one sugar is uronic acid and the other is either N-acetylglucosamine or N-acetylgalactosamine (Lodish *et al*., 2000). Frequently some of the residues in a GAG chain are modified after synthesis; dermatan sulfate is formed from chondroitin sulfate, for instance. Similarly, heparin is formed only in mast cells, as a result of enzymatic addition of sulfate groups at specific sites in heparan sulfate (Fig. 1.7).

Proteoglycans can be found in the extracellular matrix as well as on the surface of many cells, particularly epithelial cells. A class of proteoglycans present in the basal lamina (syndecan) consists of a core protein to which are attached several heparan sulfate chains. Such proteoglycans bind to type IV collagen and other structural proteins, thereby imparting structure to the basal lamina (Lodish *et al*., 2000). The core protein of cell-surface proteoglycans spans the plasma membrane and contains a short cytosolic domain, as well as a long external domain to which a small number of heparan sulfate chains are attached. Some cell surface proteoglycans also contain chondroitin sulfate (Lodish *et al*., 2000).

(a) Hyaluron ($n \leq 50{,}000$)

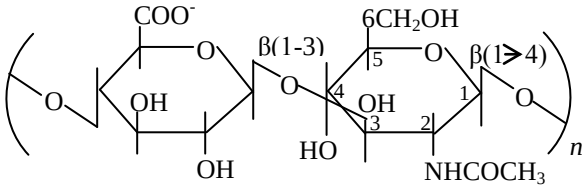

D-Glucuronic acid *N*-Acetyl-D-glucosamine

(b) Chondroitin sulfate ($n \leq 250$)

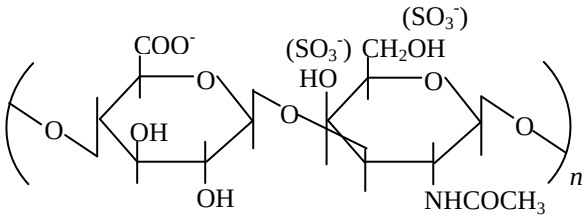

D-Glucuronic acid *N*-Acetyl-D-galactosamine

Dermatan sulfate

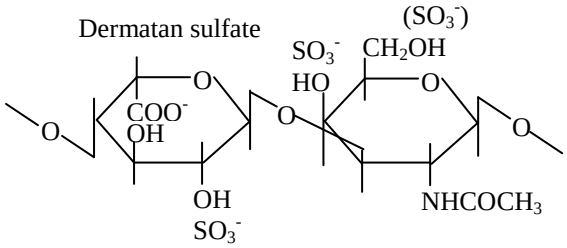

L-Iduronic acid *N*-Acetyl-D-galactosamine

(c) Heparin/Heparan sulfate (n = 15-30)

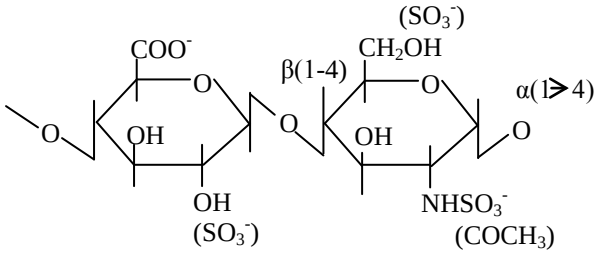

D-Glucuronic or L-Iduronic acid *N*-Acetyl- or *N*-sulfo-D-glucosamine

(d) Keratan sulfate (n =20-40)

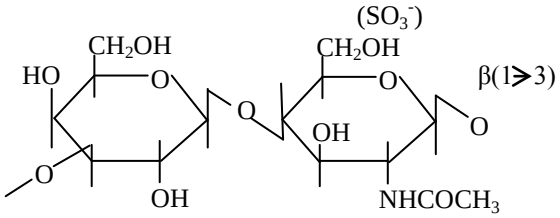

D-Galactose *N*-Acetyl-D-glucosamine

Fig. 1.7. Structure of various glycosaminoglycans, the polysaccharide components of proteoglycans. The number (*n*) of disaccharides typically found in each glycosaminoglycan chain is given (adapted from Lodish *et al*., 2000).

1.7.3.1 Heparin and heparan sulfate

Heparin is a highly sulfated polysaccharide that is similar in structure to heparan sulfate. Heparin is made up of repeating units of disaccharides containing a uronic acid residue (either D-glucuronic acid or L-iduronic acid) and D-glucosamine, which is either N-sulfated or N-acetylated. Heparin is an intracellular product found in the secretory granules of mast cells in complexes with basic proteases. Heparan sulfate (originally called "heparitin sulfate") on the other hand is produced by most animal cells and is structurally similar to heparin. It is less highly sulfated but contains all of the structural motifs found in heparin. Heparan sulfate, in contrast to heparin is normally secreted from cells. As a major component of the extracellular matrix, it is well positioned to play a prominent role in the physiology of the cell. Heparin and heparan sulphate are unique among the glycosaminoglycans in their ability to bind to a large number of different (primarily extracellular) proteins (Conrad, 1998). It is often convenient, because of the structural similarities between these two polymers, to refer to them together as "heparinoids".

A number of bacterial (*Chlamydia trachomatis, Helicobacter pylori, Neisseria gonorrhoeae*), viral (herpes simplex virus, cytomegalovirus, human immunodeficiency virus) and parasitic (*Leishmania donovani*, *Plasmodium* spp.) pathogens have been shown to express surface proteins that interact with specific glycoconjugates on cell surfaces (Rostand and Esko, 1997; Norkin, 1995). Many of these pathogens have evolved to use these cell surface glycolipids, glycoproteins and GAGs as receptor molecules for cell attachment, as well as eukaryotic cell invasion and intercellular migration processes (Wadström and Ljungh, 1999).

A novel strategy in microbial pathogenesis has been described which involves specific bacterial recruitment of glycosaminoglycans such as heparin, or related sulfated polysaccharides, which in turn serve as universal binding sites for a diverse array of mammalian heparin binding proteins, including adhesive glycoproteins (vitronectin and fibronectin), inflammatory and immunomodulatory intermediates, and fibroblast growth factor (Duensing *et al*., 1999). Adhesive proteins such as fibronectin and vitronectin have been implicated as intermediates in bacterial interactions with host cell integrin receptors, resulting in bacterial colonisation and invasion of epithelial cells (Ljungh *et al*., 1996). This process is utlilised by *Neisseria gonorrhoeae* where the OpaA adhesin binds proteoglycans, resulting in bacterial adherence, and vitronectin acts as a bridging molecule linking the Opa-proteoglycan complex and integrin receptors at the host cell surface, resulting in internalization of the bacteria by HEp-2 epithelial cells (Van Putten *et al*., 1998).

Studies of *Listeria monocytogenes*, *Helicobacter pylori* and *Neisseria gonorrhoeae* (Alvarez-Dominguez *et al*., 1997; Chen *et al*., 1995a,b; Chmiela *et al*., 1997) suggest that GAG-binding surface molecules confer resistance to phagocytosis. For example, treatment of *H. pylori* with heparin caused a decrease in phagocytosis by 55 to 70% (Dubreuil *et al*., 2002).

1.7.4 Laminin

After type IV collagen, laminin, a large multi-adhesive matrix protein, is the most prevalent constituent of all basal lamina. Laminin is important for the structure of the basement membrane by its formation of networks with type IV collagen, entactin/nidogen, and heparan sulfate proteoglycans such as perlecan (Yurchenco and

Schnittny, 1990) (Fig. 1.8). The laminin molecule is a 900-kDa glycoprotein consisting of multiple domains, arranged in an extended four-armed cruciform shape (Beck *et al.*, 1990) (Fig. 1.9). In addition to domains binding collagen and heparan sulfate in the basement membrane, other domains include a cell-signalling site with mitogenic action, a region involved in calcium-dependent aggregation, and a receptor-mediated cell attachment site (Beck *et al.*, 1990; Gehlsen *et al.*, 1988; Liotta *et al.*, 1986). Laminin is composed of three polypeptide chains: an A chain (400 kDa), a B1 chain (220 kDa), and a B2 chain (220 kDa) (Beck *et al.*, 1990; Timpl, 1989). A characteristic feature of the laminin molecule is its high carbohydrate content of 12 to 27%, most of which is present in complex-type oligosaccharides (Arumugham *et al.*, 1986; Fujiwara *et al.*, 1988; Knibbs *et al.*, 1989) which plays a role in cellular adhesion processes (Dean *et al.*, 1988; Dennis *et al.*, 1984; Zhou and Cummings, 1990).

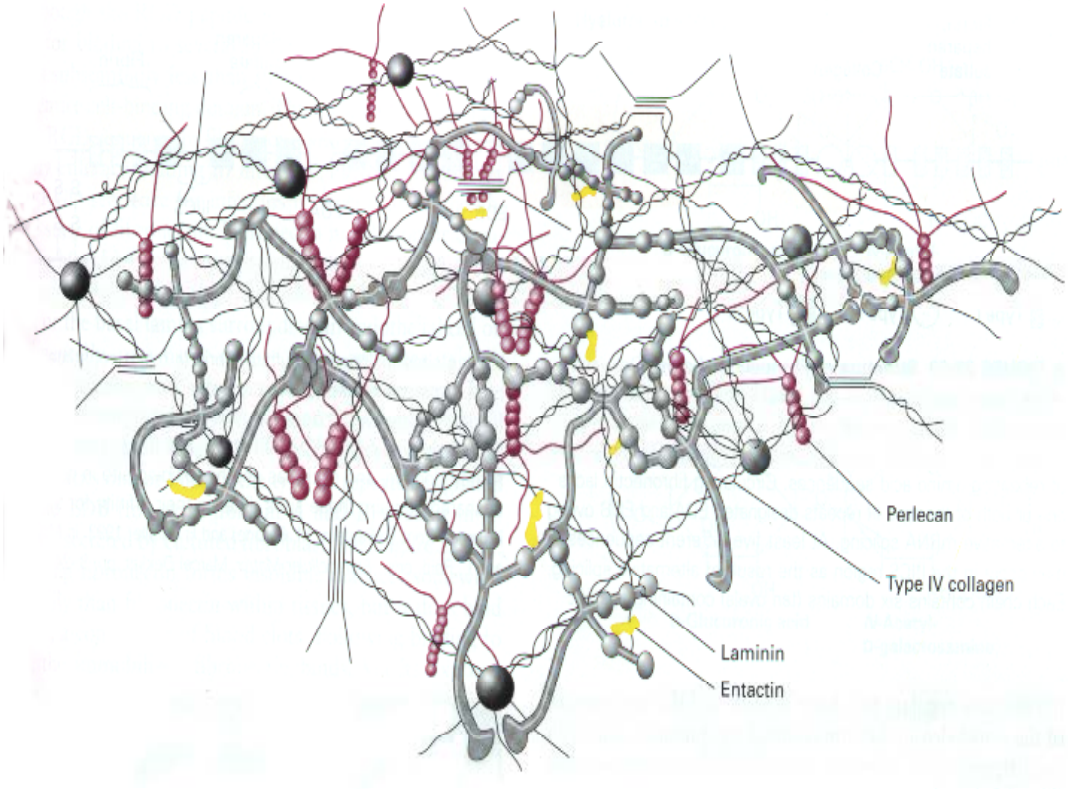

Fig. 1.8. Model of the basal lamina (Yurchenco and Schittny, 1990).

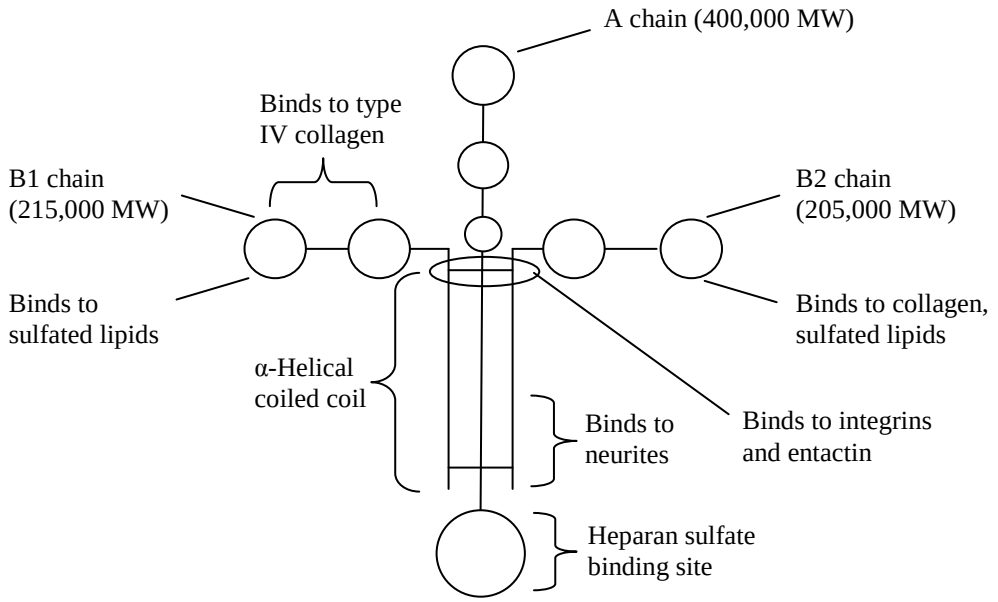

Fig. 1.9. Structure of laminin. The cross-shaped molecule contains globular domains and a coiled-coil region in which three chains are covalently linked via several disulphide bonds. Different regions of laminin bind to cell-surface receptors and various matrix components (adapted from Lodish *et al*., 2000).

H. pylori is the primary cause of active chronic gastritis and plays a pivotal role in the development of peptic ulcer disease (Blaser and Parsonnet, 1994; Graham *et al*., 1992; Marshall and Warren, 1984; Rauws and Tytgat, 1990; Warren and Marshall, 1983). The maintenance of the integrity of the gastric epithelium involves specific interaction of epithelial cell surface, integrins, with distinct extracellular matrix adhesive proteins, one of which is laminin (Gehlsen *et al*., 1988; Ruoslahti and Pierschbacher, 1987). *H. pylori*, particularly haemagglutinating strains, were earlier shown to bind the basement membrane protein laminin (Valkonen *et al*., 1993). Ljungh and colleagues (1996) suggest that laminin binding by *H. pylori* is unlikely to play a role in the initial adherence mechanisms. However, once adherent to gastric epithelium, laminin binding expressed by *H. pylori* lipopolysaccharide may inhibit the binding between laminin and its cell receptor on the gastric epithelium (Slomiany *et al*., 1991;Wadström *et al*., 1996).

1.7.5 Fibronectin

Fibronectin is a mammalian glycoprotein found in a soluble form (molecular mass, 550 kDa) in body fluid such as plasma as well as in an insoluble form in the interstitial connective tissues and extracellular matrices (Peterson *et al.*, 1989; Ruoslahti, 1988). Differences in structure between plasma and cellular fibronectin result partly from distinct splicing patterns of the fibronectin gene (Peterson *et al*., 1989; Schwarzbauer, 1991). Fibronectin serves diverse biological functions including cell to cell adhesion, spreading, and migration, tissue development and differentiation, blood clot stabilisation, and wound healing (Carson, 1989; Ruoslahti, 1988; Yamada, 1989).

Fibronectin is composed of repeating structural units, presented in two similar disulphide-linked subunits (Fig. 1.10) (Naito *et al.*, 2000). Fibronectin contains distinct binding sites for a variety of other extracellular molecules; including fibrin, heparin, and collagen, as well as for a number of cell surface integrins (Joh *et al.*, 1999; Naito *et al.*, 2000).

Many MSCRAMMs interacting with fibronectin have been characterised and fibronectin binding has been extensively studied over the past 30 years. The interaction of bacteria with fibronectin is believed to contribute significantly to the virulence of a number of microorganisms (Joh *et al.*, 1999). Fn-binding MSCRAMMs have been implicated in the pathogenic process of a number of infectious diseases such as urinary tract infections (Westerlund *et al*., 1991), pharingitis (Molinari *et al*., 1997) and infective endocarditis (Kuypers and Proctor, 1989).

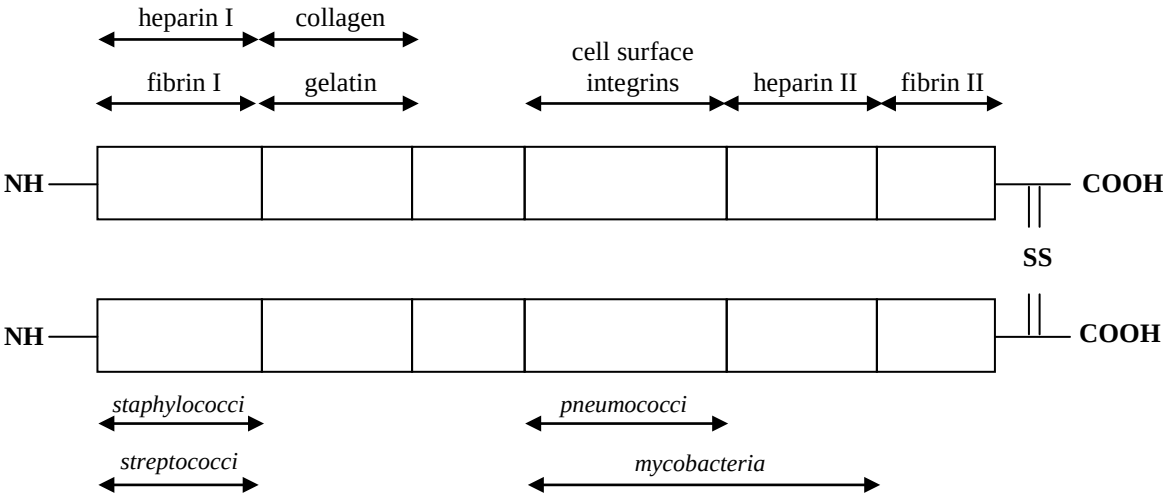

Fig. 1.10. Schematic representation of the domains of the fibronectin molecule. Fibronectin consists of two similar disulphide linked subunits. Functional domains that interact with heparin (I and II), fibrin (I and II), collagen, gelatin, and cell surface integrins are labelled above the respective domains. Binding to integrins is dependent on an Arg-Gly-Asp (RGD) sequence. Bacterial binding regions are indicated in italics (adapted from Naito *et al.*, 2000; van der Flier *et al.*, 1995).

Concentrating on two of the most studied interactions; fibronectin binding by *S. aureus* is mediated by two surface-exposed proteins with molecular weights of 110 kDa, designated FNBP-A and FNBP-B. The genes encoding these proteins have been cloned and sequenced (Jonsson *et al.*, 1991). The fibronectin binding region is found in a 38 amino acid repeated domain (D repeat region) located outside a segment rich in proline residues. Williams *et al*. (2002) identified a second binding region within the N-terminal part of FNBP-A and FNBP-B. The *S. pyogenes* fibronectin-binding protein SfbI interacts with fibronectin on nonphagocytic Hep-2 cells which triggers bacterial internalization, as discovered by coating inert latex beads with SfbI which were ingested by the eukaryotic cells (Molinari *et al*., 1997). *S. pyogenes* was also found to recruit collagen via surface-bound fibronectin through the SfbI protein which resulted in bacterial aggregation, colonization of collagen fibres and protection from adhering to human polymorphonuclear cells in the presence of opsonizing antibodies (Dinkla *et al*., 2003).

1.7.6 Collagen

Collagen is the major insoluble fibrous protein in the ECM and in connective tissue and is a major constituent of cartilage. In fact, collagen is the single most abundant protein in the animal kingdom. There are at least 16 types of collagen, but 80-90% of the collagen in the body consists of types I, II and III. Type IV is a major constituent of the basal lamina of the ECM. It was thought that all collagens were secreted by fibroblasts in connective tissue, but we now know that numerous epithelial cells make certain types of collagen. Staphylococci express surface antigens that bind collagen. The role of collagen binding by *S. aureus* in arthritis was elucidated using polystyrene beads coated with purified collagen binding protein (CNBP). Beads coated with CNBP adhered to cartilage whereas beads coated with FNBP did not (Switalski *et al*., 1993). Studies have shown that the collagen-binding MSCRAMM on *S. aureus* is both necessary and sufficient for the adhesion of these cells to cartilage (Patti *et al*., 1994b).

1.7.7 Interactions of bacteria with the ECM

Table 1.2 shows some bacterial species and the proteins at the site of tissue injury with which they interact. Both structural and adhesive components of the ECM are utilised in bacterial adherence. Just as an example, the capacity of *Streptococcus pyogenes* to invade host cells is thought to provide a mechanism whereby the organism can gain access to deep tissue and blood, providing at least partial protection from host defences and antibiotics (Cue *et al*., 1998) and it may be that the *S. pyogenes* binding to ECM proteins is what allows this microorganism to invade host cells. MSCRAMMs that act as adhesins and virulence determinants represent potential targets for the development of novel antimicrobial agents, including vaccines and adhesion blockers. In summary, the initial

studies of MSCRAMMs have revealed a family of microbial proteins that participate in host interactions in a sophisticated fashion.

Table 1.2. Some examples of bacterial species capable of binding proteins of the ECM.

Species	Host protein used for bacterial binding	Reference
Mycoplasma fermentans	Plasminogen	Yavlovich *et al*., 2001
Mycoplasma sp. bovine group 7	Plasminogen	Bower *et al*., 2003
Staphylococcus aureus	Fibronectin	Cho *et al*., 2001
	Fibrinogen	Cho *et al*., 2001
	Vitronectin	McGavin *et al*., 1993
	Collagens	Switalski *et al*., 1989
Yersinia enterocolitica	Collagens	Shultze-Koops *et al*., 1992
	Laminin	Flugel *et al*., 1994; Skurnik *et al*., 1994
	Fibronectin	Tertti *et al*., 1992
Enterococcus faecalis	Collagen I, IV	Xiao *et al*., 1998
	Laminin	Xiao *et al*., 1998
Pseudomonas aeruginosa	Laminin	de Bentzmann *et al*., 1996
	Collagen I, IV	de Bentzmann *et al*., 1996
Helicobacter pylori	Laminin	Trust *et al*., 1991; Valkonen *et al*., 1993; Valkonen *et al*., 1994
	Collagen IV	Trust *et al*., 1991
	Vitronectin	Ringner *et al*., 1992
Streptococcus pyogenes	Fibronectin	Courtney *et al*., 1994
	Fibrinogen	Katerov *et al*., 1998
	Laminin	Cue *et al*., 1998
	Plasminogen	Winram and Lottenberg, 1996
Neisseria meningitidis	Fibronectin	Eberhard *et al*., 1998
	Collagens I, III, V	Eberhard *et al*., 1998
	Plasminogen	Ullberg *et al*., 1992
Haemophilus influenzae	Fibronectin	Virkola *et al*., 1996
	Laminin	Virkola *et al*., 1996
	Collagen I, III	Virkola *et al*., 1996
	Plasminogen	Virkola *et al*., 1996
Haemophilus ducreyi	Fibronectin	Bauer and Spinola, 1999
	Collagens I, III	Bauer and Spinola, 1999
	Laminin	Bauer and Spinola, 1999
Treponema denticola	Fibronectin	Umemoto *et al*., 1993, Haapasalo *et al*., 1992
	Plasminogen	Fenno *et al*., 2000
	Laminin	Haapasalo *et al*., 1992
	Fibronectin	Haapasalo *et al*., 1992

Chapter 2: General Methods

This section contains methods that are common to more than one chapter of this thesis and the specific details of each experiment can be found in the proceeding chapters. A list of commonly used buffers and solutions and their ingredients can be found in Appendix A. A list of all extracellular matrix components and the kits used in this study can be found in Appendix B and C, respectively. The cell lines and bacterial strains can be found in Appendix D and maps of the vectors used for cloning in this project are given in Appendix E.

2.1 *M. hyopneumoniae in vitro* culture sample preparation

Cultures of *M. hyopneumoniae* were grown by inoculating modified Friis media (Appendix A) with a 1:50 volume inoculum of a previously grown culture (either from -80^{o}C storage or fresh). The culture was left rotating slowly at 37^{o}C until the pH in the media had changed to 6.9-7.2, resulting in a change of colour from orange to yellow (approximately 2-3 days). The cultures were then pelleted by centrifuging at 10,000 rpm for 30 min at 4°C in a Sorvall RC5C plus centrifuge (GSA rotor). The supernatant was discarded and the pellets resuspended in 2 ml of PBS. The volume was made up to 50 ml with PBS and samples were re-centrifuged as above. The supernatant was discarded and the pellets resuspended in 1 ml of PBS. The cells were transferred to pre-weighed sterile 2 ml microcentrifuge tubes and the bacteria pelleted by centrifugation using a benchtop centrifuge (Biofuge Pico, Heraeus) at 10,000 rpm for 10 min. The supernatant was removed and the weight of the bacterial pellet was determined and the pellet stored at -20°C.

2.2 Cloning

2.2.1 PCR amplification

The reaction mix for PCR consisted of 5 µl of 10X Taq buffer (Roche), 1.5 µl dNTPs (2.0 mM; Astral Scientific), 1 µl of each of the forward and reverse primers (20 pmol/µl; Sigma-Genosys), 0.2 µl Taq DNA Polymerase Enzyme (Roche), 2 µl (20 ng) of DNA and sterile MilliQ water up to a final volume of 50 µl. PCR reactions were carried out on either a PC-960G gradient thermal cycler or an FTS thermal cycler (Corbett Research). All PCR products were stored at -20^{o}C.

2.2.2 Agarose gel electrophoresis

For electrophoresis of PCR products or restriction enzyme digestion products a 1-2.5% agarose (w/v) gel was prepared in 0.5X TBE buffer. Gels were electrophoresed in 0.5X TBE Buffer (Appendix A) containing 2 µl (5 µg/ml) ethidium bromide. Approximately 2 µl of loading buffer (0.25% bromophenol blue, 15% ficoll) was added per 10 µl of sample. Electrophoresis was carried out at 100 V (constant voltage). GeneRuler™ 100 bp DNA Ladder Plus (1.5 µg; Progen) was used for sizing the resolved fragments. All gels were viewed under UV light and recorded using a GelDoc™ 1000 computer system (BioRad).

2.2.3 Restriction enzyme digestion

Restriction enzyme digestions were carried out for at least 2 h at 37^{o}C on a dry block heater (Thermoline) with the appropriate restriction enzymes according to the manufacturers' instructions. These digested products were then electrophoresed through agarose gels, to verify digestion or for gel extraction.

2.2.4 Ligation and transformation

Ligations were performed by adding appropriate amounts of the pQE-9 vector and PCR product or pPCR-Script plasmid which contains the insert that is to be ligated into pQE-9 (see appropriate chapter), in a total volume of 17 µl with MilliQ water and incubated at 65^{o}C for 1 min, 37^{o}C for 10 min, RT for 10 min and on ice for 10 min. Subsequently 2 µl of 10X T4 DNA Ligase Buffer (Roche) and 1 µl of T4 DNA Ligase (Roche) were added to the reaction mix and incubated overnight at 10^{o}C. A control with digested vector only was also included. The following day the ligation mix was transformed into either 300 µl of chemically competent ($CaCl_2$-treated) *E. coli* M15 (pREP4) cells (Appendix D) or electroporated into electro-competent *E. coli* M15 (pREP4) cells (Appendix D) using a BioRad Gene Pulsar and using the pre-set *E. coli* protocol at 2.5 kV. For chemical transformations the tubes containing cells and vector were left on ice for 30 min and then placed in a 37^{o}C incubator for 5 min and subsequently centrifuged at 14,000 rpm on a bench-top microcentrifuge (Biofuge Pico, Heraeus) for 1 min. The supernatant was discarded and the pellet resuspended in 0.5 ml of LB broth. The tubes were then incubated at 37^{o}C for 1 h with shaking at 150 rpm (Certomat® R, B-Braun). The cells were then plated on appropriate selective medium (LB with 25 µg/ml kanamycin and 100 µg/ml ampicillin) and incubated overnight at 37^{o}C. The electroporated cells were added to 1ml of LB media and incubated at 37^{o}C with shaking at 250 rpm for 1 h. The cells were then plated onto appropriate selective media and incubated overnight at 37^{o}C.

2.2.5 DNA sequence analysis of *M. hyopneumoniae* genes

The primers pQEF (5'-CGGATAACAATTTCACACAG-3') and pQER (5'-GTTCTGAGGTCATTACTGG-3') (Sigma-Genosys) were used to sequence *M. hyopneumoniae* genes inserted into the pQE-9 vector. Two PCR sequencing reaction

mixes containing 5 µl MilliQ water, 5 µl purified pQE-9 clone DNA, 8 µl DTCS Quickstart Master Mix (Beckman Coulter) and 3 µl pQEF or pQER primer (3.2 pmol/µl; Sigma-Genosys) were prepared. The cycle sequencing protocol for the reactions was as follows 96°C, 20 sec; 50°C, 20 sec; 60°C, 4 min (30 cycles) (FTS-960 Thermal Sequencer, Corbett Research). Sequencing reactions were stopped by addition of 5 µl of stop solution premix (Appendix A). Then, 60 µl of cold 95% (v/v) ethanol was added to the reaction mix which was centrifuged immediately at 14,000 rpm (Biofuge Pico, Heraeus) for 15 min at 4°C. The supernatant was removed and the pellet rinsed twice with 200 µl of 70% (v/v) ethanol, followed by centrifugation at 14,000 rpm for 5 min at 4°C. The pellets were resuspended in 40 µl of sample loading solution (Beckman Coulter) and the samples analysed using a CEQ8000 Genetic Analyser (Beckman Coulter).

2.2.6 Plasmid mini-preparations

Transformants were screened through small-scale plasmid preparations using a FlexiPrep™ Kit (Amersham Pharmacia Biotech). The method was as follows: a 3 ml overnight *E. coli* culture was transferred into a microcentrifuge tube and centrifuged at 13,000 rpm (Biofuge Pico, Heraeus) for 30 sec to pellet the cells. The supernatant was removed and the pellet resuspended in 200 µl of Solution I by vigorous vortexing. 200 µl of Solution II was added (mixed by inversion) followed by 200 µl of Solution III (mixed by inversion). The tube was centrifuged at 13,000 rpm (Biofuge Pico, Heraeus) for 5 min and the supernatant removed. 420 µl of isopropanol (0.7 volume) was added to the supernatant which was then vortexed and incubated for 10 min at RT. The sample was centrifuged at 13,000 rpm for 10 min to pellet plasmid DNA, after which 150 µl of Sephaglas FP slurry was added to the pellet, vortexed gently for 1 min and centrifuged at

13,000 rpm for 15 sec. The Sephaglas pellet was washed with 200 µl of Wash Buffer and centrifuged at 13,000 rpm for 15 sec (Biofuge Pico, Heraeus). A 300 µl aliquot of 70% ethanol was added to the pellet to resuspend it before centrifugation at 13,000 rpm for 15 sec. The supernatant was removed and the tube vortexed to disperse the pellet before air-drying for 10 min. Then, 50µl of sterile MilliQ water was added to the pellet to elute bound DNA, the tube vortexed and incubated for 10-30 min at RT (vortexing occasionally). Tubes were centrifuged at 13,000 rpm for 1 min and the supernatant transferred to a clean microcentrifuge tube. Plasmid preparations were analyzed using agarose gel electrophoresis and restriction enzyme analysis was performed which was subsequently analysed by agarose gel electrophoresis.

2.2.7 Plasmid DNA Extraction - Midi/Maxi Preparation

A culture of *E. coli* JM109 (pQE-9) was harvested and the plasmid extracted using a Midi/Maxi Prep Kit (Qiagen) as described below. Recombinant plasmids from positive clones were also extracted using this method. A 400 ml overnight culture was centrifuged at 6,000 g for 15 min in a Sorvall RC5C Plus centrifuge and the supernatant discarded. Kit buffers P1, P2, P3, QBT, QC and QF are shown in Appendix A. The bacterial pellet was resuspended in Buffer P1 (10 ml). Buffer P2 was added (10 ml), mixed gently by inversion and incubated at RT for 5 min. Buffer P3 (10 ml) was added and the solutions mixed immediately and incubated on ice for 20 min. The solution was centrifuged at 20,000 g (Sorvall RC5C Plus centrifuge) for 30 min and the supernatant promptly removed. The supernatant was then applied to a QIAGEN-tip 100 that had been equilibrated in Buffer QBT (10 ml). The column was washed with Buffer QC (35 ml) and DNA eluted with Buffer QF (14 ml). The DNA was precipitated with 0.7 volumes of isopropanol and pelleted by centrifugation at 15,000 g (Sorvall RC-5C Plus centrifuge)

for 30 min. The supernatant was removed and the plasmid DNA washed with 3 ml of 70% ethanol, centrifuged at 15,000 g (Sorvall RC-5C Plus centrifuge) for 10 min and the pellet allowed to air dry. The pellet was resuspended in 250 μL of TE Buffer. The resulting DNA was analysed by agarose gel electrophoresis.

2.3 Protein expression

100 ml *E. coli* cultures containing the pQE-9-based isopropyl-β-D-thiogalactopyranosidase (IPTG) inducible plasmids were grown to an optical density at 600 nm of 0.6 (measured with an Ultrospec 3300 Pro, Amersham) and induced with 0.1-1.0 mM IPTG (Roche) final concentration. 1 ml SDS-PAGE samples were taken at pre-induction, 1 h, 2 h, 4 h and overnight post-induction and centrifuged at 13,000 rpm (Biofuge Pico, Heraeus) for 2 min. Cell pellets were stored at –20^{o}C. These samples were analysed to determine the optimum IPTG concentration and induction times. Larger scale cultures (500-2000 ml, inoculated with a 5% starter culture) were then grown and induced for the optimal times.

2.4 Protein purification under denaturing conditions

After the cultures were induced for the optimal time the cells were harvested by centrifugation at 4,000 g and at 4^{o}C for 30 min (Sorvall RC5C Plus centrifuge). The pellet from a 250 ml culture was resuspended in 20-30 ml of urea buffer B (Appendix A) and rocked on ice for 30 min until cell lysis was complete. The lysate was centrifuged at 10,000 g for 30 min (Sorvall RC5C Plus centrifuge). The cleared lysate was removed and 10 ml of 50% Ni-NTA superflow resin (Qiagen) was added and the tube rocked at RT for 1 h. The lysate-resin mixture was loaded onto an empty column and the flow-through discarded. The columns were washed with 100 ml of urea buffer C (Appendix A), and

bound 6x His-tagged protein was eluted from the columns with 4 x 5 ml of urea buffer D (Appendix A) and 4 x 5 ml of urea buffer E (Appendix A). These volumes were altered to scale depending on the culture size. A 25 mm YM10 ultrafiltration membrane (Millipore) was equilibrated in MilliQ water. An ultrafiltration cell (Amicon) was assembled, and purified protein in urea buffer was ultrafiltered with sterile PBS to ensure removal of the urea from the sample and replacement with PBS and the initial volume was reduced to concentrate the protein samples.

2.5 Bradford assay to calculate protein concentration

Protein standards were made by dissolving BSA in sample buffer to give concentrations ranging from 0.2-1.0 mg/ml. Samples were routinely diluted 1:2, 1:5 and 1:10 in sample buffer to a final volume of 30 µl. A total volume of 20 µl of each standard and diluted sample were mixed with 1 ml of Bradford reagent (Appendix A) in a plastic cuvette. Cuvettes were incubated for 5 min at RT. The OD at a wavelength of 600 nm was determined for each standard and sample using an Ultraspec 3300 Pro spectrophotometer (Amersham Pharmacia). The spectrophotometer was set to generate a regression line and if that was linear then the OD measurement and concentration were determined for the test samples.

2.6 Generation of polyclonal antiserum in rabbits

A New Zealand White rabbit was injected subcutaneously with a mixture of purified protein in PBS and Freund's incomplete adjuvant (Sigma-Aldrich) with a total injection volume of 500 µl. Prior to immunisation, a sample of blood was taken and the serum collected, representing the pre-immune serum. A 500 µl booster injection was given

subcutaneously after 14-21 days. Marginal ear vein test bleeds were taken at 2 weeks post-immunisation, and blood left to clot overnight at 4°C. Clear serum was collected in microcentrifuge tubes and the remaining clot separated into quarters and centrifuged at 2,300 rpm (Beckman GS-6 centrifuge) for 10 min at RT. The red serum was collected in microcentrifuge tubes, and all tubes centrifuged at 5,300 rpm (Biofuge pico, Heraeus) for 5 min to pellet red blood cells. Antiserum was collected in fresh sterile microcentrifuge tubes and stored at –20°C.

2.7 One-Dimensional protein gel electrophoresis (SDS-PAGE)

Whole-cell extracts of bacterial cells and expressed proteins in PBS or PBS with 0.1% SDS were reduced in SDS-PAGE reducing solution (Appendix A) and boiled for 5 min. Proteins in urea buffer were combined with 5 µl of bromophenol blue loading dye (Appendix A) for every 25 µl of sample. Samples were loaded onto 12-15% acrylamide resolving gels (Appendix A) and electrophoresed with SDS-PAGE running buffer (Appendix A) in a Hoefer Scientific Mighty Small II electrophoresis unit at 20-30 mA (maximum voltage) for at least 1 h using the method described by Laemmli (1970). The stacking gel was discarded and the resolving gel stained in Gel Code Blue (Progen) or Coomassie (Appendix A) for at least 1 h, and de-stained with washes in MilliQ water or Coomassie de-stain solution (Appendix A).

2.8 Mass spectrometry analysis of proteins

SDS-PAGE gels were run as previously described and stained with colloidal Coomassie (Appendix A). The resulting protein bands of interest were then excised from the gel using a sterile scalpel blade and placed into 96-well V bottom trays (Greiner), analysed by mass spectrophotometry (courtesy of APAF) and resulting peptide fragment sizes were

analysed against the *M. hyopneumoniae* database for peptide matches. The method used is as described in Djordjevic *et al*. (2004). Briefly, the gel pieces in the tray were washed with 100 µl 50 mM ammonium bicarbonate-100% acetonitrile (60:40 v/v) by shaking at RT for 1 h, the buffer was then removed and the gel pieces dried in a vacuum desiccator for 90 min. Gel pieces were hydrated in 8 µl of 17 ng/µl sequencing-grade modified trypsin (Promega) for 1 h at 4^{o}C. Excess trypsin solution was removed, and the gel pieces were immersed in 25 µl of 50 mM ammonium bicarbonate and incubated overnight at 37^{o}C with gentle shaking. Eluted peptides were concentrated and desalted using C_{18} Zip-Tips (Millipore). The peptides were washed on a column with 10 µl of 5% formic acid. The bound peptides were eluted from the Zip-Tip in 0.8 µl matrix solution (10 mg of α–cyano-4-hydroxycinnamic acid [Sigma-Aldrich]/ml in 70% acetonitrile) directly onto the target plate. Matrix-assisted laser desorption ionization-time-of-flight (mass spectrometry) (MALDI-TOF [MS]) mass spectra were acquired using a Voyager DE-STR apparatus (PerSeptive Biosystems). The instrument was equipped with 337 nm nitrogen lasers and all spectra were obtained in reflectron-delayed extraction mode, averaging 256 laser shots per sample. Two-point internal calibration of spectra was performed on the basis of the use of internal porcine trypsin autolysis peptides (842.5 and 2211.10 $[M+H]^{+}$ ions). A list of monoisotopic peaks corresponding to the mass of generated tryptic peptides was used to search a modified translated version of the *M. hyopneumoniae* genome (Minion *et al*., 2004). Successful identification of proteins was made on the basis of the number of matching peptide masses and the percentage of sequence coverage afforded to those matches.

2.9 Western transfer and ligand/western blot

For specific and sensitive detection of proteins, western transfer and blotting techniques were performed using the method described by Burnette (1981). Proteins were

transferred from the polyacrylamide gels onto a polyvinylidene difluoride membrane (PVDF) in western transfer buffer (Appendix A) using a Hoefer Scientific TE Series Transphor Electrophoresis Unit. The membrane was cut to the size of the gel and the gel was western transferred onto the membrane at 268 mA and maximum volts for 1.5 h for 2-D gels and 20-30 V overnight for 1-D gels. After transfer the membrane was blocked overnight (16 h) for 2-D gels and for 1 h for 1-D gels at RT in 5% w/v skim milk in tris-saline, unless otherwise indicated. The blot was then incubated with ligand if needed for 1-1.5 h at RT with gentle agitation and then washed 3 x 10 min using 0.1% w/v skim milk in tris-saline, unless otherwise indicated. The primary antibody was then added and incubated for 1-1.5 h at RT with gentle agitation. The membrane was washed as above and incubated with the secondary antibody for 1 h at RT with gentle agitation. After 3 final washes, the membrane was equilibrated in 100 mM Tris, pH 7.6 for 5 min and developed in DAB (Appendix A) for up to 1 h. The membrane was rinsed in MilliQ water and air dried. The resulting blot was scanned using a BioRad scanning densitometer (GS-800).

2.10 ELISA

The basic protocol for an ELISA consisted of coating 100 µl total volume of proteins (5-10 µg/ml) overnight in carbonate coating buffer (Appendix A) onto wells of an ELISA plate (Linbro/Titretek; ICN Biochemicals). The plates were washed five times in an automated plate washer (SLT Lab instruments) with 0.05% v/v Tween20 in PBS (200 µl per well) patted dry and then blocked for 1 h by addition of 100 µl per well blocking solution (2% w/v skim milk in PBS). The plates were stored in the humidifying chamber at RT for 1 h. The plates were washed again as above and the ligands (if necessary, e.g. fibronectin, heparin, fibrinogen, laminin) were added to appropriate wells at varying

concentrations. Dilutions of the ligands were made in 1% w/v skim milk in PBS to generate varying concentrations. The plates were then incubated for 1.5 h in the humidifying chamber at RT. The plates were washed as above and 100 µl of primary antibody was added to the appropriate wells diluted in 1% w/v skim milk in PBS. The plates were incubated in the humidifying chamber at RT for 1.5 h. After this time the plates were washed as above and secondary antibody was added to the appropriate wells. The plates were incubated for 1 h in the humidifying chamber, then washed and developed by the addition of ABTS substrate (Appendix A). The substrate was added to each well (100 µl) and the plates were left shaking on an ELISA plate shaker (Heidolph Titramax 1000) and the absorbance values read at 414 nm after various time periods up to 1 h using a Multiskan Ascent ELISA plate reader (Thermo Labsystems). Controls were included throughout this assay to ensure that there was no false positive reactivity due to components of the detection system binding non-specifically to the ELISA plate. Controls ensuring the proteins were binding adequately to the plate were also included.

Chapter 3: P159 is an immunogenic surface antigen of *M. hyopneumoniae* that is proteolytically processed

3.1 Introduction

Current commercial vaccines against *M. hyopneumoniae* are limited in their effectiveness; they do not protect against colonization of the organism and herds are breaking with the disease. Since adherence to epithelial surfaces is the initial event in colonization and disease, a better understanding of the adherence mechanisms of *M. hyopneumoniae* will improve our chances of developing more effective vaccines.

Little is known concerning the adherence mechanisms of *M. hyopneumoniae*, but it is clear that this species adheres only to the cilia of the respiratory epithelium and not to other cells in the upper respiratory tract (Hsu and Minion, 1998b). This is in contrast to other mycoplasmal species that adhere to various cell types, including epithelial and tissue culture cells (Razin and Jacobs, 1992). Because of this binding specificity, *in vitro* models have relied upon swine ciliated cells or purified swine cilia (DeBey and Ross, 1994; Zhang *et al*., 1994b; Zielinski and Ross, 1993). These studies led to the identification of the ciliary adhesin P97. Although studies of this molecule represent an important first step in our understanding of the adherence mechanisms of *M. hyopneumoniae*, studies with other mycoplasmal pathogens indicate that adherence is a complex process involving multiple gene products (Layh-Schmitt *et al*., 2000; Papazisi *et al*., 2002). Adhesins of other mycoplasma species are found within multigene operons (Inamine *et al*., 1988; Reddy *et al*., 1995) and are present as multiple copies within the chromosome (Baseggio *et al*., 1996; Dallo and Baseman, 1991; Su *et al*., 1988).

Further analysis of the DNA sequences surrounding the *p97* structural gene revealed an operon composed of two ORFs, *p97* and one coding for a 102.3-kDa protein designated P102, the function of this protein is poorly understood. Further investigations into the genome sequence of *M. hyopneumoniae* by Minion and colleagues (Minion *et al*., 2004) identified several paralogs of the cilium adhesin *p97* residing in two-gene operons mostly with paralogs of *p102* and Fig. 3.1 below shows the structure of these gene families (Minion *et al*., 2004). One exception is a gene termed *p159*, which resides in a two gene operon with a paralog of *p97* (*p216*) but it has no significant homology to *p102* (see operon 1 in Fig. 3.1). As shown for the cilium adhesin P97 (Djordjevic *et al*., 2004), P159 also seems to undergo post-translational modification generating various sized products ranging from 27 to 110 kDa. This protein is therefore the focus of the following chapter. The post-translational modification of this protein, its localization in the *M. hyopneumoniae* cell, the P159 protein expression differences between a pathogenic (232) and a non-pathogenic (J) strain of *M. hyopneumoniae* and its ability to be recognised during an immunogenic response using sera from pigs that have naturally been infected with *M. hyopneumoniae* have been investigated.

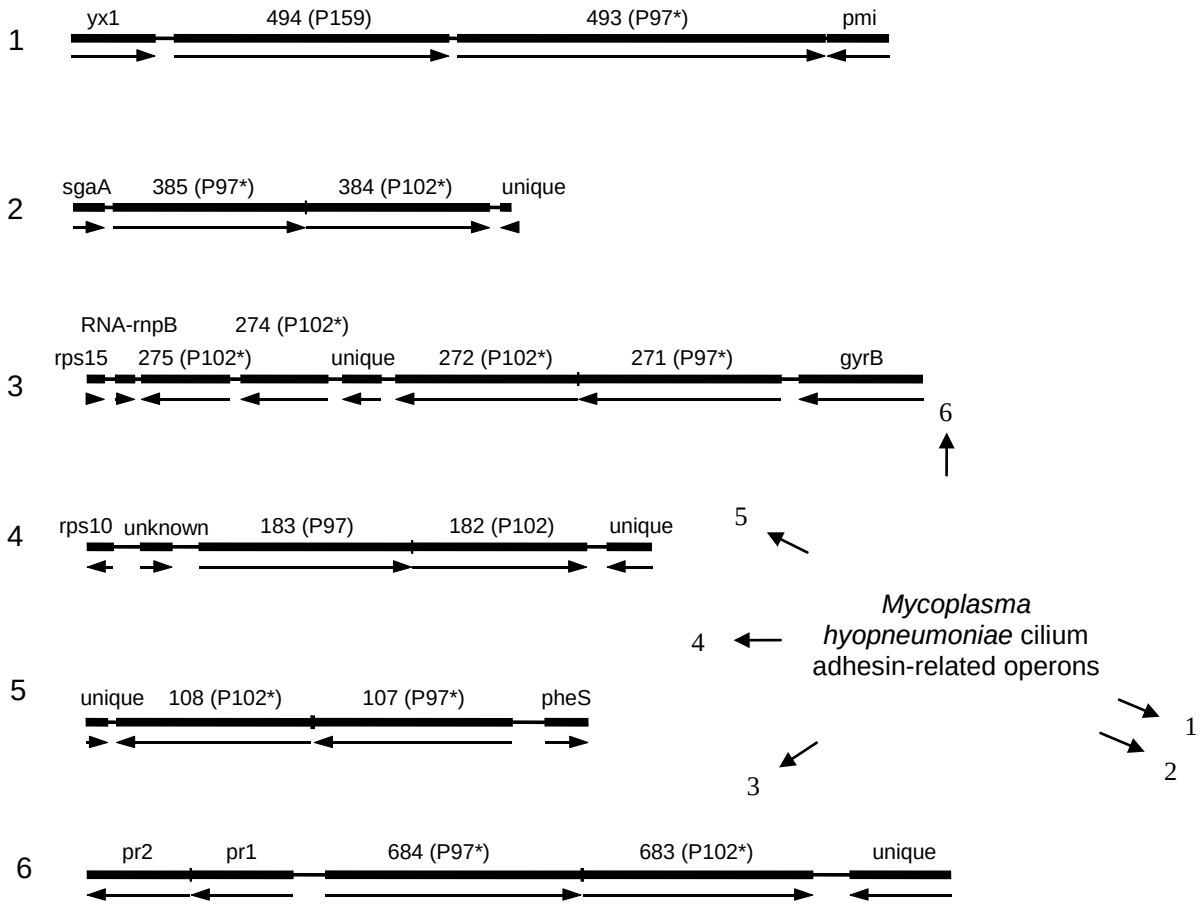

Fig. 3.1. Diagram of the *p97*/*p102* gene families in *M. hyopneumoniae* 232 strain. Number 4 is the *p97*/*p102* operon and others show the *p102* gene paralogs (P102*) in conjunction with *p97* gene paralogs. The diagram to the right shows their location in the genome of *M. hyopneumoniae* strain 232. Adapted from Minion *et al*., 2004.

Chapter 3: P159 is an immunogenic surface antigen of *M. hyopneumoniae* that is proteolytically processed

3.2 Methods

3.2.1 Detection of transmembrane domains in protein P159

Programs available through the Expert Protein Analysis System (Expasy) website (ca.expasy.org) were used to perform database searches and alignments. Sequences of P159 from strains 232 (GenBank accession number AF279292) and J (GenBank accession number AF279293) of *M. hyopneumoniae* were aligned using Eclustalw mutiple sequence analysis. Trans-membrane regions of the *M. hyopneumoniae* P159 protein sequence were predicted using the TMpred program located on the European Molecular Biology website (www.ch.embnet.org).

3.2.2 Proteomic analyses: 2-D gel electrophoresis

Two-dimensional gel electrophoresis (2-DGE) was carried out essentially as described by Cordwell and colleagues (Cordwell *et al.*, 1997). Dimension immobilized pH gradient (IPG) strips (Amersham Biosciences) were prepared for focusing by submersion in 2-DGE buffer (Appendix A) overnight. A *M. hyopneumoniae* bacterial pellet (strain 232) prepared as in 2.1 was resuspended in 1 ml lysis buffer (Appendix A) for each 0.1 g of bacterial pellet. The cells were disrupted with a Microson Ultrasonic sonicator (Misonix) for 6 x 30 sec and centrifuged at 50,000 g for 2 h at 15°C in an ultracentrifuge TL 100 (TLA 100.3 rotor, Beckman). The supernatant and pellet were both stored at -80°C. A total of 300-350 µg or 800 µg of *M. hyopneumoniae* protein extract was diluted with sample buffer to a volume of 100 µl for application to the anodic end of each re-hydrated

11 cm or 17 cm pH 3-10 first dimension IPG strip (BioRad), respectively, in an applicator cup using a horizontal Multiphor electrophoresis apparatus (Amersham Pharmacia). The IPG strip was then subjected to the electrophoresis protocol shown in Table 3.1 at 20^{o}C. Following electrophoresis the IPG strip was frozen at -80^{o}C until electrophoresis in the second dimension was performed. IPG strips were detergent exchanged, reduced, and alkylated in equilibration buffer (Appendix A) for 20 min prior to loading the IPG strip onto the top of a 8-18% 20cm by 20 cm polyacrylamide gel. Second-dimension electrophoresis was carried out at 5^{o}C using the electrophoretic conditions described in Table 3.2 and using a Multiphor horizontal electrophoresis unit. Gels were fixed in 40% methanol and 10% acetic acid for 1 h, then stained overnight in Sypro Ruby (Molecular Probes). Images were acquired using a Molecular Imager Fx apparatus (Bio-Rad). Gels were then stained in colloidal Coomassie (Appendix A). Selected proteins covering the entire proteome were excised and subjected to mass-spectrometry analysis as described in section 2.8.

Table 3.1. First dimension electrophoresis protocol for 11 cm or 17 cm IPG strips.

Phase	Volts	Current	Watts	Time (h)	
				11cm	17cm
1	150	1	5	0.01	0.01
2	150	1	5	0.5	0.5
3	300	1	5	0.01	0.01
4	300	1	5	5	6
5	3500	1	5	5	5
6	3500	1	5	10	37.40
Total				20.52	48.92

Table 3.2. Second dimension electrophoresis protocol.

Phase	Volts	Current	Watts	Time (h)
1	200	10	30	1.20
2	200	10	30	0.15
3	600	30	30	4

3.2.3 N-terminal sequencing of P159 cleavage products

N-terminal Edman sequencing was performed as described previously (Nouwens *et al*., 2000). The procedure was as follows; protein spots were excised from 2-D gels and the protein eluted overnight in 100 µl of buffer containing 100 mM sodium acetate (unbuffered), 0.1% SDS and 50 mM DTT at 37ºC with shaking. The eluant was removed and spotted onto a ProSorb Insert (PE Biosystems) membrane wetted with methanol. The protein was washed twice with 200 µl 0.1% (v/v) trifluoroacetic acid and allowed to dry. Edman sequencing was conducted on a Procise 494 protein sequencer (PE Biosystems) for five residues per protein to obtain an N-terminal tag.

3.2.4 PCR amplification of the *p159* gene of *M. hyopneumoniae*

Combinations of the various primers listed in Table 3.3 were used to PCR amplify fragments of the *p159* gene from *M. hyopneumoniae* strain 232 chromosomal DNA. The template for the amplification of *p159* sequences was Hyop 232p110 SDM c1 supplied by Steven Geary (University of Connecticut). This pPCR2.1 TA plasmid (Invitrogen) contained the entire open reading frame of *p159* which had all 9 mycoplasma tryptophan-encoding TGA codons modified to TGG by site-directed mutagenesis. This mutagenised pPCR2.1 plasmid was supplied in *E. coli* TOP_{10} cells and plasmid DNA was prepared

using a QIAGEN MidiPrep. kit as described in 2.2.7 and the DNA used in these PCR's. P159Ff and P159Rd were combined to amplify P159 fragment 1 (minus the signal peptide), P159Fb and P159Rb were combined to amplify P159 fragment 2, P159Fc and P159Rc were combined to amplify P159 fragment 3, P159Fd and P159Ra were combined to amplify P159 fragment 4, P159Ff and P159Ra were combined to amplify the whole P159 gene (minus the signal peptide), P159Ff and P159Re were combined to amplify P159 fragment 5 (N-terminal half of *pP159* minus the signal peptide), P159Fe and P159Ra were combined to amplify P159 fragment 6 (C-terminal half of *pP159*). *Sal*I and *Pst*I restriction enzyme sites incorporated into the forward and reverse primers respectively are underlined. An initial gradient PCR was setup to establish the optimal PCR conditions for each primer pair, as described in 2.2.1. The established conditions are listed in Table 3.4. The reaction mix was the same as outlined in section 2.2.1 although 4 µl dNTPs were used and 0.6µl Expand DNA Polymerase Enzyme (Boehringer Mannheim) was used instead of Taq.

For electrophoresis of PCR products, 1% agarose (w/v) gels were used as described in section 2.2.2. GeneRuler™ 100 bp DNA Ladder Plus (1.5 µg, Progen) or Hyper I DNA ladder (Bioline) were added for sizing the resolved fragments.

Table 3.3. Primer sequences used to amplify various fragments of the *p159* gene. The incorporated restriction enzyme sites are underlined.

Primer name	Sequence 5'-3'
P159Fa	GGGTCGACATGAAGAAACAAATTCGCAAC
P159Fb	GGGTCGACCAAACAAGTCAAAGCTCAGAA
P159Fc	GGGTCGACAAGACCTCAGAGGCAAGTAAT
P159Fd	GGGTCGACCACAAAATAACAACTTTCCAA
P159Fe	GGGTCGACTATAAATTAGAATTTGATCTT
P159Ff	GGGTCGACAATTCAGCGCTTAGATCC
P159Ra	GGCTGCAGTCAATATTGATCCATAAAGGC
P159Rb	GGCTGCAGTCATGGTGCTGTCTCTGGTGA
P159Rc	GGCTGCAGTCAATCTTTTTCTTGGTCATG
P159Rd	GGCTGCAGTCACCCTTTTTGATCTGTTGA
P159Re	GGCTGCAGTCATATTTGTCCGGCGTCAAT

Table 3.4. Reaction conditions of the various P159 primer combinations.

Primer pair	Amplified product	Reaction conditions x30 [a]
P159Ff + P159Rd	P159 fragment 1 - 699bp	92°C 30 sec, 60°C 30 sec, 68°C 2.5 min
P159Fb + P159Rb	P159 fragment 2 - 764bp	92°C 15 sec, 65°C 30 sec, 68°C 2 min
P159Fc + P159Rc	P159 fragment 3 - 1052bp	92°C 15 sec, 65°C 30 sec, 68°C 2 min
P159Fd + P159Ra	P159 fragment 4 - 1340bp	92°C 15 sec, 60°C 30 sec, 68°C 2 min
P159Ff + P159Ra	Whole P159 – 4125 bp	92°C 15 sec, 65°C 30 sec, 68°C 4 min
P159Ff + P159Re	P159 fragment 5 – 2043 bp	92°C 15 sec, 60°C 30 sec, 68°C 2.5 min
P159Fe + P159Ra	P159 fragment 6 – 2244 bp	92°C 15 sec, 57°C 30 sec, 68°C 2.5 min

[a] Note: Each PCR cycle began with an initial denaturation step at 92°C for 4 min followed at the end by a final extension at 68°C for 7 min.

3.2.5 Construction of a pQE9-based expression plasmid system for *M. hyopneumoniae* P159 proteins

3.2.5.1 Cloning into pPCR-Script plasmid

The PCR products for P159 fragments 1-4 obtained in 3.2.4 were cloned into the pPCR-Script Amp SK (+) Cloning Vector using pPCR-Script Cloning Kit (Stratgene). The PCR products were purified and polished to ensure blunt-ended products using the StrataPrep PCR Purification Kit available in the pPCR-Script Cloning Kit. A ligation reaction consisting of 4 µl of the blunt-ended PCR product, 1 µl 10X Reaction Buffer, 1 µl pPCR-Script Amp SK (+) cloning vector (10 ng/µl), 0.5 µl of 10 mM rATP, 1 µl of *Srf*I restriction enzyme (5 U/µl), 1 µl T4 DNA Ligase (4 U/µl) and 1.5 µl sterile MilliQ water was incubated at RT (25^{o}C) for 1 h. The ligation reaction was then heated for 10 min at 65^{o}C and stored on ice until ready for transformation or stored long term at -20^{o}C. An aliquot of 40 µl of XL10-Gold Kan ultra-competent cells was incubated with 1.6 µl of the XL10-Gold ß-mercaptoethanol mix provided with the kit for 10 min on ice to ensure highest transformation efficiency. Then 2 µl of each ligation mix was added directly to the cells, mixed gently and incubated on ice for 30 min. The reaction was heat shocked at 42^{o}C for 30 sec then placed on ice for 2 min. Then 450 µl of NZY^{+} media (Appendix A) was added to the reactions and incubated at 37^{o}C for 1 h shaking at 250 rpm, before plating on appropriate selective media and incubated at 37^{o}C overnight. Resulting white colonies containing recombinant plasmids were screened for the PCR product insert using a Flexiprep Kit (Amersham Biosciences) as described in section 2.2.6. DNA samples were digested overnight at 37^{o}C using *Pst*I and *Sal*I according to the manufacturer's instructions and analysed by agarose gel electrophoresis as described previously.

3.2.5.2 Cloning into pQE9 plasmid

A 400 ml culture of *E. coli* JM109 (containing the pQE9 plasmid) was harvested and extracted using a Maxi Prep Kit (Qiagen) exactly as described in section 2.2.7. The P159 fragments now cloned into pPCR-Script (section 3.2.5.1), and the pQE9 plasmid were digested overnight at 37^{o}C on a dry block heater (Thermoline) with restriction enzymes *Pst*I and *Sal*I according to the manufacturers instructions. The enzymes in the digestions were then heat-inactivated by heating at 80^{o}C for 20 min before ligation. The P159 fragments in pPCR-Script were cloned into pQE9 by incubating overnight digestions of each in different ratios (1:1, 5:3, 3:1) as described in section 2.2.4. The ligations were then electroporated into *E. coli* M15 (containing the plasmid pREP4) cells (Appendix D) using a BioRad Gene Pulser as described in 2.2.4. The electroporated cells were then placed into 1 ml of LB media and incubated at 37^{o}C shaking at 250 rpm for 1 h (Certomat® R, B-Braun). The cultures were than plated on appropriate selective media and incubated overnight at 37^{o}C. Recombinant plasmids were screened through colony blotting, for large screening.

3.2.5.3 Colony blotting for screening of recombinants

The PCR method was followed exactly as stated in section 3.2.4 with the following modification to produce DIG-labeled P159 fragments 1-4 only. The PCR DIG-labeling mix contained 2.0 mM each of dCTP, dGTP and dATP, along with 1.9 mM of dTTP and 0.1 mM DIG-dUTP (Roche). After the PCR, the DIG-labeled products were passed through a QIAquick PCR column to remove unincorporated PCR reagents, using the protocol supplied with the QIAquick PCR purification kit (Qiagen). Colonies from the transformation of 3.2.5.2 were picked and patched onto a nitrocellulose membrane (Hybond N^{+}) placed onto an LB agar plate (plus 100 µg/ml ampicillin and 25 µg/ml

kanamycin) and incubated overnight at 37°C. The colonies on the nitrocellulose were then lysed by treatment in denaturation solution (Appendix A) for 30 min, neutralisation solution (Appendix A) for 30 min, followed by 2X SSC (Appendix A) for 20 min. The membranes were then left to air dry and the DNA was bound to the nitrocellulose by baking at 80°C for 30 min. The membranes were then subjected to proteinase K treatment by adding a 2 mg/ml solution of Proteinase K to each membrane and incubating at 37°C for 1 h. The hybridization method used reagents from the Roche DIG wash and block buffer set. The membranes were placed in a hybridisation bottle with EasyHyb solution (Roche) and pre-hybridised at 58°C for 2 h in a Hybaid hybridisation oven. The probe (QIAquick cleaned up DIG-labeled PCR product from above) was denatured by heating to 100°C for 10 min. The pre-hybridisation solution was then replaced with hybridisation solution (5 µl denatured probe in 25 ml EasyHyb solution). Hybridisation was carried out at 65°C for 1.5 h and then at 42°C overnight with the same solution. The next day the hybridisation solution was removed and stored at -20°C for possible re-use. The membranes were washed 2 x 15 min at RT (25°C) with 2X SSC/0.1% SDS and then 2 x 15 min at 68°C with 0.5X SSC/0.1% SDS. The membranes were equilibrated for 1 min at RT with wash buffer (2X SSC/0.1% SDS) after which they were blocked with blocking solution (made up in 1X maleic acid, from kit) at RT for 80 min. The anti-DIG-AP (antibody; 1:10,000 dilution, Roche) was added to the membranes and incubated at RT for 30 min. The membranes were finally washed at RT for 2 x 15 min with wash buffer before transferring to a plastic bag for detection. Detection buffer (5 ml; Roche) was added to the membranes and then 50 µl CSPD chemiluminescent substrate [Disodium 3-(4-metho xyspiro {1,2-dioxetane-3,2-(5-chloro)tricyclo [3.3.1.1^{3},7]decan}-4-yl)phenyl phosphate] was added and the membranes kept in the dark. The bag was sealed and placed in an x-ray cassette against autoradiography film (Hyperfilm MP) in the dark. Exposure was carried out for varying times from 5 min to 2 h to obtain the most

information from the blot. Each film was then developed with Kodak developer for 2-5 min, placed in water (stop solution) for 1 min and fixed (Kodak fixer) for 2-3 min. Recombinant plasmids that hybridised to the DIG-labelled probes were then screened to confirm the presence of the *p159* fragment insert using the Flexiprep. Kit (Amersham Biosciences) as described in 2.2.6 for plasmid DNA extraction, followed by digestion overnight and analysis by agarose gel electrophoresis. A 100 ml culture of *E. coli* M15 (pREP4 pQE9) was harvested and extracted using a Midi Prep Kit (Qiagen) essentially as described in 2.2.7.

3.2.5.4 DNA sequencing of the *M. hyopneumoniae p159* fragment gene inserts

The primers pQEF (5'-CGGATAACAATTTCACACAG-3') and pQER (5'-GTTCTGAGGTCATTACTGG-3') were used to sequence the *M. hyopneumoniae* P159 fragment gene inserts in the pQE9 vector as described in 2.2.5.

3.2.6 Expression of P159 protein fragments

A 200 ml culture containing each *E. coli* M15 (pREP4 pQE9) was grown to an optical density at 600nm of 0.6 and induced with 0.1 mM IPTG final concentration. Based on the samples from the test induction (see 2.3), the cultures were left for 1 h, 2 h or 4 h and then centrifuged at 6,000 rpm at 4^{o}C for 30 min (Sorvall RC5C Plus) and stored at –20^{o}C overnight. Purification was carried out as described in section 2.4. Whole-cell extracts of *E. coli* M15 (pREP4 pQE9) were prepared by resuspending cells in SDS-PAGE cracking buffer (Appendix A) and boiling for 5 min. 5 µl of bromophenol blue loading dye (Appendix A) was combined with 25 µl of eluted P159 protein fragments from the purification. Samples were loaded onto either 10% or 12% acrylamide resolving gels (Appendix A) and electrophoresed with SDS-PAGE Running Buffer as outlined in 2.7.

Mass spectrometry was carried out on the purification products as shown in section 2.8 to confirm the integrity of the cloning process. 10ml of purified P159 protein fragments from section 3.2.6 were ultrafiltered with sterile PBS (see 2.4) to a final volume of approximately 3 ml. P159 fragment 4 was unstable in PBS alone and therefore was ultrafiltered with PBS containing 0.1% SDS.

3.2.7 Generation of polyclonal antiserum in rabbits

A New Zealand White rabbit was injected subcutaneously with each P159 protein fragment in Freund's incomplete adjuvant (Sigma-Aldrich) as described in 2.6. P159 proteins were loaded onto 12% acrylamide gels as outlined in 2.7 and western transferred from the polyacrylamide gels onto a polyvinylidene difluoride membrane (PVDF) by electrophoresis with western transfer buffer and blotted as in section 2.9. The membrane was then incubated with primary antibody (pre-immune sera diluted 1:200, or anti-P159 fragments rabbit sera diluted 1:250-1:500. Sheep anti-rabbit HRP conjugated secondary antibody (Silenus) was used at a dilution of 1:1000.

3.2.8 Growth time-course assay for detecting P159 expression

This assay was conducted to see the expression levels of P159 during the entire growth cycle of *M. hyopneumoniae* by taking whole cell samples of a culture during the entire growth cycle and immunoblotting the protein profiles with antisera for the proteins to be detected. Numerous tubes with 6 ml of *M. hyopneumoniae* medium were inoculated with a viable culture of *M. hyopneumoniae* strain J and another with strain 232. These tubes were then left slowly rolling at 37^{o}C. Over various times up until 72 h post-inoculation the tubes were removed, the optical densities of each sample were determined at 560 nm using an Ultraspec 3300 Pro spectrophotometer (Amersham Pharmacia) and then the

samples were centrifuged at 13,000 rpm (Biofuge Pico, Heraeus) for 6 min. The pellets were washed twice with PBS and then resuspended in 1 ml of PBS. These samples were then separated using reducing 15% SDS-PAGE gels and subsequently western blotted as described previously.

3.2.9 Determining cellular location of P159

3.2.9.1 Trypsin treatment of *M. hyopneumoniae*

Cells of *M. hyopneumoniae* strains 232 and J from 250 ml cultures were harvested by centrifugation at 9,000 rpm (Sorvall, GSA rotor) for 30 min. The pellets were gently washed in 50 ml PBS and re-centrifuged as above. The pellets were then gently resuspended in 5 ml PBS and frozen until subjected to trypsin treatment. The OD of the cells was determined so that a comparative number of cells were subjected to the treatment. A total of 0.5 ml of cells for each strain was aliquoted into 10 separate microcentrifuge tubes and warmed to 37^{o}C in a dry block heater. Dilutions of trypsin were prepared in PBS ranging from 0, 0.1, 0.5, 1.0, 3.0, 5.0, 10.0, 50 and 150 µg/ml and were warmed to 37^{o}C. A volume of 0.5 ml of pre-warmed trypsin was mixed with the cells and incubated at 37^{o}C for 15 min. Finally 100 µl of reducing solution was added to the samples and they were boiled for 5 min before being subjected to reducing SDS-PAGE as described in 2.7. The lane loadings were optimised for western analysis and consisted of loading 17µl of the 232 strain samples and 25µl of the J strain samples onto reducing 12% SDS-PAGE gels and western transfer onto PVDF at 20 V overnight. The membranes were blocked in 5% skim milk and reacted with a pool of rabbit sera from the four P159 recombinant fragments or rpL7/L12 antisera (see Chapter 5), all at 1:100 for 1.5 h. After subsequent washing the membranes were incubated with sheep anti-rabbit

HRP-conjugated antibodies for 1 h. The membranes were equilibrated and developed in a DAB solution.

3.2.9.2 Immuno-electron microscopy of intact *M. hyopneumoniae*

Immunogold labelling of whole *M. hyopneumoniae* cells was performed as follows: Parlodion/carbon coated 300 mesh nickel grids (Pro. Sci. Tech.) were floated on drops of a fresh *M. hyopneumoniae* (strain 232) suspension in a moist petridish for 2 min. The grids were floated on drops of undiluted anti-P159 sera, pre-immune for control and post-immune for tests, and incubated at 37^{o}C for 90 min. The grids were washed with phosphate buffer (pH 6.8) 3 x 5 min and then floated on drops of protein A gold (15 nm, BBInternational) diluted 1:50 for 45 min. The grids were washed with phosphate buffer and distilled water and stained with 2% aqueous uranyl acetate (Merck). The grids were blotted dry and examined under a Phillips 208 transmission electron microscope.

3.2.10 Triton X-114 extraction of *M. hyopneumoniae* for 2-DGE

A 250mL *Mycoplasma* sp. culture was prepared as outlined in 2.1. A triton solution of 1% triton X-114 (Appendix A) was added at approximately 1 ml per 0.1 g of bacterial pellet. The bacterial pellet was completely resuspended in the triton solution and then left shaking overnight at 4°C. The samples were then centrifuged at 15,000 rpm (Biofuge Pico, Heraeus) for 15 min at 4°C. The supernatant was removed and the pellet (insoluble prep.) frozen at -20°C. The supernatant was heated at 37°C for 10 min on a dry cell heating block (Thermoline) to induce condensation of TX-114 then centrifuged at 13,000 rpm (Biofuge Pico, Heraeus) for 5 min at RT. After this centrifugation two phases are produced; an aqueous (top) phase and a detergent (bottom) phase. The aqueous phase was removed to a new microcentrifuge tube upon which neat triton X-114 was added to give a

1% solution (approximately 20 µl). The detergent phase had 1 ml of the 1% triton solution added. Both microcentrifuge tubes were then left shaking at 37°C for at least 3 h. The microcentrifuge tubes were then heated again at 37°C for 10 min on a dry cell heating block (Thermoline) and centrifuged as stated above to generate the two phases. The top aqueous phases from both tubes were pooled as were the bottom detergent phases for both.

A 10X volume of cold 100% acetone was added to each preparation (aqueous and detergent), mixed and then left at –20°C overnight. The tubes were then centrifuged at 13,000 rpm in a Sorvall SS-34 rotor at 4°C for 30 min. The supernatant was removed and the centrifuge tubes containing the pellet were dried in a vacuum desiccator for approximately 1 h or until completely dry and free of acetone.

The pellet of the aqueous phase was resuspended in SSS (standard solubilisation solution, Appendix A) at a volume of approximately 1 ml per 0.25 g initial bacterial pellet weight. The pellet of the detergent phase was resuspended in MSS (multiple surfactant solution, Appendix A) at a volume half that of the aqueous phase sample (1 ml per 0.5 g initial bacterial pellet weight). The tubes were left to stand at RT for 30 min to help resuspend the pellets. The suspensions were aliquoted into microcentrifuge tubes and subjected to sonication for Mycoplasma cell disruption for 4 x 90 sec cycles. After this the samples were centrifuged at 13,000 rpm for 15 min at RT on a bench top microcentrifuge (Biofuge Pico, Heraeus). The supernatant was transferred to a new microcentrifuge tube and the pellet and supernatant were frozen at -80°C. These samples were subsequently analysed by 2-DGE as outlined in 3.2.2. Duplicate gels were subjected to western transfer and blotted with anti-P159 rabbit sera as outlined in section 2.9.

3.2.11 Convalescent pig sera ELISA

This assay followed the method outlined in section 2.10 and was as follows: wells were coated with 5 μg of recombinant P159 proteins in PBS or PBS with 0.1% SDS (from section 3.2.6). A total of 16 different pig sera were chosen from a collection held at EMAI. Sera from pigs that had been subjected for *M. hyopneumoniae* testing using the *M. hyopneumoniae* ELISA diagnostic test used at EMAI were chosen. Pigs with various ELISA ratios (which indicate a positive or negative reaction, Djordjevic *et al*., 1994), ranging from 0-3 (negative), 5-10, 10-15 and 15 or above were used. These sera were diluted 1:100 with 1% w/v skim milk in PBS after which 100 μl of each were added to the wells of an ELISA plate. Goat anti-swine HRP conjugated antibody (Silenus) diluted 1:1000 in 1% w/v skim milk in PBS was then added to the ELISA plate. The plate was then developed in ABTS, and readings taken over various times up to 1 h.

Chapter 3: P159 is an immunogenic surface antigen of *M. hyopneumoniae* that is proteolytically processed

3.3 Results

3.3.1 P159 possesses a transmembrane domain

The *p159* gene contains 4230 nucleotides coding for a protein 1410 amino acids long with a predicted molecular mass of 158.67 kDa and pI 8.50. A search of protein databases with BlastP found no significant matches for P159, indicating that this is a novel protein. Using the TMpred program (EMBnet website; www.ch.embnet.org/software/TMPRED_form.html), a transmembrane domain was found at the N-terminus of P159 (Fig. 3.2) with the sequence ^{9}AIIVLAGLSFIGTAGVGLAV^{29}. The scores for an inside (cytoplasmic) to outside (luminal) and outside to inside transmembrane helix were 2150 and 2028, respectively. These values are significantly higher than the statistically significant cut-off value of 500, with an inside to outside helix being the preferred conformation. This data suggests that the N-terminus of P159 is located inside the cell while the C-terminus is exposed on the outside of the cell membrane in *M. hyopneumoniae*.

3.3.2 Proteomic analysis of P159 expression in *M. hyopneumoniae*

Initial proteomic analysis of *M. hyopneumoniae* strain 232 whole cell extracts identified three protein spots (P27, P52 and P110) with apparent molecular masses of 27, 52 and 110 kDa (Fig. 3.3A) that represented different fragments of P159 spanning the entire molecule (Fig. 3.3B; GenBank accession number AF279292). Fragments were identified on the basis of molecular weight and peptide mass fingerprint. The N-terminal sequence of P27 (MKKQIRN) mapped to amino acids 1 to 7 in the N terminus of P159. TMpred

predicts that this N-terminus contains the transmembrane domain (amino acids 1-29); this transmembrane domain is not cleaved during *in vitro* expression. The peptide matches of P27 from MALDI-TOF (MS) covered amino acids 36-219 of the P159 sequence (Fig. 3.3B). N-terminal sequencing of P110 and P52 were unsuccessful (data not shown), however, the peptide matches for P110 spanned amino acids 303-841 while the peptide matches for P52 covered amino acids 978-1387 (Fig. 3.3B). Therefore a cleavage event appears to have occurred between amino acids 220-302 and 842-977. P110 is the largest P159 product found in the proteome of *M. hyopneumoniae* with an apparent molecular weight of 110 kDa (based on the 2-DGE size markers). The peptide matches spanned an area representing approximately 61 kDa of the P159 protein however, as the exact cleavage site of P110 is unknown the product could be as large as 85 kDa. This indicates that this protein may migrate aberrantly during SDS-PAGE. The full-length P159 product is not seen in 2-D gels and perhaps it is not present in any significant amount *in vivo*. Protein fragments will henceforth be referred to by their apparent molecular weights (P27, P52 and P110) while the full-length molecule will be referred to as P159 (Fig. 3.3C).

3.3.3 Cloning and expression of different regions of P159 within *E. coli*

Upon analysis of the above data, which showed production of various P159 products by *M. hyopneumoniae*, we set out to clone and over-express four fragments of P159 (Fig. 3.3C) representing the length of the *p159* gene product (AF279292). Expression of large AT rich genes in *Escherichia coli* has proven difficult in the past so the P110 fragment was cloned in two halves (F2 and F3). Attempts to clone the entire *p159* gene into *E. coli* were unsuccessful; however, recombinant expression and Nickel-NTA agarose affinity chromatography of the four P159 fragments was achieved (fragment 1 [F1], amino acids

31-264; fragment 2 [F2], 265-519; fragment 3 [F3], 558-909; and fragment 4 [F4], 958-1405). All clones generated in this study were DNA sequenced to confirm the integrity of the constructs. Purified recombinant proteins were subjected to MALDI-TOF mass-spectrometry and their identities as P159 fragments confirmed (results not shown).

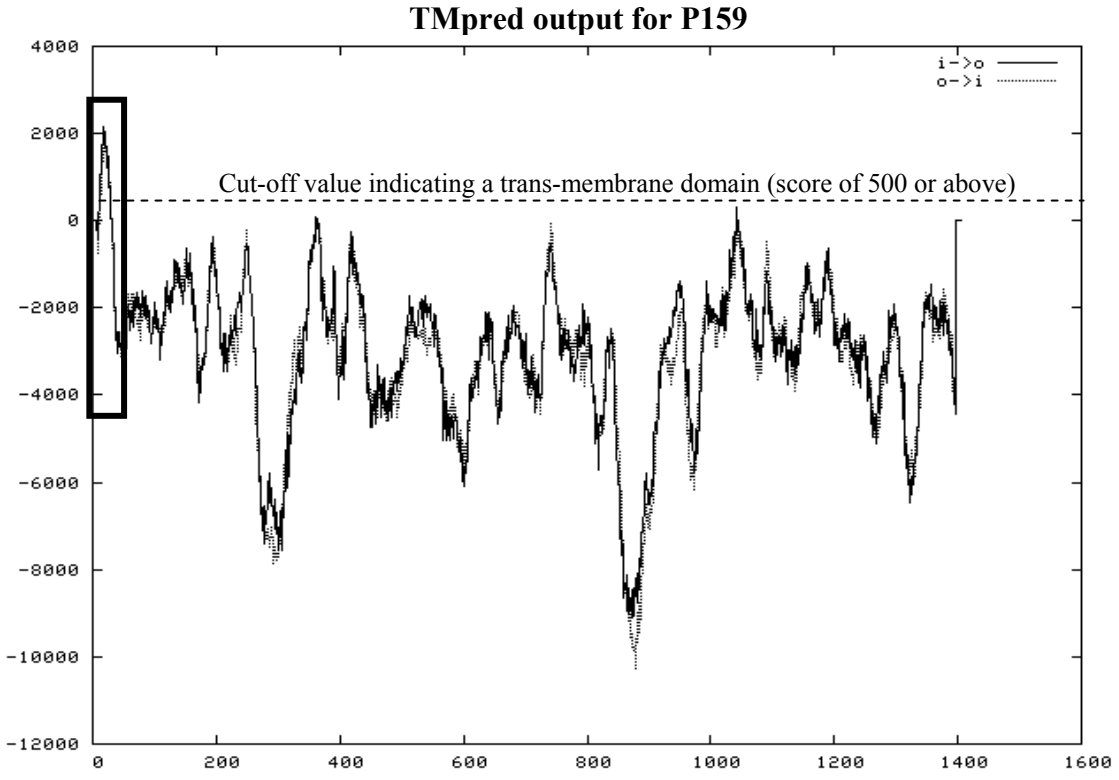

Fig. 3.2. TMpred output for P159. The boxed area shows the potential trans-membrane domain in P159, located at the N-terminus of the protein. This trans-membrane domain scored 2150 and 2028 in TMpred, showing that it is a significant trans-membrane domain as it scored well above the 500 cut-off value (broken line).

A

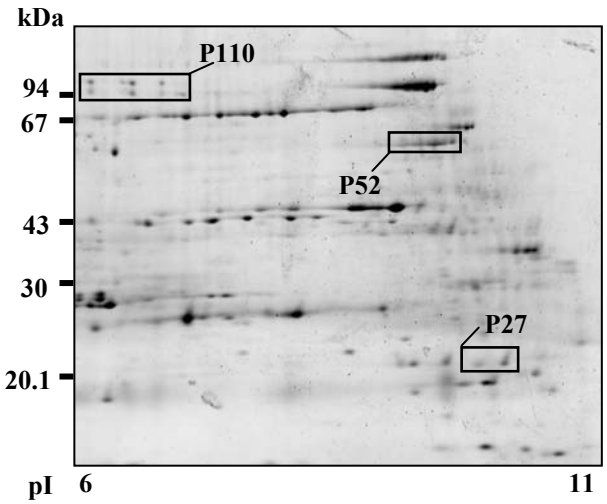

B

MKKQIRNKAIIVLAGLSFIGITAGVGLAVQNSALRSSYLNQFKNDKSATELLSPINDTELSKIISNFSLKE
NWSKISAGQAFELHKNPLYAFKLTDAIDFSKIDKKFAHLFFNVQVNDNTKVEGNSIRNLTVFVFDAITKKE
VATRAFHTSLSGFSSVAKEDFIENFVAESSTYELDKDQLKKNFATEIVLPSAFSIKFQDVLLTHLRKTSPE
SFQETKTIQVRALTNSITEFQQQQQEGGSGGSGTSGGSSGGSSSGSTDQKGQTSQSSEKESKSEKEKGKDQ
QSTQGSEQKQDQKQQKPKEAEKPAQEKPAQEKPAETPKVKAPVIEPVKKLVFENEKLNQALLETLKDFGGL
KLLAASGLQGLLPNEYTLLPVSSDKSLIKLDIDDQAGTASIHLKLLDKNKKEKNLILPINGLASIGAIKDK
VFSQIFRNQNAYLTIRPQINEYLRKNPRKKIQEVIWSFSREKFDQLRGQNEVEKFLEELYNPTQTSQSPQK
SKSSDSAKNNVATIQASPETAPKTTTTNSNTQSSSTSTNNQSSNGSQQMASPQTESSLSTAKTSEASNSSE
ESSSETKGTKEQANSETNPMGKSQAKPEAKPEEKQINLEDQAKTELKEILKIHGWNYRTLLKDQNQKVILP
DNINFWFDLRNKRSSYENYKLEFDLVKKTGQIQAGDVIDANKIRLNLKISPLANLKLEVDSKNKQYIDAGQ
IGDYVEFDKQGKKLVEQGKSLDLKVGASAANSIFSPEIRYSAYELKGWTYPIDIDIKGNPIQQELEKLVGN
FHKVGINKNNQYQIYSTDIDKIFAQAKLDKYFELSQEEKQASKKYLQEKLNPISEITIVKLPPKEEVLPPL
EEEKKPEQDQKAQEKQEDKQNQKQQEKQEDKKEQDQQKHSQSPDQKTETQTHDQEKDKQTSSETSPSNTNE
SSGTQNTAQNSQTNQANSGQGQSQQAASSSTSYQTHKITTFQDDQKDQTNEQTEKEIEPEKLAFGDYLVKY
LDIFETFKVGPDQKLSIGRWYNAPQRTYNVIFRVLDKENIQVAASLFQLHGISATNIALEKSLRYAPDIFL
DGTSGLEYKQDTGDKPYLQGRQFVSAINSINNTKSSYRVHKLFDNLPLSEESSQGLRLKSSLVYDYQKNDP
YTFQASKEALRKTALTKGVLYLAFKPEQILGIKGSKTAPGRNYKLLSTTNVHFKSLYGLSNLELVKTKYQE
NLKLVWKLIGAKPVNDDKILPPQVADLPRHRSTEIILLEDSKPGASSSPQTKENSQNKEAETFNLDIRQTK
PNQIEPLEHYLGQTWLMEIRIDDESATITIIPEQQEREDSKLKVWKSEIKIKDKNKYQNQDTNWETELASV
LGRGFDYGQIGDTTPQASNPQDRVGMTFKGFAVFKGDKLLNDKARLNVRKAFMDQYFKNYS

P27 P110 P52

C

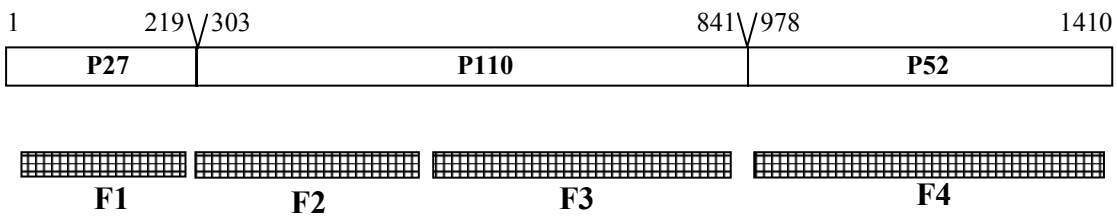

Fig. 3.4A shows the expressed products of P159 F1-F4 as they resolve on a 15% reducing SDS-PAGE gel. Clearly visible for F4 is the presence of two higher bands (circled), as well as the expected (52 kDa) band. Mass-spectrometry analysis gave peptide matches corresponding to F4 for the higher molecular weight bands indicating that these are multimeric or modified forms of F4 (Fig. 3.4B).

Rabbit antisera raised against each recombinant purified P159 fragment was used to investigate the post-translational cleavage pattern of P159 in *M. hyopneumoniae*. Western blots were performed on purified F1-F4 and *M. hyopneumoniae* 232 whole cell extracts (Fig. 3.5 panels A-D). Antisera raised against recombinant F1 (panel A, lane 2) weakly recognizes a *M. hyopneumoniae* protein equivalent in size to native P27 (panel A, lane 1). The size difference between F1 and this protein may be attributed to the 6x His-tag contained within F1. The antiserum raised against F2 and F3 reacted with a *M. hyopneumoniae* protein equivalent in size to native P110. Additional lower molecular weight bands (panel B and C, lane 1), including a strongly immunogenic band of 78 kDa (P78), were also detected which may represent additional cleavage products of P159 not identified in proteomic analyses. Anti-F4 sera reacted with a *M. hyopneumoniae* protein equivalent in size to native P52 (panel D, lane 1).

A

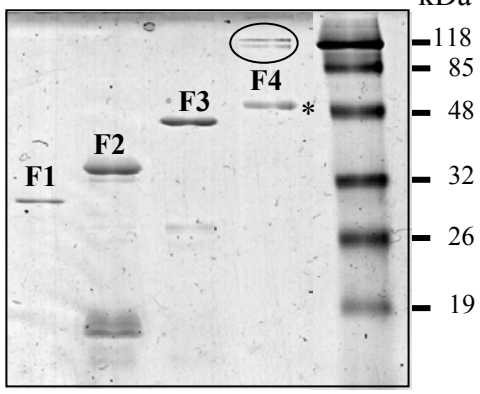

B

MKKQIRNKAI IVLAGLSFIG ITAGVGLAVQ NSALRSSYLN QFKNDKSATE LLSPINDTEL
SKIISNFSLK ENWSKISAGQ AFELHKNPLY AFKLTDAIDF SKIDKKFAHL FFNVQVNDNT
KVEGNSIRNL TVFVFDAITK KEVATRAFHT SLSGFSSVAK EDFIENFVAE SSTYELDKDQ
LKKNFATEIV LPSAFSIKFQ DVLLTHLRKT SPESFQETKT IQVRALTNSI TEFQQQQQEG
GSGGSGTSGG SSGGSSSGST DQKGQTSQSS EKESKSEKEK GKDQQSTQGS EQKQDQKQQK
PKEAEKPAQE KPAQEKPAET PKVKAPVIEP VKKLVFENEK LNQALLETLK DFGGLKLLAA
SGLQGLLPNE YTLLPVSSDK SLIKLDIDDQ AGTASIHLKL LDKNKKEKNL ILPINGLASI
GAIKDKVFSQ IFRNQNAYLT IRPQINEYLR KNPRKKIQEV IWSFSREKFD QLRGQNEVEK
FLEELYNPTQ TSQSPQKSKS SDSAKNNVAT IQASPETAPK TTTTNSNTQS SSTSTNNQSS
NGSQQMASPQ TESSLSTAKT SEASNSSEES SSETKGTKEQ ANSETNPMGK SQAKPEAKPE
EKQINLEDQA KTELKEILKI HGWNYRTLLK DQNQKVILPD NINFWFDLRN KRSSYENYKL
EFDLVKKTGQ IQAGDVIDAN KIRLNLKISP LANLKLEVDS KNKQYIDAGQ IGDYVEFDKQ
GKKLVEQGKS LDLKVGASAA NSIFSPEIRY SAYELKGWTY PIDIDIKGNP IQQELEKLVG
NFHKVGINKN NQYQIYSTDI DKIFAQAKLD KYFELSQEEK QASKKYLQEK LNPISEITIV
KLPPKEEVLP PLEEEKKPEQ DQKAQEKQED KQNQKQQEKQ EDKKEQDQQK HSQSPDQKTE
TQTHDQEKDK QTSSETSPSN TNESSGTQNT AQNSQTNQAN SGQGQSQQAA SSSTSYQTHK
ITTFQDDQKD QTNEQTEKEI EPEKLAFGDY LVKYLDIFET FKVGPDQKLS IGRWYNAPQR
TYNVIFRVLD KENIQVAASL FQLHGISATN IALEKSLRYA PDIFLDGTSG LEYKQDTGDK
PYLQGRQFVS AINSINNTKS SYRVHKLFDN LPLSEESSQG LRLKSSLVYD YQKNDPYTFQ
ASKEALRKTA LTKGVLYLAF KPEQILGIKG SKTAPGRNYK LLSTTNVHFK SLYGLSNLEL
VKTKYQENLK LVWKLIGAKP VNDDKILPPQ VADLPRHRST EIILLEDSKP GASSSPQTKE
NSQNKEAETF NLDIRQTKPN QIEPLEHYLG QTWLMEIRID DESATITIIP EQQEREDSKL
KVWKSEIKIK DKNKYQNQDT NWETELASVL GRGFDYGQIG DTTPQASNPQ DRVGMTFKGF
AVFKGDKLLN DKARLNVRKA FMDQYFKNYS

Fig. 3.4. (A) Recombinant P159 expression products as they resolve on a 15% reducing SDS-PAGE gel. (B) Peptide matches from MALDI-TOF mass spectrometry of F4. The sequence of F4 is highlighted in grey. The solid underlines represent matches for the higher F4 bands (circled), dashed underlines represent matches for the lower F4 band (asterix) and double underlines represent those that match both.

To determine if the P159 protein was expressed continuously during the growth cycle, a series of samples from an *in vitro* grown culture of *M. hyopneumoniae* strain 232 were taken at various time points and then reacted with a pool of anti-P159 rabbit sera from the four recombinant fragments. The expression pattern of P159 during the growth cycle from early log (8 h), through mid-log (16 to 28 h) and into the stationary phase (40 to 72 h) was analysed. P159 was shown to be expressed and always cleaved over the entire *M. hyopneumoniae* strain 232 growth cycle (Fig. 3.5 panel E). P159 was also found to be constitutively expressed and cleaved in a similar experiment with *M. hyopneumoniae* strain J (results not shown).

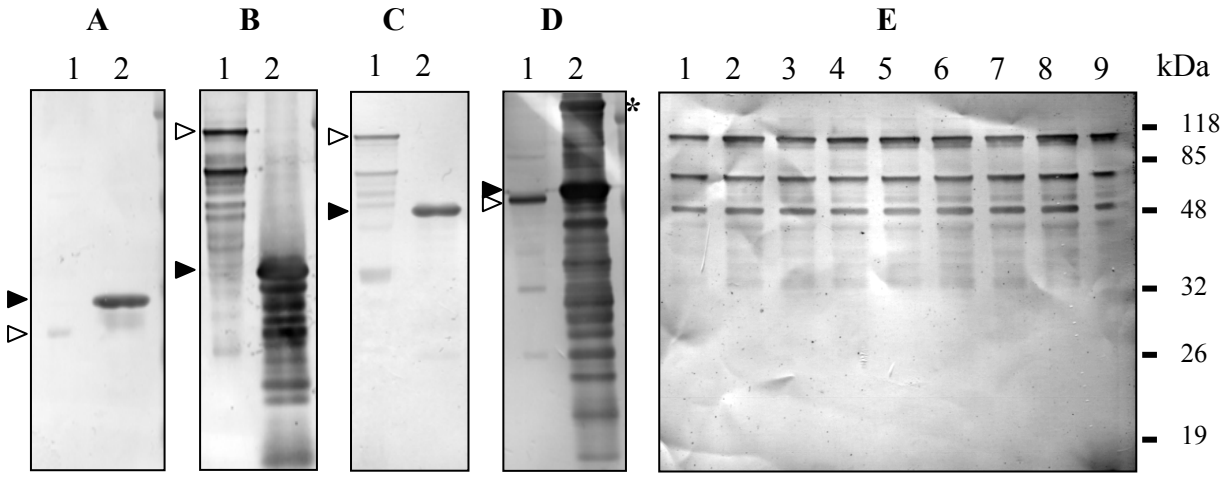

Fig. 3.5. Immunoblot analyses with anti-P159 sera. (A-D) contain a whole cell protein extract of *M. hyopneumoniae* strain 232 (Lane 1, panels A-D) and a sample of purified F1, F2, F3 and F4 (Lane 2, panels A-D respectively). After western transfer these samples were reacted with each P159 rabbit serum: anti-F1, anti-F2, anti-F3 and anti-F4, respectively. Highlighted with closed arrows are the recombinant F1-F4 bands, open arrows represent the expected cleavage product in the *M. hyopneumoniae* whole cell protein extract. Highlighted with an asterix (*) is the multimeric form of F4. (E) Immunoblot patterns of *M. hyopneumoniae* strain 232 cultures harvested at different times post-inoculation. The blot was reacted with a pool of the four anti-P159 rabbit sera. Equivalent amounts of protein were loaded in each lane. Lanes 1-9 correspond to *M. hyopneumoniae* growth times (in hours) of 8, 16, 24, 28, 32, 40, 48, 56 and 72.

3.3.4 Cellular location of P159 fragments

Immunoblot analysis of *M. hyopneumoniae* strain 232 cells digested with increasing concentrations of trypsin (0-150 μg/ml) was used to investigate the cellular location of P159 cleavage fragments. Exposure of intact *M. hyopneumoniae* cells to trypsin concentrations from 0.1 to 10 μg/ml showed a gradual loss of the high molecular weight P159 cleavage fragments; all immunoreactive P159 protein fragments were lost at a trypsin concentration of 50 μg/ml (Fig. 3.6A). This observation suggests that the P159 cleavage products are surface accessible. As a control, identical blots (Fig. 3.6B) were reacted with antiserum raised against recombinant ribosomal protein L7/L12 (a known cytoplasmically located protein of *M. hyopneumoniae*; see Chapter 5). These experiments show that rpL7/L12 remained detectable with trypsin concentrations of up to 150 μg/ml, indicating that the integrity of the cells was not significantly disrupted during digestion with up to 150 μg/ml trypsin. Thus, digestion of the P159 fragments at low trypsin concentration was attributed to surface accessibility.

To confirm the surface location of P159, immuno-gold labeling of intact *M. hyopneumoniae* cells was conducted using antisera raised against F2 and F4 (Fig. 3.7 panel B and D) and pre-immune serum (Fig. 3.7 panel A and C). The abundance of gold particles observed on the anti-F2 and anti-F4 treated cells, but not the cells treated with pre-immune serum further supports the hypothesis that P159 fragments are surface located on *M. hyopneumoniae*. Experiments with anti-F1 and anti-F3 serum were inconclusive due to the considerably high cross-reactivity with the pre-immune serum (results not shown).

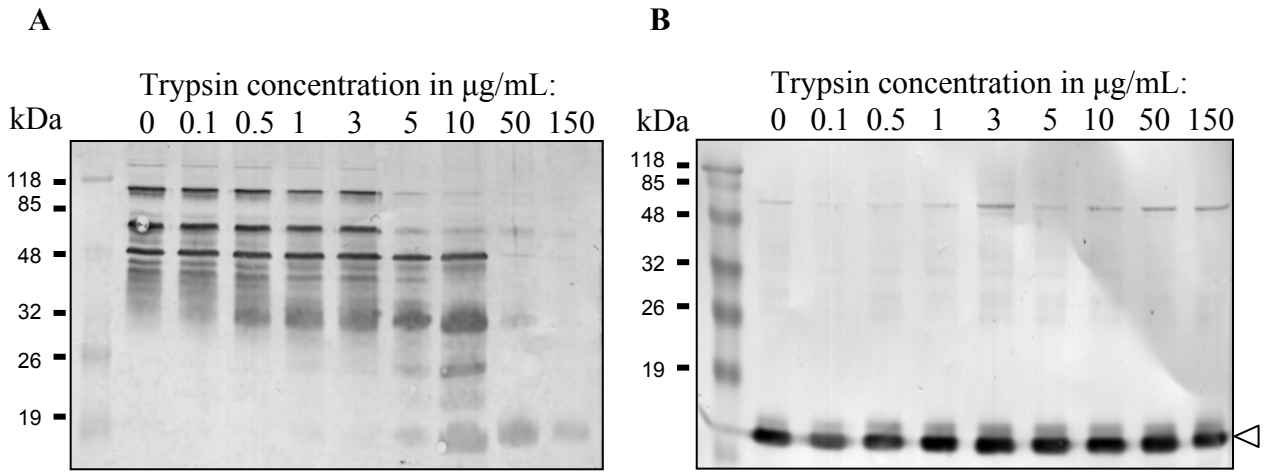

Fig. 3.6. Whole cell preparations of *M. hyopneumoniae* strain 232 subjected to trypsin treatment. The concentrations of trypsin are 0, 0.1, 0.5, 1, 3, 5, 10, 50 and 150 µg/ml (lanes 2-10). The trypsin treated cells were then subjected to immunoblot analyses with a pool of anti-P159 rabbit sera (A) and anti-rpL7/L12 rabbit sera (B). Open arrow indicates position of the rpL7/L12 protein.

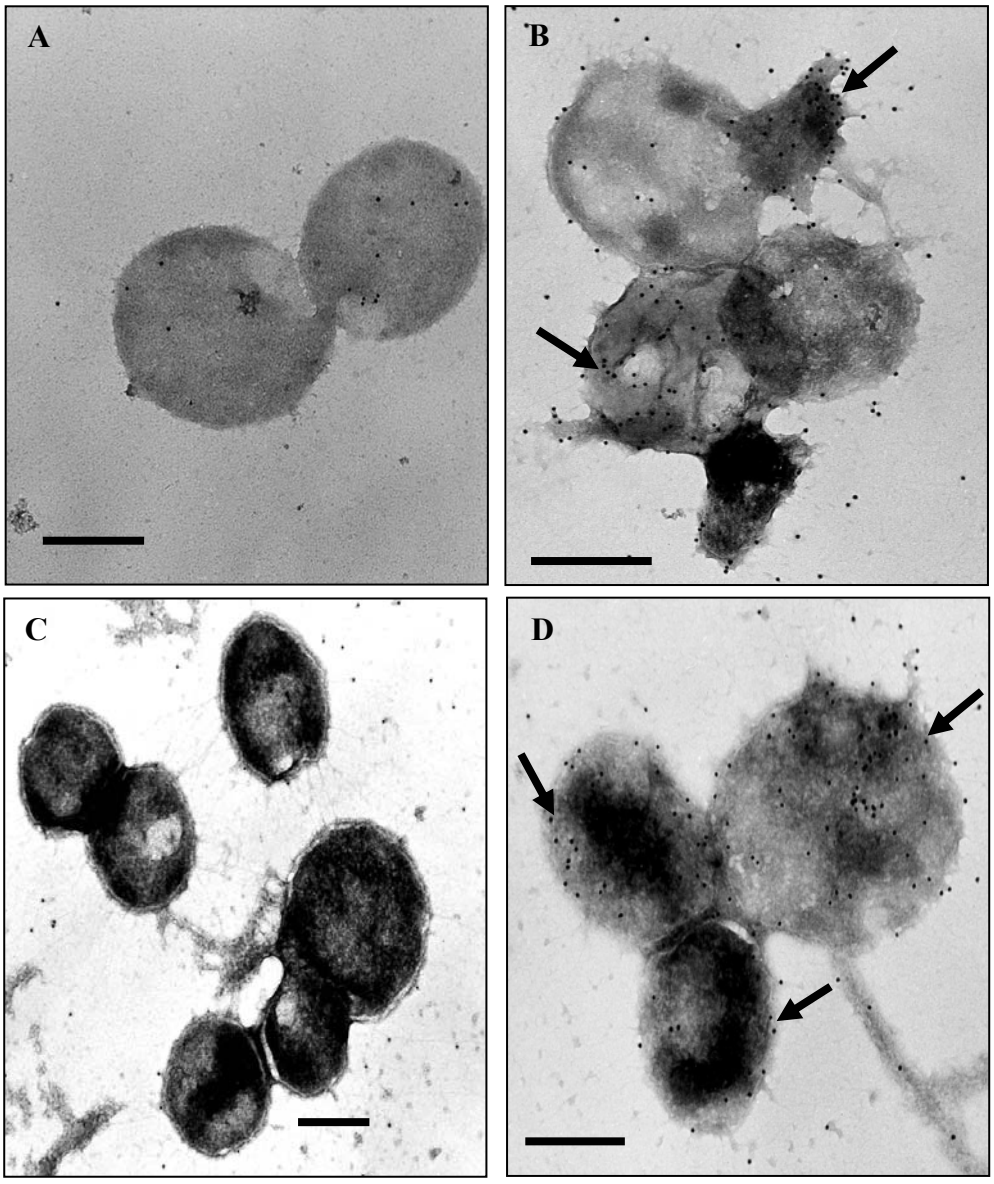

Fig. 3.7. Immunolocalization of P159 cleavage products on the surface of *M. hyopneumoniae* strain 232. Cells were successively labeled with pre-immune rabbit antiserum of F2 (A), rabbit anti-F2 serum (B), pre-immune rabbit antiserum of F4 (C), and rabbit anti-F4 serum (D) and 15-nm-diameter gold-conjugated protein A and stained with 2% aqueous uranyl acetate. Arrows indicate gold particles. Bars, 500 nm.

3.3.5 Comparison of P159 from *M. hyopneumoniae* strains 232 and J

3.3.5.1 Sequence comparison

Fig. 3.8 shows the Eclustalw (ANGIS website: www.angis.org.au/html/index.html) alignment of the P159 sequence from *M. hyopneumoniae* strains J (Genbank accession AF279293) and 232 (GenBank accession AF279292). The two sequences were found to be 95.7% identical with a total of 61 differences which included several insertions/deletions and conserved and non-conserved amino acid substitutions. The largest difference was a 12 amino acid deletion in strain 232 (or insertion in strain J) between amino acids 870 and 882.

3.3.5.2 Comparison of P159 expression products

From 1-D western blots many of the P159 expression products are common to both the pathogenic strain 232 and the non-pathogenic strain J of *M. hyopneumoniae*. There are three highly expressed proteins present in both strains. The approximate sizes of these proteins are 110, 78 and 52 kDa (P110, P78, P52). However, an immunoreactive protein of approximately 38 kDa (P38) was found to be highly expressed in J strain and not in 232 (Fig. 3.9). This expression product was also detected when using anti-F3 serum alone (results not shown) indicating it reacts with anti-F3 serum and may represent a protein within the F3 region of P159. Expression of the N-terminal P27 protein was not readily detected by the pooled antiserum.

```
                  10        20        30        40        50        60
                   .         .         .         .         .         .
P159_J    MKKQIRNKAIIVLAGLSFIGITAGVGLAVQNSALRSSYLNQFKNDKSATELLSPINDTEL
P159_232  MKKQIRNKAIIVLAGLSFIGITAGVGLAVQNSALRSSYLNQFKNDKSATELLSPINDTEL
          ************************************************************

P159_J    SKIISNFSLKENWSKISAGQAFELHKNPLYAFKLTDAIDFSKIDKKFAHLFFNVQVNDNT
P159_232  SKIISNFSLKENWSKISAGQAFELHKNPLYAFKLTDAIDFSKIDKKFAHLFFNVQVNDNT
          ************************************************************

P159_J    KVEGNSIRNLTVFVFDAITKKEVATRAFHTSLSGFSSVAKEDFIENFVAESSTYELDKDQ
P159_232  KVEGNSIRNLTVFVFDAITKKEVATRAFHTSLSGFSSVAKEDFIENFVAESSTYELDKDQ
          ************************************************************

P159_J    LKKNFATEIVLPSAFSIKFQDVLLTHLRKTSPESFQETKTIQVRALTNSITEFQQQQQQE
P159_232  LKKNFATEIVLPSAFSIKFQDVLLTHLRKTSPESFQETKTIQVRALTNSITEFQQQQQ-E
          ************************************************************ *

P159_J    GGSGG---SGGSSGGSSSGSTDQTAQTSQSSEKESKSEKEKGKDQQSTQGSEQKQDQKQE
P159_232  GGSGGGSGTSGGSSGGSSSGSTDQKGQTSQSSEKESKSEKEKGKDQQSTQGSEQKQDQKQQ
          *****   ***************  *********************************.

P159_J    KPKEAEKPAQEKSAQEKPAQEKPAEAPKVAAPVIEPVKKLVFENEKLNQALLETLKDFGG
P159_232  KPKEAEKPAQEK-----PAQEKPAETPKVKAPVIEPVKKLVFENEKLNQALLETLKDFGG
          ************     ********.*** ****************************

P159_J    LKLLAASGLQGLLPNEYTLLPVSSDKSLIKLDIDDQAGTASIHLKLLDKNRKEKNLILPI
P159_232  LKLLAASGLQGLLPNEYTLLPVSSDKSLIKLDIDDQAGTASIHLKLLDKNKKEKNLILPI
          ************************************************.*********

P159_J    NGLASIGEIKDKVFSQIFRNQNAYLTIRPQINEYLRKNPRKKIQEVIWSFSREKFDQLRG
P159_232  NGLASIGAIKDKVFSQIFRNQNAYLTIRPQINEYLRKNPRKKIQEVIWSFSREKFDQLRG
          ******* ************************************************

P159_J    QNEVEKFLEELYKPSQTSQSPQKSKSSDSGKNNVATIQASPETPPKTPAPTTNSNTEQGS
P159_232  QNEVEKFLEELYNPTQTSQSPQKSKSSDSAKNNVATIQASPETAPKT--TTTNSNTQSSS
          ************ *.************** ************* ***   ******.  *

P159_J    TSTNNQSSNGAQQMASPQTESSHSTAKTSEASNSSNESSSETKATQEQANPETNPKTKSQ
P159_232  TSTNNQSSNGSQQMASPQTESSLSTAKTSEASNSSEESSSETKGTKEQANSETNPMGKSQ
          **********.********** ************ ******* *.**** ****  ***

P159_J    AKPEAKPEEKPINLEDQAKTELKEILKIHGWNYRTLLKDQNQKVILPDNINFWFDLRNKR
P159_232  AKPEAKPEEKQINLEDQAKTELKEILKIHGWNYRTLLKDQNQKVILPDNINFWFDLRNKR
          ********** ************************************************

P159_J    SSYENYKLEFDLAKKTGQIQAGDVIDANKIRLNLKISPLANLKLEVDSKNKQYIDAGEIG
P159_232  SSYENYKLEFDLVKKTGQIQAGDVIDANKIRLNLKISPLANLKLEVDSKNKQYIDAGQIG
          ************ ********************************************.**

P159_J    DYVEFDKQGKKLVEQGKSLDLKVGAAAANSIFSSEIRYSAYELKGWTYPIDIDIKGNPIQ
P159_232  DYVEFDKQGKKLVEQGKSLDLKVGASAANSIFSPEIRYSAYELKGWTYPIDIDIKGNPIQ
          ************************.******* ************************

P159_J    QELEKLVGNFHRVGINKNNQYQIYSTDIDKIFAQAKLDKYFELSQEEKQASKKYLQEKLN
P159_232  QELEKLVGNFHKVGINKNNQYQIYSTDIDKIFAQAKLDKYFELSQEEKQASKKYLQEKLN
          ***********.************************************************

P159_J    PISEITIVKLPPKEEVLPPLEEEKKPEQDEKPQEKQEDKQNQKPQEKQEDKQNQKQQEKQ
P159_232  PISEITIVKLPPKEEVLPPLEEEKKPEQD-----------QKAQEKQEDKQNQKQQEKQ
          ****************************           ** ****************
```

```
P159_J   EDKKEQDQQKHSQSPEQKTETQTQNQEKDKQTSSETSPSNTNESSGTQNTAQNSQTNQAN
P159_232 EDKKEQDQQKHSQSPDQKTETQTHDQEKDKQTSSETSPSNTNESSGTQNTAQNSQTNQAN
         ***************.*******. **********************************

P159_J   SGQGQSQQAASSSASYQTHKITTFQDDQKDQTNEQTEKEIEPEKLAFGDYLVKYLDIFET
P159_232 SGQGQSQQAASSSTSYQTHKITTFQDDQKDQTNEQTEKEIEPEKLAFGDYLVKYLDIFET
         *************.********************************************

P159_J   FKVGPDQKLSLSRWYNTPQRTYNVIFRVLDKENIQVAASLFQLHGISATNIALEKSLRYA
P159_232 FKVGPDQKLSIGRWYNAPQRTYNVIFRVLDKENIQVAASLFQLHGISATNIALEKSLRYA
         **********. ****.****************************************

P159_J   PDIFLDGTSGLEYKQDTGDKPYLQGRQFVSAINSINNTKSSYRVHKLFDNLPLSEESSQG
P159_232 PDIFLDGTSGLEYKQDTGDKPYLQGRQFVSAINSINNTKSSYRVHKLFDNLPLSEESSQG
         ************************************************************

P159_J   LRLKSSLVYDYQKNDPYTFQASKEALRKTALTKGVLYLAFKPEQILGIKGSKTAPGRNYK
P159_232 LRLKSSLVYDYQKNDPYTFQASKEALRKTALTKGVLYLAFKPEQILGIKGSKTAPGRNYK
         ************************************************************

P159_J   LLSTTNVHFKSLYGLSNLELVKTKYQENLKLVWKLIGAKPVNDDKILPPQVADLPRHKST
P159_232 LLSTTNVHFKSLYGLSNLELVKTKYQENLKLVWKLIGAKPVNDDKILPPQVADLPRHRST
         ************************************************************.**

P159_J   EIILLEDSKPGASSSPQTKENSQNKEAETFNLDIRQTKPNQIEPLEHYLGQTWLMEIRID
P159_232 EIILLEDSKPGASSSPQTKENSQNKEAETFNLDIRQTKPNQIEPLEHYLGQTWLMEIRID
         ************************************************************

P159_J   DESATITIIPEQQEREDSKLKVWKSEIKIKDKNKYQNQDTNWETELASVLGRGFDYGQIG
P159_232 DESATITIIPEQQEREDSKLKVWKSEIKIKDKNKYQNQDTNWETELASVLGRGFDYGQIG
         ************************************************************

P159_J   DTTPQASNPQDRVGMTFKGFAVFKGDKLLNDKARLNVRKAFMDQYFKNYS
P159_232 DTTPQASNPQDRVGMTFKGFAVFKGDKLLNDKARLNVRKAFMDQY-----
         *******************************************
```

Fig. 3.8. Eclustalw alignment of the P159 protein sequence from *M. hyopneumoniae* strains J and 232. An asterix (*) indicates where the two sequences are identical. Insertions and deletions are highlighted in green, while conserved amino acid changes are highlighted in blue and non-conserved in yellow. The various coloured lettering on the 232 strain sequence represents the peptide matches from mass-spectrometry of P27, P110 and P52.

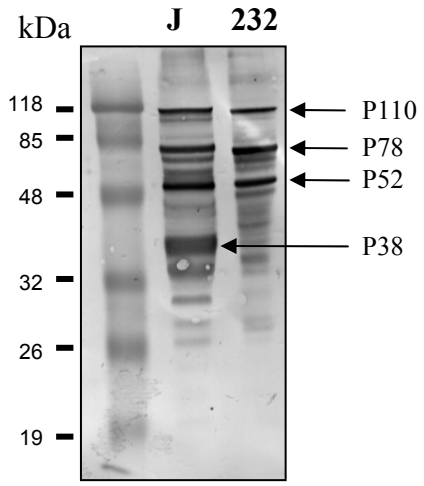

Fig. 3.9. Whole cell extracts of *M. hyopneumoniae* strains J and 232 after western blotting with a pool of anti-P159 sera. The major expression products are highlighted with arrows.

To further compare the cleavage pattern of P159 between *M. hyopneumoniae* strains 232 and J an aqueous phase protein preparation from a TX-114 extraction of each strain was subjected to 2-DGE (Fig. 3.10). Duplicate gels were western transferred and reacted with a pool of the anti-P159 sera generated from the four recombinant fragments. The protein loadings are comparable between the two strains as shown in Fig. 3.10A. There are slight differences in the expression of the P159 products between the two *M. hyopneumoniae* strains and a protein appearing to correlate to the 38 kDa protein (it appears to resolve at approximately 33 kDa) can be seen in both strains, however the size varies slightly (smaller in strain 232) based on the comparative positions of these spots in the proteome. This protein also appears to be more highly expressed in strain J based on the relative intensities of this protein spot on the western blot. In the 2-D blot (Fig. 3.10B) expression of P110 and the C-terminal P52 protein was detected, but due to the limitations of this proteomic analysis and the high pI of the N-terminal cleavage product P27, this protein was not visualised. The protein representing P78 (Fig. 3.5 and 3.9) appears to migrate at a lower molecular weight during 2-DGE (approximately 70 kDa). Further work is needed to confirm these spots are the same protein products.

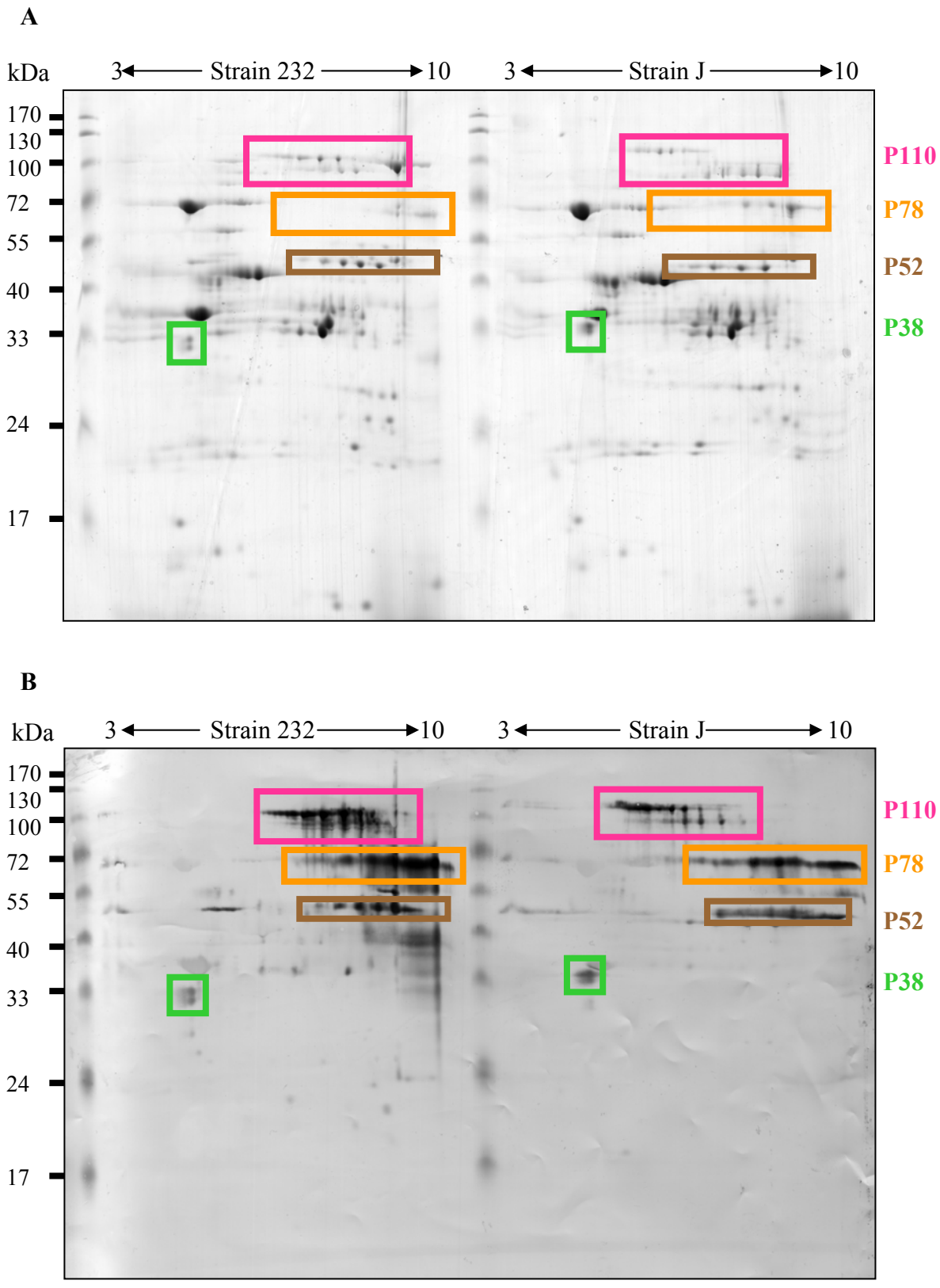

Fig. 3.10. P159 expression products of *M. hyopneumoniae*. (A) 2-D gel of *M. hyopneumoniae* 232 and J strain separated by a molecular weight marker, highlighting the P159 cleavage products corresponding to (B) which is a second identical 2D gel western transferred and blotted with pooled anti-P159 sera generated from the four recombinant fragments. Highlighted are those spots corresponding to the gel above. The first dimension of both gels had a non-linear pH range of 3-10 and the second dimension was a 12.5% SDS-PAGE gel.

3.3.6 P159 reacts with convalescent pig sera

An ELISA assay was conducted using convalescent pig serum attained from pigs in NSW that had been subjected to the *M. hyopneumoniae* ELISA assay at EMAI in 2002. The pig sera were separated into four groups based on their resulting ELISA ratios (indicates reactivity to a *M. hyopneumoniae* specific antigen, Djordjevic *et al*., 1994). Negative samples were those with an ELISA ratio below 3. Three more groups were analysed, those with ratios between 5 and 10, 10 and 15, and 15 or above. Any sera between 3 and 5 are considered inconclusive and none of these sera were investigated. Table 3.5 shows the optical density values obtained when each of the four P159 fragments were coated onto ELISA plates and then incubated with the different pig sera. The pig sera showing significant OD values above an arbitrary cut-off value of 0.2 are highlighted. There does not appear to be a trend between the OD values obtained and the previous ELISA ratio values.

Table 3.5. P159 reactivity with convalescent pig sera. Average OD values obtained when F1-F4 were coated onto an ELISA plate and incubated with 16 different pig sera from EMAI. Highlighted in grey are those with significant OD values (above 0.2).

Pig	*M. hyopneumoniae* ELISA ratio	OD values for P159F1	OD values for P159F2	OD values for P159F3	OD values for P159F4
Pig 1	negative	0.075	0.066	0.217	0.332
Pig 2	negative	0.161	0.100	0.297	0.090
Pig 3	negative	0.140	0.077	1.105	0.085
Pig 4	5-10	0.136	0.089	0.517	2.012
Pig 5	5-10	0.133	0.256	0.903	1.567
Pig 6	5-10	0.271	0.095	0.830	0.122
Pig 7	5-10	0.336	0.222	1.166	0.172
Pig 8	10-15	0.095	0.128	4.723	0.484
Pig 9	10-15	0.146	0.090	0.682	0.231
Pig 10	10-15	1.950	0.318	2.448	0.349
Pig 11	10-15	0.231	0.111	0.883	0.088
Pig 12	≥15	0.103	0.121	0.594	0.431
Pig 13	≥15	0.065	0.074	0.310	0.286
Pig 14	≥15	0.071	0.082	0.519	0.258
Pig 15	≥15	0.447	0.408	1.206	0.667
Pig 16	≥15	0.130	0.090	0.942	0.227

3.4 Discussion

Knowledge of the mechanism by which *M. hyopneumoniae* cells adhere to the porcine respiratory tract is currently limited to the cilium adhesin P97. While studies on P97 have demonstrated that it plays a vital role in adherence it has also been suggested that P97 is not the only molecule involved in host cell attachment (Zhang *et al*., 1995). Genome sequencing studies have identified several paralogs of P97 that are scattered at various sites around the *M. hyopneumoniae* genome (Minion *et al.*, 2004). One of these (*p216*) is preceded by a novel gene identified here as *p159*, which together comprise a two-gene operon. The observations that (i) adhesins of mycoplasmas are often found in multi-gene operons, (ii) genes in operons often share common functions, and (iii) adherence in mycoplasmas often involves several gene products acting in concert (Layh-Schmitt *et al.*, 2000; Papazisi *et al.*, 2002), suggests that the product of the *p159* gene may play a role in adherence of *M. hyopneumoniae* to swine ciliated respiratory cells.

The *p159* gene is predicted to encode a protein of 159 kDa (identified here as P159). Computational analyses identified a putative N-terminal transmembrane domain within P159 indicating that this protein may be membrane associated, secreted or on the surface of *M. hyopneumoniae*. The predicted conformation suggests that the majority of the protein is on the outside of the cell with the N-terminus of the protein anchoring it to the membrane. This conformation would allow P159 to be involved in cellular interactions such as adhesion or to be processed on the surface of the *M. hyopneumoniae* cell, possibly by extracellular proteases. Trypsin digestion studies of whole *M. hyopneumoniae* cells

suggest that P159 is surface exposed. Concentrations of 50 μg/mL of trypsin or above resulted in loss of all the P159 fragments; a pattern mimicking that of the cilium adhesin, a molecule that is known to be surface expressed (Djordjevic *et al.*, 2004). Immunogold studies with F2 and F4 antisera also indicated that P159 is expressed on the surface of *M. hyopneumoniae.*

Mycoplasmas are not known to contain components of the secretion apparatus (i.e. SecE, SecG or SecF along with GroES and GroEL) described in many other bacteria (Burns, 1999; Fath and Kolter, 1993; Hueck, 1998; Sandkvist, 2001). However, the recently sequenced genome of *M. hyopneumoniae* strain 232 (Minion *et al.*, 2004) shows the presence of genes encoding proteins analogous to SecA, SecY, SecD, DnaK/DnaJ, GrpE, PrsA, LepB (signal peptidase I) and LepA. The presence of these genes suggests that a potential pathway for the biogenesis of the P159 fragments is Sec-dependent translocation of P159 then subsequent proteolytic processing of the mature P159 protein external to the plasma membrane to create the various products. Alternatively, as the nascent protein emerges from the translating ribosome, P159 may be recognised by the signal recognition particle (SRP, Ffh) (Luirink and Dobberstein, 1994). SRP in prokaryotes binds the nascent peptide and slows down or arrests protein synthesis, the SRP then targets the arrested translational complex to the SRP receptor (FtsY) and eventually to the translocation machinery. *M. hyopneumoniae* strain 232 contains Ffh and FtsY homologues (Minion *et al.*, 2004). Powers and Walter (1997) have found that Ffh and FtsY of *E. coli* can function directly in protein targeting. Work by Valent and colleagues (Valent *et al.*, 1998) shows that while two distinct protein targeting pathways exist in *E. coli*, once released from SRP, the targeted nascent protein then inserts into a minimum translocon containing SecA, SecY and SecG. Thus, it would appear that the SRP and Sec

targeting pathways converge at the same translocon in the membrane, thereby linking these two pathways in prokaryotes (Valent *et al*., 1998).

Proteomic analyses indicated that P159 is cleaved at two distinct sites generating P27 (N-terminal region of P159), the central P110, and a C-terminal fragment P52. However, subsequent immunoblotting studies detected the presence of a 78 kDa (P78) and a 38 kDa (P38) product whose cleavage sites and sequence remain to be determined. P38 appears to be more highly expressed in strain J based on 1-DGE and 2-DGE, however relative protein concentrations need to be quantified before suggesting that there is a significant difference between strains with respect to P38. This is the focus of future work. The determination of the site within P159 that is cleaved to generate P110 and P52 is the focus of current work. Initial N-terminal sequencing of P110 and P52 was unsuccessful.

Intact P159 is not present in significant quantities in *M. hyopneumoniae* cells *in vitro* and expression of the N-terminal P27 fragment was not readily detected. However, the cleavage products P52, P78 and P110 were found to be constitutively expressed throughout the entire growth cycle of *M. hyopneumoniae* strains 232 and J. The fact that these products are highly expressed during the entire growth cycle and consistently cleaved suggests they may play an important role in this pathogen. *M. hyopneumoniae* possesses a small genome and therefore limited gene set; cleavage of surface proteins may allow such proteins to fulfil multiple functions. *M. hyopneumoniae*, like other mycoplasmas, contain an unusually large number of lipoproteins (Minion *et al*., 2004), with 8.5% of the entire genome coding for lipoproteins (compared to 1.93% for *M. gallisepticum* and 5.79% for *M. penetrans*), but unlike other mycoplasmas these lipoproteins have not been shown to undergo antigenic and/or size variation. It is possible

that differential cleavage of surface exposed proteins in *M. hyopneumoniae* provides this variation.

The post-translational cleavage of proteins in mycoplasmas has been reported for the surface lipoprotein MALP-404 of *M. fermentans* (Davis and Wise, 2002) where MALP-404 is cleaved to produce cell-bound MALP-2 and soluble released fragment (RF) products. The authors suggest that the specific cleavage of some surface proteins may confer efficient "secretion" of extracellular products by these organisms, with concurrent changes in the surface phenotype (Davis and Wise, 2002). Post-translational cleavage has also been reported in the assembly of a complex mycoplasma adhesin organelle (Krause, 1998; Popham *et al.*, 1997). The attachment organelle of *M. pneumoniae* is a polar structure that orients mycoplasma binding to host respiratory epithelium and functions in cell division and gliding motility. The two accessory proteins B (P90) and C (P40) are post-translational cleavage fragments of the ORF6 gene product, which is encoded by an ORF of the P1 operon adjacent to the *p1* gene (Inamine *et al*., 1988; Sperker *et al*., 1991). These proteins act in concert with others in stabilising and forming the attachment organelle of *M. pneumoniae*. Additionally, spontaneously arising mutants of *M. pneumoniae* that fail to cytadhere have been found (Krause *et al*., 1982). The high molecular weight proteins HMW1-3 are required for the stability and assembly of the terminal organelle of *M. pneumoniae* (Krause and Balish, 2004). In class I mutants the levels of HMW1 and HMW3 are greatly reduced and HMW2 is completely absent (Popham *et al*., 1997). This results in the inability of the mutants to cluster the adhesin P1 at the attachment organelle. Loss of HMW1 and HMW3 occurs via post-translational proteolytic processing and raises the possibility of a role for proteolysis in regulating components of this attachment organelle in *M. pneumoniae*. Extensive post-translational cleavage of the secreted *M. hyopneumoniae* P97 cilium adhesin has also been observed

(Djordjevic *et al.*, 2004) and these authors hypothesise that this event provides the pathogen with a capacity to alter its surface architecture, thereby potentially playing an important role in the disease process of *M. hyopneumoniae*. The post-translational cleavage of P159 may also alter the surface architecture of *M. hyopneumoniae* and therefore allow evasion of the host immune system or may have functional implications for host-pathogen interactions.

An unknown feature of P159 proteolysis is the identity and specificity of the corresponding protease. Analysis of the *M. hyopneumoniae* genome identifies five proteins with aminopeptidase signatures (GenBank accession number AAV27465.1, Map; AAV27896.1, PepA; AAV27937.1, PepF; AAV27669.1, PepP; and AAV28011.1, Gcp) and a further two with serine protease signatures (GenBank accession numbers AAV27500.1 and AAV27502.1). We hypothesise that one or more of these proteases plays a role in processing of surface proteins such as P159 and the cilium adhesin P97 in *M. hyopneumoniae*.

Recombinant poly-histidine fusion protein F4 displayed an ability to form multimers even when solubilised in 8M urea and after being subjected to reducing SDS-PAGE analysis. The formation of multimeric forms of proteins has not been previously observed in *M. hyopneumoniae* but has been reported elsewhere. For example, *Shigella flexineri* protein Wzz has been shown to form multimers of at least six units and the dimeric form is highly stable even after heating at 100^{o}C in the presence of SDS (Daniels and Morona, 1999). The role of the multimeric form of F4 (equivalent to P52) is unknown. However, it is becoming increasingly evident that the formation of bacterial aggregates is an important step in colonization of some pathogenic bacteria. For example, M protein mediated aggregation has been reported to contribute to adherence of *Streptococcus pyogenes* to

some epithelial cell types (Caparon *et al.*, 1991) and *Bordetella pertussis* has been shown to grow in aggregates resulting from homophilic protein-protein interactions within the lungs of infected mice (Menozzi *et al.*, 1994). *Staphylococcus aureus* forms aggregates through fibrinogen-binding surface proteins (McDevitt *et al.*, 1994) and in its aggregated state *S. aureus* has been suggested to be protected against phagocytosis (Kapral *et al.*, 1980). The multimerization of P159 via the F4 domain may allow bacterial aggregation and thereby contribute to cell-cell adhesion. Another possibility is that the dimer of F4 may be the functional form of this molecule. F4 corresponds to the *M. hyopneumoniae* C-terminal cleavage product P52 and further study is required to determine whether this protein forms dimers and the functional consequence of such dimerisation.

ELISA assays with convalescent sera from pigs that had naturally been infected with *M. hyopneumoniae* demonstrate the immunogenic properties of P159. F1 reacted with 5/16 (31%) of convalescent pig sera, whereas F2 reacted with 4/16 (25%), F3 reacted with 16/16 (100%) and F4 reacted with 11/16 (69%). This data shows that the various cleavage products have different immunogenic properties. F3, which represents the P110 cleavage product, is highly immunogenic and reacted even with those sera showing negative ELISA values in the *M. hyopneumoniae* ELISA and may be useful as a diagnostic tool. These data suggest that F3 is more sensitive in detecting the exposure of a pig to *M. hyopneumoniae* than the antigen currently in use in this diagnostic assay. The fact that P159 is immunogenic means it may be a good target for vaccine development and as it is surface exposed it is freely available as a target of the swine humoral immune response.

Chapter 4: *M. hyopneumoniae* surface antigen P159 binds heparin and promotes adhesion to and internalization of eukaryotic (PK15) cells

4.1 Introduction

The *p159* gene resides in a two gene operon with a paralog of *p97* (*p216*) but it has no significant homology to *p102*, the second gene found in the two gene operon with *p97*. As shown for the cilium adhesin P97 (Djordjevic *et al*., 2004), P159 also seems to undergo post-translational modification generating various sized products ranging from 27 to 110 kDa. The cleavage and expression pattern appears to vary between the pathogenic strain 232 and the non-pathogenic J strain and at least parts of this molecule are found to be expressed on the surface of *M. hyopneumoniae*, as presented in Chapter 3. It is thought that adherence in *M. hyopneumoniae* is multi-factorial involving other adhesins, possibly working in combination with the cilium adhesin P97. This idea evolved from the work of Zhang and colleagues (Zhang *et al*., 1995) who showed that MAbs F1B6 and F2G5, which recognise P97 in immunoblots, reduce adherence (*in vitro*) to purified cilia and to ciliated cells by only 67%. These authors proposed the idea that other molecules must be involved in adherence.

Recent studies on pathogenic mechanisms of bacteria have focused on the ability of bacteria to bind to components of the extracellular matrix (ECM) as a mechanism to adhere to host cells and tissue. Zhang and colleagues had also shown that glycosaminoglycans and ECM components, namely dextran sulfate, heparin, chondroitin sulfate, laminin, mucin and fucoidan inhibit the binding of *M. hyopneumoniae* to tracheal cilia (Zhang *et al*., 1994b). The P159 antigen was therefore screened for its ability to bind to a range of ECM components and glycosaminoglycans, namely fibronectin, laminin,

fibrinogen, type IV collagen, keratin and heparin. Finally, the ability of this protein to adhere to a porcine epithelial-like cell line was investigated.

Chapter 4: *M. hyopneumoniae* surface antigen P159 binds heparin and promotes adhesion to and internalization of eukaryotic (PK15) cells

4.2 Methods

4.2.1 Ligand blots

Samples of purified recombinant P159 proteins (generated in Chapter 3) were equally loaded onto multiple 15% SDS-PAGE gels and western transferred onto PVDF at 20 V overnight as described in 2.9. Blots were subjected to western blotting as described in section 2.9, incubating with human fibronectin (40 μg/ml), laminin (30 μg/ml), human fibrinogen (50 μg/ml), chondroitin sulphate A (40 μg/ml) and biotinylated heparin (10 μg/ml). The membranes were then incubated with the appropriate primary antibody: anti-fibronectin at 1:500, anti-laminin at 1:500, anti-fibrinogen at 50 μg/ml, and anti-chondroitin sulphate at 1:500. Then the membranes were incubated with the appropriate HRP-conjugated secondary antibody: sheep anti-rabbit at 1:1000, anti-mouse at 1:1000 for the chondroitin sulphate blot and streptavidin-peroxidase (1:3000) for the biotinylated heparin blot. Control blots were also conducted with the ECM components which involved exactly the same method as above but without incubating the membranes with the ECM ligand.

4.2.2 Fibronectin and Fibrinogen ELISA

This method is described in detail in 2.10. Aliquots (100 μl) of F1-F4 (5 μg/ml) were applied to ELISA trays (Linbro/Titretek; ICN Biochemicals) and allowed to adsorb overnight at RT. The wells were then blocked for 1 h at RT. Fibronectin and fibrinogen in PBS containing 1% skim milk were next applied to the wells in 100 μl aliquots and

incubated for 1.5 h at RT. The primary antibodies, anti-fibronectin or anti-fibrinogen diluted 1:3000, were added and incubated for 1 h at RT. The secondary antibodies of HRP conjugated anti-rabbit Ig (Silenus) at 1:1000 for those wells with fibronectin and HRP conjugated anti-goat Ig (KPL) diluted 1:1000 for fibrinogen were then added. The wells were washed 3 times with 0.05% (v/v) Tween20 in PBS between each of the above steps. The substrate solution used was 100 µl aliquots of ABTS solution (Appendix A). The absorbance of the product formed was measured at 414 nm using a Multiskan Ascent ELISA plate reader (Thermo Labsystems).

4.2.3 Radioactive pull-downs and western blots

4.2.3.1 Radioactively labelling ECM proteins

To determine whether P159 recombinant fragments could bind ECM components radioactive labelling of the ECM proteins was performed and these were then subjected to pull-down experiments and western blotting. The following ECM components were used: fibronectin (whole [ICN], alpha-chymotryptic 120kDa fragment [Chemicon], and the proteolytic fragments 70, 45 and 30kDa [Sigma-Aldrich]), type IV collagen (Sigma-Aldrich), laminin (Calbiochem), fibrinogen (Calbiochem) and keratin (Sigma-Aldrich), see Appendix B. 100 µg aliquots of each protein solution were transferred into silicon coated glass tubes. 3 µl of radioactive I^{125} (Amersham Pharmacia Biotech) and 20 µg of Chloramin T (Sigma; made in PB buffer, Appendix A) were added to each tube. After 1 min the labelling reaction was stopped by the addition of 20 µg of sodium metabisulphite (Sigma; made in PB buffer, Appendix A). The binding efficiency was then calculated by adding 1 µl of the newly labelled protein to a microcentrifuge tube containing 20 µl of foetal calf serum (FCS) and the counts per minute (CPM) determined over 30 sec. The labelled protein was then precipitated by addition of 1 ml of a 10% tricarboxylic acid

(TCA) solution and centrifuged at 12,000 g for 3 min. The supernatant was removed and the CPM of the resulting pellet was determined. A binding efficiency of 60% or greater was considered adequate. The unbound I^{125} was removed from the remaining labelled mix by adding PBST (PBS with 0.5% tween 20) to a total volume of 2.5 ml to each labelled protein mix. This solution was put onto a PBST equilibrated PD10 column (Pharmacia). The void volume was discarded and the labelled protein was eluted in a further 3.5 ml of PBST. The labelled protein was aliquoted into microcentrifuge tubes and stored at 4^{o}C.

4.2.3.2 Radioactivity pull-down experiments

The P159 recombinant fragments were subsequently screened for their ability to bind the radioactively labelled ECM compounds by a pull-down assay which allowed any proteins binding to the radioactive ECM compounds to be isolated by nickel affinity chromatography due to the presence of the His-tag on the recombinant proteins. Subsequently these would be detected due to the presence of radioactivity on the ECM compound bound to the P159 protein. The method was as follows: 50 µg of protein (in PBS or PBS with 0.1% SDS) were aliquoted into microcentrifuge tubes. A volume of 50 µl of PBS was added to another microcentrifuge tube as a negative control. A "total counts" control tube containing the total CPM values possible for the particular labelled ECM component was set up in duplicate containing 20 µl of FCS due to its ability to bind the radioactively labelled compounds and be precipitated with TCA. A volume of 20 µl of each I^{125}-labelled ECM component was added to the P159 protein (F1-F4), PBS or FCS in the microcentrifuge tubes. These were left rotating at RT for 45 min. The protein mixtures and negative (PBS) control were added to a microcentrifuge tube containing a pellet from 100 µl of a 50:50 solution of Ni-NTA sepharose (washed 2 times in PBS + 20 mM imidazole, centrifuged at 500 g for 5 min; Qiagen). These were again left rotating at

RT for 45 min, the total counts control tubes were left standing (no resin). After this time the microcentrifuge tubes were centrifuged at 12,000 g for 25 sec. The supernatant was removed and 1 ml of PBS + 20 mM imidazole was added to remove any unbound protein. The tube was then centrifuged as above. This was repeated again for a total of two washes. The CPM of the resin pellets were determined. A total of 1 ml of a 10% TCA solution was added to the "total counts" tubes. The tubes were centrifuged at 12,000 g for 3 min, upon which the CPM of the pellet was determined.

4.2.3.3 Radioactivity western blots

A total of 10 µg of each purified F1-F4 protein was loaded onto a 15% SDS-PAGE gel and western transferred onto PVDF at 90 V for 1.5 h. The membranes were blocked overnight with 5% w/v skim milk in PBS at 4^{o}C and subsequently washed in PBST for 20-30 min. The I^{125}–labelled ECM components (diluted 1:30) were added and the membranes incubated for 1 h at RT with shaking. The membranes were subsequently washed in PBST and the washes transferred to a clean container and the radioactivity detected with a gamma-counter. Washing was continued until the radioactivity in the wash had stabilised and reached background level (approximately 10 x 10 min washes). The membranes were then placed in an X-ray cassette sealed between two sheets of plastic. A piece of x-ray film (Kodak) was then placed over the membrane and the cassette sealed for 1-7 days and the film developed.

4.2.4 Heparin binding assays

Aliquots (100 µl) of F1-F4 (5 µg/ml) were applied to ELISA trays and allowed to adsorb overnight at RT as described in 2.10. The wells were then blocked with 100 µl aliquots of PBS containing 2% (w/v) skim milk for 1 h at RT. Biotinylated heparin (Sigma-Aldrich)

in PBS containing 1% skim milk was next applied to the wells in 100 µl aliquots and incubated for 1.5 h at RT. Bound biotinylated heparin was detected using 100 µl aliquots of peroxidase conjugated streptavidin (Roche) diluted 1:3000 with a 1 h incubation at RT. The wells were washed 3 times with 0.05% (v/v) Tween20 in PBS between each of the above steps. The substrate solution used was 100 µl aliquots of ABTS solution, Appendix A. The absorbance of the product formed was measured at 414 nm using a Multiskan Ascent ELISA plate reader (Thermo Labsystems). In other experiments, a competition binding assay was used in which unlabeled glycosaminoglycans: heparin, fucoidan, heparan sulfate, chondroitin sulphate A and chondroitin sulfate B (all from Sigma-Aldrich) were pre-incubated with biotinylated heparin before the addition of 100 µl aliquots of the mixture to coated and blocked wells. Control experiments showed that none of the P159 fragments could bind to streptavidin-peroxidase or the ABTS solution, establishing that the heparin binding is not an artifact of binding to a compound used in the detection system. Graph construction and non-linear regression with one-site binding and one-site competition analysis was performed using GraphPad Prism version 4 (GraphPad Software).

4.2.5 Adherence/invasion assay of P159 fragments with PK15 cells

4.2.5.1 Coating latex beads with F1-F4 and incubation with PK15 cells

As per previously published methods (Dombek *et al.*, 1999; Molinari *et al.*, 1997), latex beads (3 µm; Sigma-Aldrich) were coated with purified recombinant P159 fragments F1-F4. Briefly, 10^8 bead particles in 20 µl PBS were incubated with 5 µg of purified proteins in PBS overnight at 4^oC. After washing steps, free binding sites on the bead surface were blocked by incubation with 200 µl of PBS with 10 mg/ml BSA for 1 h at RT. The efficiency of particle loading was verified by fluorescence-activated cell sorter (FACS)

analysis with anti-F1-F4 rabbit serum (results not shown). Beads were washed and the volume adjusted to 2.5 ml with Dulbecco modified Eagle medium (Invitrogen GmbH) with HEPES and 1% foetal calf serum. PK15 cells (American type culture collection certified cell line 33) were seeded on 12-mm-diamater glass coverslips (Nunc Gmbh and Co.) placed on the bottom of 24-well tissue culture plates (Nunc Gmbh and Co.) at 1.5 x 10^5 cells per well and allowed to grow to semiconfluent monolayers at 37^{o}C under a 5% CO_2 atmosphere. After addition of 250 µl of the bead suspension, the cells were incubated for 2, 4, 7 and 22 h at 37^{o}C under a 5% CO_2 atmosphere. Cells were washed three times with PBS to remove unbound beads. Cells were either processed for scanning electron microscopy (Molinari *et al.*, 1997, outlined in section 4.2.6) or for double immunofluorescence as described below.

4.2.5.2 Double immunofluorescence detection of F1-F4 beads

PK15 cells (after incubation with the coated latex beads) were washed with PBS and then fixed by the addition of 0.5 ml/well of pre-cooled fixation buffer (1% paraformaldehyde in PBS), the tray was placed on ice for 1 h and then stored at 4^{o}C overnight. The PK15 cells were blocked by the addition of 200 µl/well of PBS with 10% FCS and incubated for 30 min at RT. The blocking solution was then removed and the cells incubated separately with 200 µl/well of the anti-F1-F4 rabbit polyclonal antibodies (40-50 µg/ml) for 45 min at RT. Cells were incubated with goat anti-rabbit Alexa 488 (green) (Molecular Probes) for 1 h at RT and subsequently washed with PBS. Cells were permeabilized with Triton X-100 (200 µl/well of a 0.1% triton X-100 in PBS solution) for 5 min at RT, washed in PBS, followed by incubation with 200 µl/well of the anti-F1-F4 rabbit polyclonal antibodies (40-50 µg/ml) for 45 min at RT. After washing, cells were treated with goat anti-rabbit Alexa 568 (red) (Molecular Probes) for 1 h, washed three times in PBS and

then mounted onto glass slides. After this labelling procedure, extracellular beads appear yellow/green whereas intracellular beads are stained orange/red. Images were recorded using a Zeiss inverted microscope 100 M with an attached Zeiss Axiocam HRc digital camera.

4.2.6 Incubation of PK15 cells with *M. hyopneumoniae*

A *M. hyopneumoniae* J strain culture was kindly supplied by the Microbiology Institute (Hannover). A 5 ml fresh *M. hyopneumoniae* culture was centrifuged at 10,000 g and resuspended in 100 µl of infection medium. 10 µl of *M. hyopneumoniae* suspension per well was added to 0.5 ml PK15 cell culture infection medium in a 24 well tray and incubated at 37^{o}C for 5 and 24 h. The wells were washed 3 times with cacodylate buffer (Appendix A) and the cells fixed in 2% formaldehyde and 3% glutaraldehyde in cacodylate buffer for 1 h on ice. The wells were then washed three times in cacodylate buffer and then in TE buffer (20 mM Tris, 2 mM EDTA, pH 6.9). The cells were dehydrated with a graded series of acetone (10, 30, 50, 70, 90, 100%) with each step being for 15 min on ice, the 100% step was conducted at RT. Critical point drying was carried out using liquid CO_2 and the samples examined in a Zeiss DSM982 field emission electron microscope at an acceleration voltage of 5 kV.

Chapter 4: *M. hyopneumoniae* surface antigen P159 binds heparin and promotes adhesion to and internalization of eukaryotic (PK15) cells

4.3 Results

4.3.1 Recombinant P159 proteins bind heparin

Parts of the P159 molecule were shown to bind laminin and fibronectin using affinity chromatography (results not shown). This binding to laminin and fibronectin along with other ECM components was investigated further using the P159 recombinant fragments generated in Chapter 3. Western blots were conducted with fibronectin, fibrinogen, laminin, chondroitin sulphate A and biotinylated heparin. From these blots it was found that recombinant fragment F2 reacts non-specifically by binding to secondary antibodies and to streptavidin-peroxidase (results not shown). F1, F3 and F4 did not bind significantly to any of these compounds under these conditions. Experiments using radioactively labeled ECM components showed that the P159 fragments did not bind to type IV collagen, laminin, fibrinogen, keratin, whole fibronectin or proteolytic fragments of fibronectin. This was found when using either radioactive pull-down experiments or when using radioactive proteins for western blot detection (results not shown).

ELISA assays showed no significant binding of any of the four P159 recombinant fragments to fibronectin or fibrinogen (results not shown), however, F3 and F4 were shown to bind biotinylated heparin in a saturable and dose-dependent manner with saturation occurring at 15-20 μg/ml of biotinylated heparin. A 50-fold excess of unlabelled heparin was found to extinguish the majority of the signal by competitively inhibiting biotinylated heparin binding (Fig. 4.1), thus indicating that heparin occupies specific binding sites on the F3 and F4 proteins. Non-linear regression and one-site

binding analysis was performed on the specific binding data which gave an estimate of the apparent dissociation constants for F3–biotinylated heparin complexes (142.37 ± 22.01 nM) and F4–biotinylated heparin complexes (75.37 ± 7.34 nM). The specificity of the biotinylated heparin binding of F3 and F4 was verified by inhibition experiments using unlabeled heparin (Fig. 4.2A). F1 and F2 were also included as non-biotinylated heparin binding P159 controls. With increasing concentration of unlabeled heparin there was a decrease in binding of biotinylated heparin to F3 and F4 (Fig. 4.2A). This data was subjected to non-linear regression with one-site competition and the 50% inhibitory concentration (IC_{50}) for F3 (52.92 ± 1.03 μg/ml) and F4 (66.63 ± 1.02 μg/ml) determined. The potent competition obtained with unlabeled heparin confirms that binding is due to interaction with heparin and not the biotin label. To examine the specificity of the interaction between F3 and F4 and heparin, we employed various glycosaminoglycans as soluble competitors of the heparin-P159 interaction (Fig. 4.2B and C). In addition to heparin, fucoidan, a highly sulfated fucose polymer, is an effective inhibitor of the binding of both F3 and F4 to biotinylated heparin giving IC_{50} values of 96.28 ± 1.19 μg/ml and 36.23 ± 1.14 μg/ml. By contrast, heparan sulfate, chondroitin sulfate A or chondroitin sulfate B did not show significant inhibition.

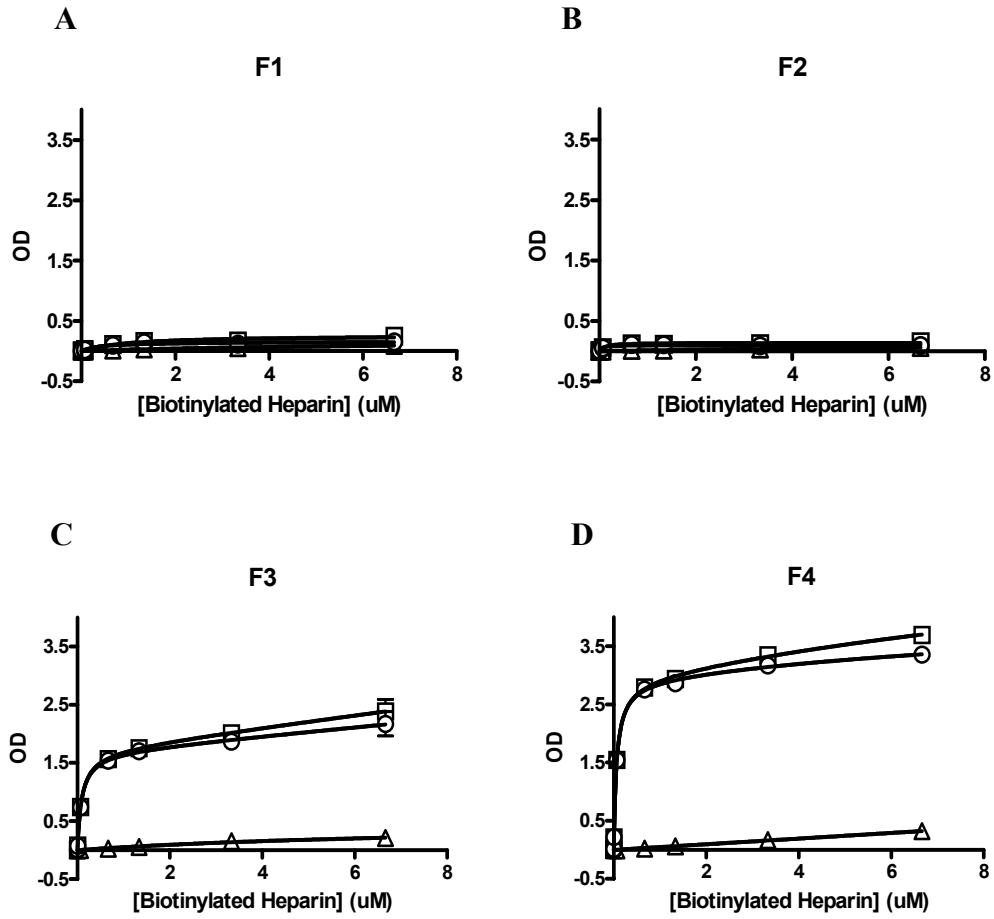

Fig. 4.1. Binding of P159 fragments to biotinylated heparin. Increasing concentrations of biotinylated heparin were added to ELISA plate wells coated with 5 μg/ml of each of the four P159 fragments. □ represents the total binding and Δ represents non-specific binding measured by mixing the biotinylated heparin with a 50 fold excess (2.4 mg/ml) of non-labeled heparin prior to incubation with the P159 fragments. The non-specific binding subtracted from the total binding generated the specific binding curve ○. Figures shown are means ± SEM of triplicate determinations, indicated by error bars where they are larger than the symbol size.

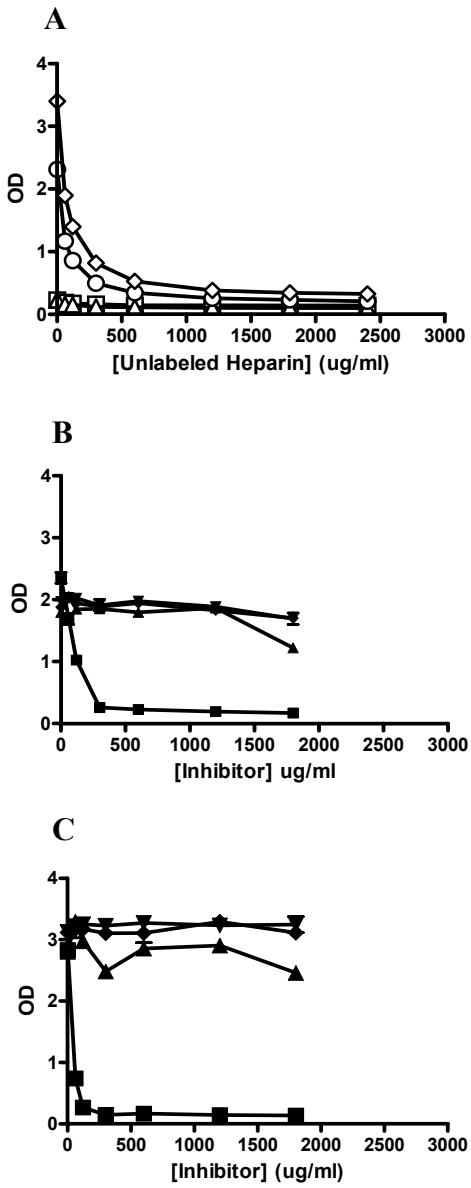

Fig. 4.2. Effect of inhibitors on P159 fragments binding to biotinylated heparin. (A) displays the results of unlabeled heparin inhibition on F1 (□), F2 (Δ), F3 (○) and F4 (◊) binding, while (B) and (C) shows the results of fucoidan ■, heparan sulfate ▲, chondroitin sulfate A ● and chondroitin sulfate B ♦ inhibition on F3 and F4 binding, respectively. Varying concentrations of inhibitor 0 to 40 times the saturating concentration of 60 µg/ml were pre-incubated with biotinylated heparin at 60 µg/ml and then added to ELISA plate wells coated in 5 µg/ml of F1-F4 before incubation with streptavidin-peroxidase and development with substrate. The data represents mean values ± SEM from triplicate determinations, shown by error bars where they are larger than the symbol size.

4.3.2 *Mycoplasma hyopnemoniae* adheres to porcine epithelial cells

Due to the procedural difficulties and unavailability of working with the natural cells in a *M. hyopneumoniae* infection, porcine respiratory cilia, a cell line from the American Type Culture Collection was chosen. This was a porcine kidney epithelial-like cell line (PK15) and Zielinski and Ross (1990) demonstrated the ability of *M. hyopneumoniae* to adhere to this cell line. However through this work it appeared that they did not investigate whether the bacterial cells had the ability to invade the PK15 cells and all data was numerical. We therefore infected PK15 cell monolayers with *M. hyopneumoniae* and looked for the adherence or invasive capabilities of the bacteria at 5 and 24 h of incubation. This involved incubating *M. hyopneumoniae* strain J (kindly supplied by the Institute for Microbiology, Hannover) with a monolayer of PK15 cells. Using electron microscopy it was found that the bacteria could adhere to these cells after 5 h of incubation (Fig. 4.3) but were not able to invade the cells even after a period of 24 h. Electron microscopic analysis of sections of the PK15 cells infected with *M. hyopneumoniae* shows the accumulation of flask or omega-shape like structures in the PK15 cell membrane (Fig. 4.3B) in the near vicinity to attached bacteria which resemble caveolae (flask- or omega-shaped non-coated invaginations, mainly 50-100 nm in size, of the plasma membrane; Rohde *et al*., 2003).

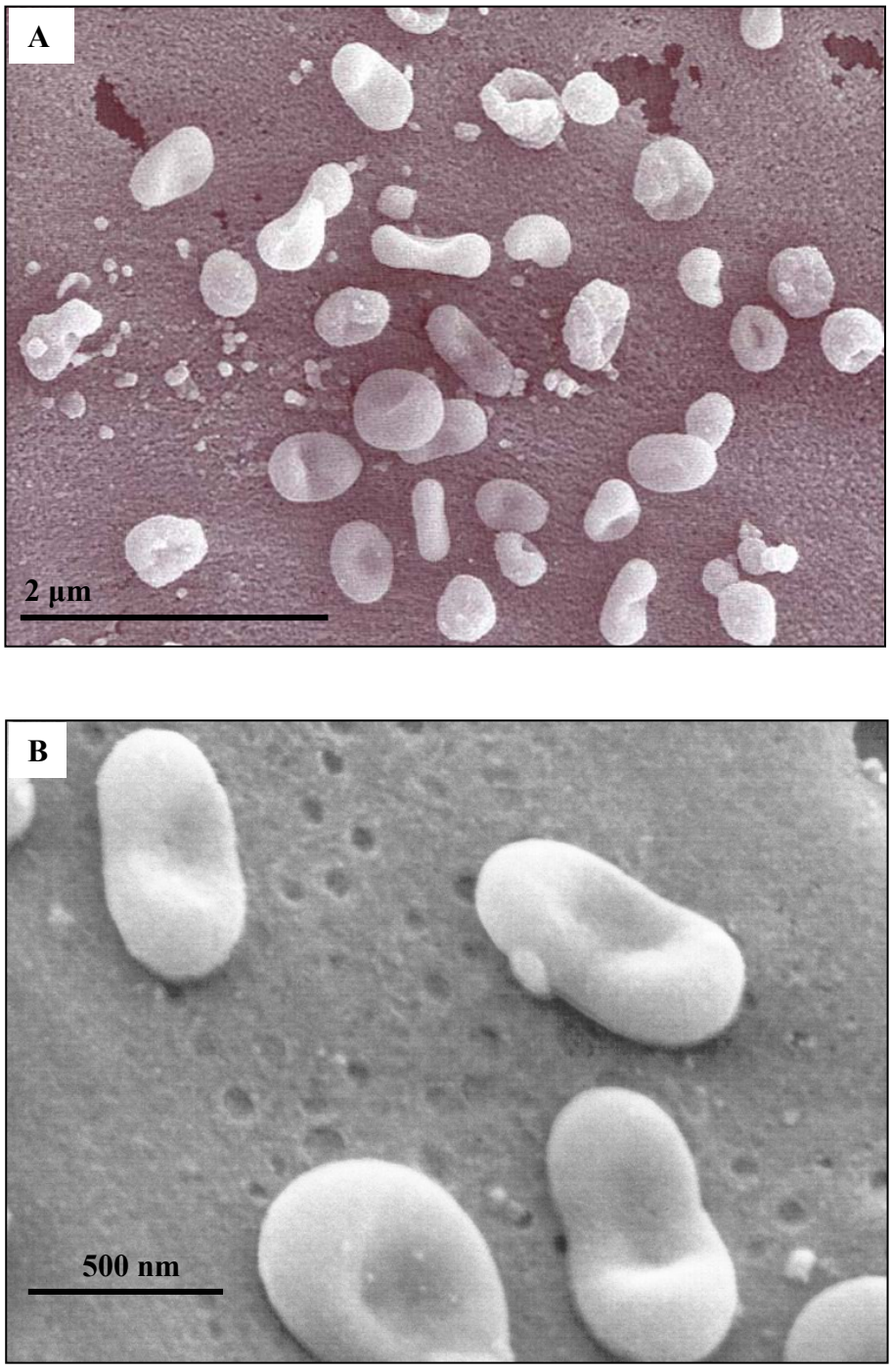

Fig. 4.3. Electron micrographs of *M. hyopneumoniae* J strain bacterial cells adhering to PK15 cells. The scale bar can be seen at the bottom of both images. (A) Bacterial cells adhering to the surface of a PK15 cell. (B) An enlargement of a small area of a PK15 cell showing the apparent pore formation on the surface of the PK15 cell at the site of bacterial adherence.

4.3.3 P159 fragments adhere to porcine epithelial cells

M. hyopneumoniae has previously been shown to adhere to the porcine kidney epithelial-like (PK15) cell line (Zielinski and Ross, 1990) and this was verified in this current study, Fig. 4.3. A coated latex bead binding assay was used to examine whether P159 adheres to PK15 cells. Latex beads and latex beads coated with each of the four purified recombinant P159 protein fragments were incubated with monolayers of PK15 cells. Scanning electron microscopy, in conjunction with double-immunofluorescence of intact and then Triton X-100 treated PK15 cells, was used to differentiate between beads adhering to the surface of the cells and those able to penetrate inside the cells. Latex beads not coated with P159 fragments neither adhered to cells nor were internalized (results not shown). Beads coated with F1 protein were unable to either adhere to or penetrate into the PK15 cells. F3 coated beads were found to adhere to PK15 cells 2 h post-incubation but were not found to penetrate cells even after 22 h. Both F2 and F4 coated beads were found to adhere to PK15 cells 2 h post-incubation and were detected inside PK15 cells from 2-22 h post-incubation. Increasing numbers of internalized beads were detected over this time course (Fig. 4.4 and Fig. 4.5; results not shown).

.

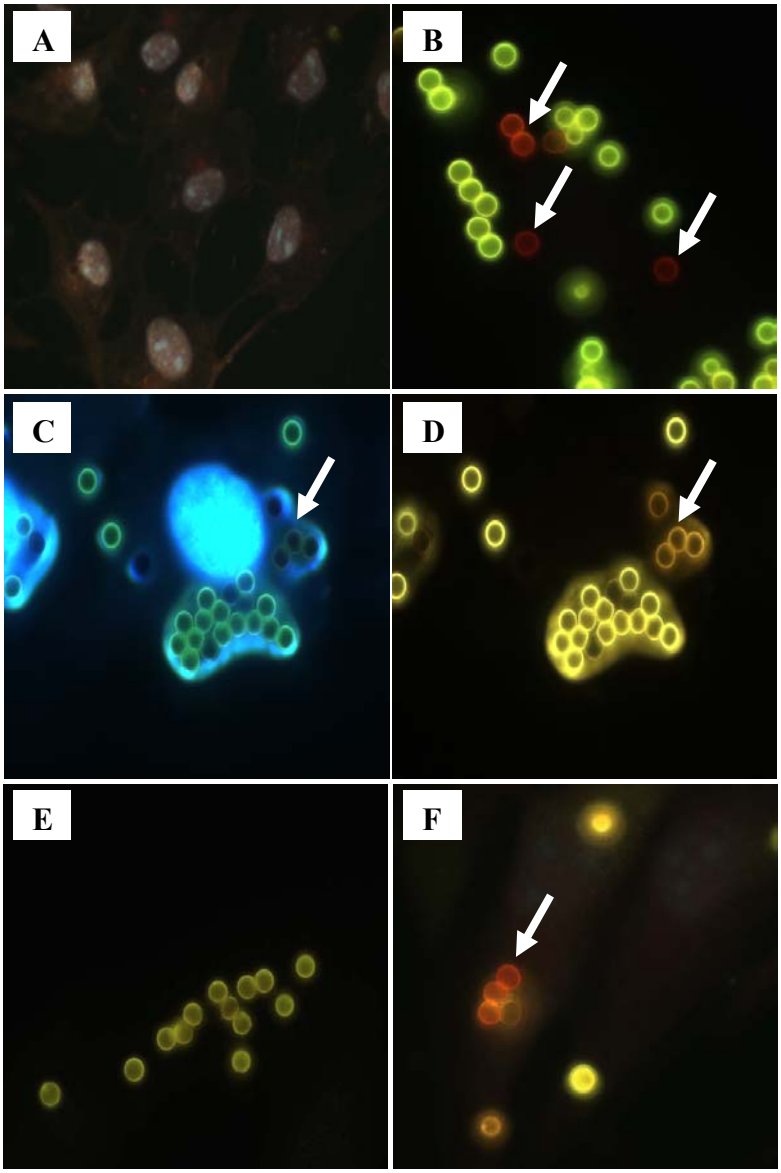

Fig. 4.4. Double immunofluorescence analysis of the adherence of P159 F1-F4 coated latex beads to PK15 cells. Intracellular beads are highlighted with white arrows. (A) PK15 cells as they appear on the glass coverslip. These cells were incubated with F1 coated latex beads for 22 h but the beads did not adhere or penetrate these cells. (B) Extracellular F2 coated latex beads (yellow/green) adhering to the PK15 cells and the intracellular F2 coated latex beads (orange/red) that have been taken up by the PK15 cells after 7 h of incubation. (C) F2 coated beads interacting with the PK15 cells after 7 h of incubation with the nucleus of the PK15 cells stained with Hoerst for orientation. (D) The same image as in C but with a different exposure time showing the extracellular (yellow/green) beads and the intracellular (orange/red) beads. (E) F3 coated beads interacting with a cluster of PK15 cells after 4 h of incubation (F) F4 coated beads interacting with PK15 cells 7 h post-incubation, highlighting the extracellular (yellow/green) beads and intracellular (orange/red) beads.

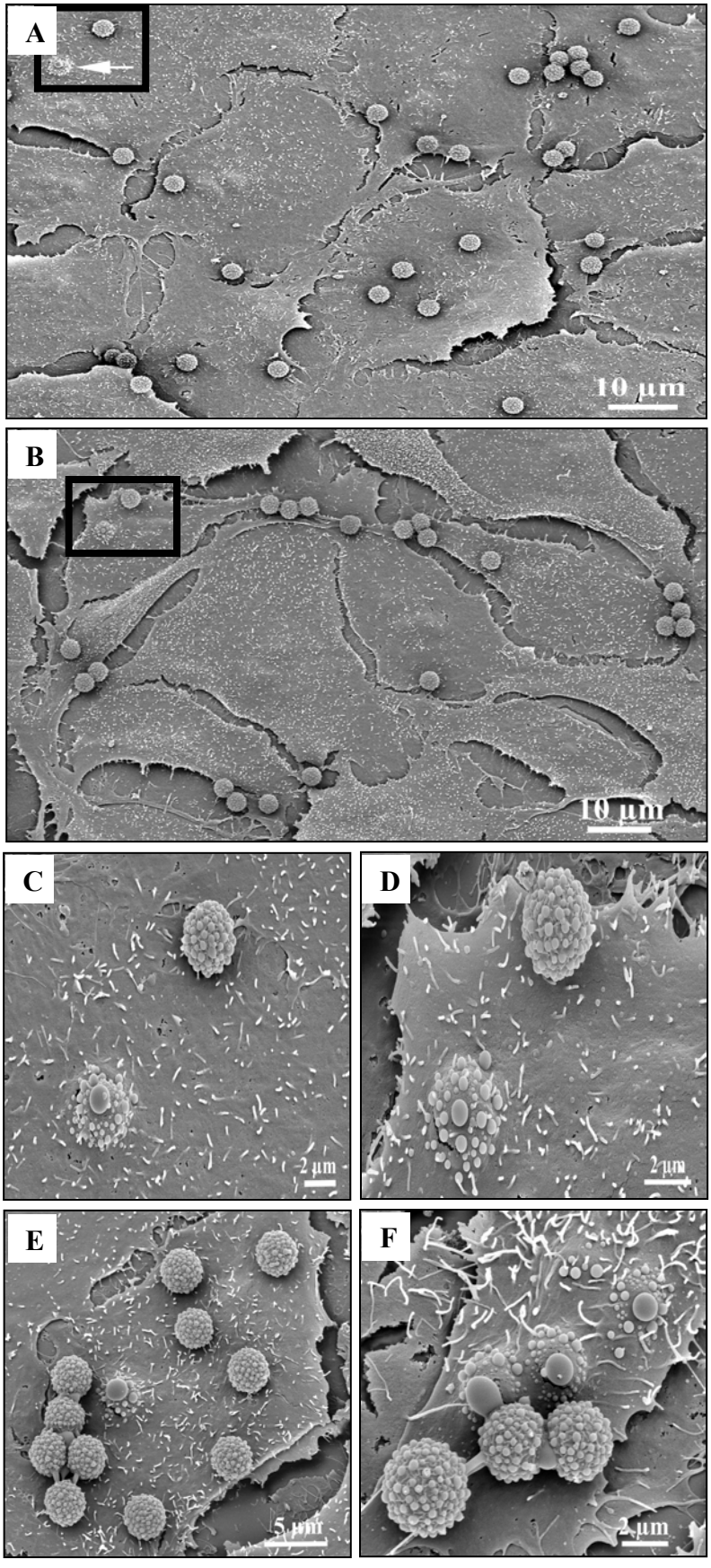
A
10 µm
B
10 µm
C
2 µm
D
2 µm
E
5 µm
F
2 µm

4.4 Discussion

The ability of pathogenic bacteria to bind components of the extracellular matrix and the role this may play in pathogenesis has been the focus of intense research in recent years. Preliminary experiments identifying ECM binding proteins in *M. hyopneumoniae* (results not shown) identified regions within P159 that were found binding to a fibronectin and laminin affinity column. Recombinant P159 fragments were screened for their ability to bind a number of ECM components by western analysis, radioactive pull-downs, radioactive western blots and finally by ELISA and all results showed the inability of any fragment of P159 to bind to fibronectin, laminin, fibrinogen, chondroitin sulphate A, type IV collagen and keratin.

Experiments using biotinylated heparin showed that the C-terminal half of the P159 molecule, represented by recombinant fragments F3 and F4, had the ability to bind to heparin in a dose-dependent saturable manner. The six histidines added at the N-terminus of the proteins during the cloning process are not playing a role in the binding ability, as other proteins containing this tag such as F1 and F2 are not able to interact with heparin. The *M. hyopneumoniae* recombinant protein RpL7/L12 (Chapter 5) was also used as a non-P159 protein 6x His-tag control due to its inability to bind to any of the ECM molecules investigated (results not shown).

The binding of heparin to F3 and F4 displays an apparent dissociation constant of 142.37 $\pm$ 22.01 nM and 75.37 $\pm$ 7.34 nM, respectively. This value is comparable to that (60 nM)

reported for the binding of clusterin to heparin (Pankhurst *et al*., 1998), to that (20 nM) of heparin binding to antithrombin (Barrow *et al*., 1994), to that of *M. tuberculosis* DNA-binding protein 1 to heparin (0.35 nM) and heparan sulfate (15.4 nM) (Aoki *et al*., 2004), to that (26 nM) of *M. tuberculosis* heparin-binding hemagglutinin adhesin binding to heparin (Pethe *et al*., 2000), to that (500 nM) of human IL-12 binding to heparin (Hasan *et al*., 1999) and falls in the midrange of other reported constants for heparin-protein interactions. These values range from 0.3 nM for heparin binding to the Alzheimer's disease amyloid precursor protein (Multhaup *et al*., 1995) to 400 nM for binding of heparin to low-density lipoproteins (Gigli *et al*., 1992).

Heparan sulfate was only a weak competitive inhibitor of heparin binding by P159 fragments and this may be due to heparin having a higher ratio of iduronate:glucuronate residues and higher sulfation than heparan sulfate. Najjam and colleagues had previously shown that only a highly sulfated form of heparan sulfate was an effective inhibitor of the binding of recombinant interleukin 2 (IL-2) to heparin (Najjam *et al.*, 1997). Frick and colleagues demonstrated that only a highly sulfated form of heparan sulfate inhibited the interaction of *Streptococcus pyogenes* strain AP1 to chondroitin sulfate B (Frick *et al.*, 2003). Fucoidan, a sulfated polysaccharide of non-mammalian origin, is shown here to be a strong competitor of the interaction between heparin and F3 and F4. It is generally the case that heparin-binding proteins also interact with fucoidan due to its high sulfate density and branched, comb-like structure, which contrasts with the linear structure of mammalian glycosaminoglycans (Patankar *et al.*, 1993). Chondroitin sulfate A, chondroitin sulfate B and mucin did not show an ability to competitively inhibit the heparin binding of the P159 fragments F3 and F4. The B variant of chondroitin sulfate contains iduronate residues, similar to heparin and heparan sulfate, which shows that inhibition is not due to the presence of iduronate, as had been found for the streptococcal

M protein (Frick *et al.*, 2003), but more likely due to the high degree of sulfation of heparin and fucoidan.

It is assumed that binding of proteins to various glycosaminoglycans (GAGs) depends on electrostatic interactions between the negatively charged sulfate groups of the GAG chains and positively charged regions of the protein. Typically, heparin-binding proteins are rich in basic amino acids that are usually clustered. There is a lack of agreement on consensus sequences found in proteins showing an ability to bind to heparin. Cardin and Weintraub (1989) proposed two heparin-binding motifs, XBBXBX and XBBBXXBX, where B represent basic amino acids and X any other amino acids. Aoki and colleagues have since shown that repeats of the residues PAKK are key residues for binding to GAGs in *M. tuberculosis* (Aoki *et al.*, 2004). P159 does not possess these motifs but has a high density of lysine (K) and arginine (R) residues in F3 (15.6% of the total sequence is K and R) and F4 (13.9% of the total sequence is K and R) which is consistent with their role as basic amino acids interacting with the negatively charged sulfate groups on the GAGs.

Pathogenic bacteria may also bind heparin which then binds to tertiary heparin binding proteins, allowing adherence to the host cells (Duensing *et al.*, 1999; van Putten *et al.*, 1998). It is known that mast cells, the primary cellular source of heparin, can be chemotactically recruited to sites of tissue damage or repair, where heparin-containing granules are released (Hamawy *et al.*, 1994). Potentially *M. hyopneumoniae*, through P159, may attach to heparin preventing it from taking part in wound healing. Furthermore, because of the multiple binding activities of GAGs, it is also possible that GAGs bound to the *M. hyopneumoniae* surface mediate binding to proteins involved in

host defense. Known relevant ligands for GAGs include growth factors, cytokines and other mediators of inflammation (Bernfield *et al.*, 1999). Trapping of these mediators could potentially provide the bacteria with means to modulate the local response to the pathogen.

Heparin was one of the molecules shown by Zhang and colleagues in 1994 to inhibit the binding of *M. hyopneumoniae* to purified porcine tracheal cilia. The results suggested that heparin interacted with the adhesive molecules on the surface of *M. hyopneumoniae*. P159 may be one of these surface molecules which bound heparin. The fact that heparin inhibited adherence may be due to the surface molecules once bound to heparin were no longer able to bind the heparin molecules present on the tracheal cilia, thereby preventing adherence. Whether or not heparin is freely available on these cells requires further investigation.

In vitro models used for investigation of mycoplasma-host cell interactions have included a model using suspensions of porcine respiratory tract ciliated epithelial cells (Zielinski and Ross, 1993) and a microtiter plate adherence assay for *M. hyopneumoniae* using purified swine tracheal cilia (Zhang *et al.*, 1994b). A porcine kidney epithelial-like cell line (PK15) was used by Zielinski and Ross (1990) where the ability of *M. hyopneumoniae* to adhere to this cell line was demonstrated and confirmed in this study. P97 has been established as an important adhesin in *M. hyopneumoniae* due to its ability to adhere to swine ciliated cells. However, monoclonal antibodies directed against P97 were only able to reduce up to 67% of adherence of *M. hyopneumoniae* to swine ciliated cells. Therefore, it was hypothesised that other molecules may be involved in adherence. F2, F3 and F4 were found to mediate the adherence of latex beads to PK15 cells. Additionally, F2 and F4 coated beads penetrated PK15 cells. This same methodology has

been used to demonstrate serum opacity factor (SOF) involvement in the fibronectin-mediated adherence of *Streptococcus pyogenes* to epithelial cells (Oehmcke *et al.*, 2004) and the fibronectin binding protein (SfbI) of *S. pyogenes* involvement in the internalization of group A streptococci by epithelial cells (Molinari *et al.*, 1997). Ectodomains 3 and 4 of human polymeric immunoglobulin receptor were shown to mediate invasion of *Streptococcus pneumoniae* into the epithelium using this same methodology (Elm *et al*., 2004) and aromatic amino acids at the surface of InlB were found to be essential for host cell invasion by *Listeria monocytogenes* using this method (Machner *et al*., 2003). The data generated in this study suggest the function of P159 as an adhesin. As whole *M. hyopneumoniae* cells were not able to invade the PK15 cells while parts of the P159 molecule were suggests that the P159 molecules are secreted from the bacteria where they invade and disturb the function of the PK15 cells, although this remains to be determined.

In conclusion the data indicating P159 as an adhesin is substantial. The gene *p159* is found in a two-gene operon with a *p97* paralog, *p216*, as one of the adhesin operon families. P159 fragments F3 and F4 exhibit the ability to bind heparin and other pathogenic bacteria have been shown to bind heparin as a potential mechanism of adherence. Inert latex beads coated with F2, F3 and F4 were able to adhere to PK15 cells whereas F2 and F4 coated beads were able to penetrate the PK15 cells. Collectively this data suggests that P159 is a good candidate for an adhesin of *M. hyopneumoniae* and thus may play a role in the colonization of the respiratory tract of swine.

Chapter 5: Characterization of *M. hyopneumoniae* ribosomal protein L7/L12

5.1 Introduction

The structure and function of ribosomal proteins, such as L7/L12 has been extensively explored. The *rplL* gene codes for a protein core, L12 which can also undergo acetylation producing L7. Within the ribosomal complex, these two ribosomal proteins are unique in their acidic nature and exist in a 4:1 ratio. The protein L7/L12 is central to the translocation step of translation, that is, the step where the peptidyl-tRNA is moved (translocated) to the next codon to continue protein synthesis. The monomer of L7/L12 has a molecular mass of 12 kDa and is organized in the ribosome as two dimers bound to one copy of protein L10, which anchors the pentamer to the large ribosomal subunit. L7/L12 was one of the first proteins isolated from 50S ribosomal particles (Moller and Castleman, 1967).

The tertiary structure model of the L7/L12 dimer (Fig. 5.1) has 3 domains. The N-termini of both monomers, comprising residues 1-37, form a four-helix bundle. This domain is responsible for dimer formation and binding to L10. The C-terminal domain (residues 50-120) consists of two associated globules that are responsible for interaction with elongation factors. The N- and C-terminal domains are connected via flexible strings (residues 38-49). The L7/L12 dimer forms a clearly defined morphological feature in the *E. coli* 50S ribosomal subunit which is called the L7/L12 stalk or protuberance (Strycharz *et al*., 1978).

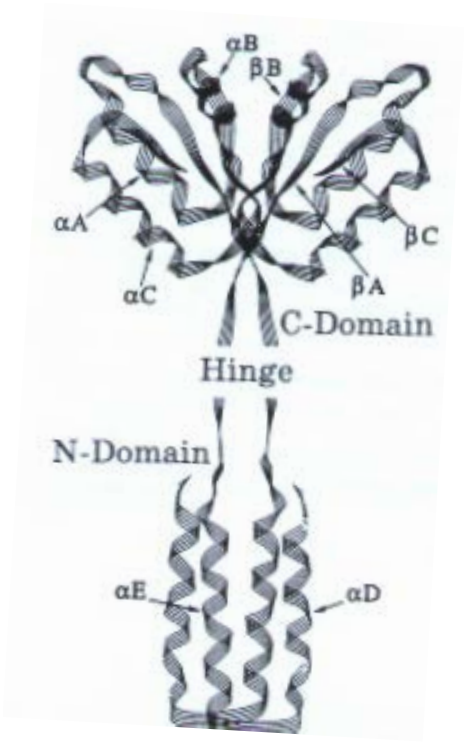

Fig. 5.1. Secondary structure of the L7/L12 dimer. N-domain comprising residues 1-37 form a four-helix bundle (αD-αE), the C-terminal domain forms two associated globules (residues 50-120), and the N- and C-terminal domains are connected with flexible strings of residues 38-49 representing a hinge region. The C-terminal domain consists of three anti-parallel β–strands (βB-βA-βC) in one layer and three α–helices (αB-αA-αC) in another (Bocharov *et al*., 1996).

In *E. coli* it has been found that a significant amount of L7/L12 exists in a non-ribosomal pool (Morrissey *et al*., 1975 and 1976). The non-ribosomal L7/L12 molecules share identical amino acid composition and electrophoretic characteristics and are immunologically identical to ribosomal L7/L12 (Morrissey *et al*., 1975) but are not able to interact with protein-stripped ribosomes, show different gel filtration profiles, and present a different trypsin digestion profile than ribosomal L7/L12. The authors postulated that the differences might be due to modification of non-ribosomal L7/L12 to inactivate excess L7/L12 or to convert it into a form with other biological activities in some organisms (Morrissey *et al*., 1975 and 1976). Spence and Clarke (2000) have also shown that L12 is membrane associated and surface exposed in *Neisseria gonorrhoeae*.

Vaccines based on ribosomal preparations have been described for over 35 years (Gregory, 1986; Thompson and Snyder, 1971; Venneman and Bigley, 1969). The use of such vaccines has been controversial, mainly due to the lack of a common mechanism explaining the protection achieved by the various ribosomal components (Gregory, 1986). Nevertheless, ribosomal preparations derived from intracellular pathogens have been shown to induce a delayed-type hypersensitivity (DTH) reaction in animals sensitized with the pathogen (Baker *et al*., 1973; Corbel, 1976; Loge *et al*., 1974; Ortiz-Ortiz *et al*., 1971). Tantimavanich *et al*. (1993) found that among all of the ribosomal proteins, L7/L12 was the only protein able to reveal a DTH reaction in guinea pigs sensitised by live BCG or killed *Mycobacterium tuberculosis*. Bachrach *et al*. (1994) found that the *Brucella melitensis* L7/L12 ribosomal protein was the main immunogenic protein in the commercial protein preparation Brucellergen responsible for DTH activity. Furthermore, Bachrach *et al*. (1997) showed that acetylation of the *B. melitensis* L7/L12 protein is crucial for the recognition of the protein by the host cells triggering the DTH reaction.

The *Brucella abortus* L7/L12 ribosomal protein has also been identified as an immunodominant antigen (Brooks-Worrell and Splitter, 1992). *B. abortus* L7/L12 ribosomal protein fused to a maltose binding protein (MBP) conferred a significant degree of protection, when compared to mice vaccinated with adjuvant alone, adjuvant plus MBP or with the *B. abortus* live attenuated vaccine strain 19 (Oliveira and Splitter, 1996). Further evidence of the immunogenicity of L7/L12 proteins come from studies of *Chlamydia trachomatis*, in which western blots of two-dimensional electrophoretic maps of proteins from this organism were probed with sera from 17 seropositive patients with genital inflammatory disease. Seven sera (41%) recognized the ribosomal protein L7/L12 (Sanchez-Campillo *et al*., 1999). Finally, Spence and Clarke (2000) have shown that pre-incubation of low invasive *N. gonorrhoeae* with micromolar amounts of purified

recombinant L12 lead to a five- to eight-fold increase in invasion of the human endometrial cell line, Hec1B. In addition, nanomolar concentrations of exogenous L12 inhibits *N. gonorrhoeae* invasion to approximately 70% of the level in controls. Thus it has been found that L7/L12 is immunogenic and surface exposed in some pathogens and in at least one case is able to increase the invasive capabilities of the pathogen.

Based on these data an investigation was commenced to determine whether the *M. hyopneumoniae* ribosomal protein L7/L12 (rpL7/L12) is expressed on the surface of the bacterial cell and whether it is an immunogenic antigen and therefore a possible target for vaccine development.

Chapter 5: Characterization of *M. hyopneumoniae* ribosomal protein L7/L12

5.2 Methods

5.2.1 Microbial rpL7/L12 gene similarity analysis

A database search was conducted to obtain the gene sequence of *rpL7/L12* genes from various bacterial species (National Centre for Biotechnology Information website: www.ncbi.nlm.nih.gov). An alignment of the complete amino acid sequences available for these 27 different bacterial species was generated using the ClustalW program available on the European Molecular Biology (EMBnet) website (www.ch.embnet.org/software/ClustalW.html). A similarity matrix was generated for this data using GeneDoc, available from the Pittsburgh Super Computing Centre website (www.psc.edu/biomed/genedoc/). A phylogenetic tree was constructed from the aligned sequences using the Phylip 3.6 package available through The University of Washington website (evolution.genetics.washington.edu/ phylip) and the Treeview program available through the University of Glasgow website (taxonomy.zoology.gla.ac.uk/rod/treeview. html). The Phylip 3.6 package consisted of: the aligned sequences were subjected to 100 bootstrap replications using Seqboot. This data was used to generate a distance matrix with the Protdist program which was run using the default parameters. A consensus tree was then constructed using the neighbour-joining method from the programs Neighbour and Consense. Treeview was used to view the resulting tree.

5.2.2 Genetic Techniques

5.2.2.1 PCR amplification of the *M. hyopneumoniae* strain 232 *rpL7/L12* gene

The *M. hyopneumoniae* rpL7/L12 nucleotide sequence was obtained from genome sequence data generated by F.C. Minion (Minion *et al*., 2004). Primers rpL7L12 forward and rpL7L12 reverse (Fig. 5.2) were used to PCR amplify the entire 363 bp *rpL7/L12* gene from *M. hyopneumoniae* strain 232 chromosomal DNA. *Bam*H1 and *Hin*DIII restriction enzyme sites were incorporated into the forward and reverse primers respectively to facilitate directional cloning.

Fig. 5.2. Primers designed to amplify the entire *rpL7/L12* gene from *M. hyopneumoniae*, rpL7/L12 forward and reverse. The incorporated restriction sites for *Bam*H1 and *Hin*DIII are underscored.

An initial gradient PCR was undertaken to establish the optimal PCR conditions. The reaction mix was the same as described in 2.2.1 and the reaction conditions are shown in Table 5.1.

Table 5.1. Reaction conditions for the rpL7/L12 PCR. Each PCR reaction began with an initial denaturation step at 94°C for 5 min and completed by a final extension at 72°C for 5 min.

Primer pair	Amplified product	PCR cycle protocol x 30
rpL7L12F rpL7L12R	rpL7/L12 363 bp	94°C 60 sec, 68°C 30 sec, 72°C 60 sec

For electrophoresis of PCR products, a 2.5% agarose (w/v) gel was prepared and run as described in 2.2.2. GeneRuler™ 100 bp DNA Ladder Plus (1.5 µg; Progen) was used for sizing the resolved fragments.

5.2.2.2 Purification of the rpL7/L12 PCR product

PCR products were purified using a QIAquick PCR Purification Kit (Qiagen) to remove any unbound dNTPs and PCR reagents essentially as described below. Products from PCR reactions were pooled into a microcentrifuge tube and a 5X volume of buffer PB (Appendix A) was added and mixed. The sample was then applied to a QIAquick spin column and centrifuged at 13,000 rpm for 1 min at RT (Biofuge Pico centrifuge, Heraeus). The flow through was discarded and 0.75 ml of buffer PE (Appendix A) was added to the spin column to wash. The column was centrifuged as above, the flowthrough discarded and then further centrifuged for 1 min to remove any residual PE buffer. The spin columns were then placed into new microcentrifuge tubes and a volume of 50 µl of sterile MilliQ water was added to the centre of the spin column and left to stand for 1-5 min. The column was then centrifuged as above and the flow through containing the purified PCR product was retained and stored at -20°C. The purified PCR product was examined on an agarose gel as described in section 2.2.2.

5.2.3 Expression of rpL7/L12 in pQE-9

5.2.3.1 Plasmid DNA extraction

A culture of *E. coli* JM109 (pQE-9) was harvested and the plasmid extracted using a Maxi Prep Kit (Qiagen) as described in section 2.2.7.

5.2.3.2 Restriction enzyme digestion and gel extraction

The purified PCR product and the pQE-9 plasmid were digested for 2 h at 37^{o}C using a dry block heater (Thermoline) with restriction enzymes *Bam*H1 and *Hin*DIII (New England Biolabs) according to the manufacturers' instructions. The digested products (60 µl of each) were electrophoresed on a 2% agarose gel in 1X TAE and stained with ethidium bromide. The bands were excised from the agarose gel using a clean scalpel blade and transferred to pre-weighed microcentrifuge tubes. Gel extraction of these products was performed using the GenElute™ Gel Extraction Kit (Sigma) as follows: a 3X gel volume of gel solubilisation solution was added to each gel slice. The tubes were incubated at 60^{o}C until the gel had completely dissolved (approximately 10 min). Afterwards, 1X gel volume of isopropanol was added and mixed. The entire sample was loaded onto a GenElute miniprep binding column placed in a collection tube and centrifuged at 14,000 rpm for 1 min using a bench-top microcentrifuge (Biofuge Pico, Heraeus). The column was washed with 0.6 ml of wash solution, centrifuged as above and then further centrifuged for 2 min to remove excess wash solution (ethanol). The DNA was eluted by transferring the column to a new microcentrifuge tube, adding 50 µl of MilliQ water to the column, incubating for 1 min and subsequently centrifuging for 1 min. The eluted DNA was stored at -20^{o}C.

5.2.3.3 Ligation and transformation

The gel extracted products (PCR and plasmid) were then mixed together in a 1:1 ratio (3:3 µl and 5:5 µl) and ligated together overnight as outlined in 2.2.4. The ligation mixes (20 µl) were then transformed into 300 µl of chemically competent *E. coli* M15 (pREP4) cells as discussed in 2.2.4.

5.2.3.4 Screening recombinant plasmids and plasmid DNA extraction

Recombinant plasmids were screened through small-scale plasmid preparations using the FlexiPrep™ Kit (Amersham Pharmacia Biotech) as described in 2.2.6. Plasmid preparations were digested for 4 h at 37^{o}C with *Bam*H1 and *Hin*DIII according to the manufacturer's instructions and analysed by agarose gel electrophoresis on a 0.8% gel for detection of the *rpL7/L12* gene insert.

5.2.3.5 DNA sequence analysis of *M. hyopneumoniae* rpL7/L12 genes

The primers pQEF (5'-CGGATAACAATTTCACACAG-3') and pQER (5'-GTTCTGAGGTCATTACTGG-3') were used to sequence the *M. hyopneumoniae* (strain 232) *rpL7/L12* gene insert in the pQE-9 vector as described in 2.2.5. The *rpL7/L12* gene from *M. hyopneumoniae* J strain was also sequenced (using primers rpL7L12 forward and rpL7L12 reverse). The PCR product was generated as described in 5.2.2.1 with *M. hyopneumoniae* J strain chromosomal DNA as the template. After PCR, the product was purified using the QIAquick PCR Purification Kit (Qiagen) (section 5.2.2.2) and then subjected to a polyethylene glycol (PEG) precipitation. This involved adding an equal amount of PEG_{8000} solution (Appendix A) to a microcentrifuge tube containing the PCR product. The sample was incubated at 4^{o}C for 24-40 h. The microcentrifuge tube was

centrifuged at 13,000 rpm for 30 min at RT using a bench-top microcentrifuge (Biofuge Pico, Heraeus). The sample was washed with 0.1 ml of 70% ethanol and centrifuged at 13,000 rpm for 10 min at RT. This was repeated with 0.1 ml of 95% ethanol. The pellet was air-dried for approximately 30 min at RT and then resuspended in sterile MilliQ water back to the initial PCR volume. PCR sequencing reaction mixes containing either 10 µl of the PEG precipitated DNA or 5 µl MilliQ water and 5 µl of pQE-9 clone DNA (pTB1), with 8 µL DTCS Quickstart Master Mix (Beckman Coulter) and 2 µl of primer (1 pmol/µl) were prepared. The reaction mixes were then thermocycled at 96^{o}C, 20 sec; 50^{o}C, 20 sec; 60^{o}C, 4 min (30 cycles) (FTS-960 Thermal Sequencer, Corbett Research). The reaction products were then purified using ethanol precipitation and analysed on a CEQ8000 Genetic Analyser (Beckman Coulter) as described in 2.2.5.

5.2.4 Protein techniques

5.2.4.1 RpL7/L12 protein expression

A 250 ml *E. coli* M15 (pREP4) culture containing the pQE-9-based isopropyl-β-D-thiogalactopyranosidase (IPTG) inducible L7/L12 expression plasmid (pTB1) was grown to an optical density (at 600 nm) of 0.6 (Ultraspec 3300 Pro spectrophotometer, Amersham) and induced with a final concentration of 1 mM IPTG as outlined in section 2.3. The culture was incubated at 37^{o}C with shaking at 200 rpm overnight (Certomat® R, B-Braun). The overnight culture was then subjected to protein purification under denaturing conditions in a buffer containing 8M urea as described in 2.4.

5.2.4.2 Sodium dodecyl sulphate polyacrylamide gel electrophoresis (SDS-PAGE)

Whole-cell protein extracts of *E. coli* M15 (pREP4 pQE-9 L7/L12) before and after induction were prepared by resuspending cells (obtained in section 5.2.4.1) in SDS-PAGE reducing solution (Appendix A) and boiling for 5 min. Samples of the denatured rpL7/L12 purified protein in urea buffer (from section 5.2.4.1) were prepared by combining 25 µl of the protein with 5 µl of bromophenol blue loading dye (Appendix A). Samples were electrophoresed through a 15% SDS-PAGE gel (Appendix A) as described in 2.7.

5.2.5 Generation of polyclonal antiserum to recombinant rpL7/L12

20 ml of purified rpL7/L12 protein in urea buffer (from section 5.2.4.1) was ultrafiltered with sterile PBS (as described in 2.4) to a final volume of approximately 18 ml and this was used to inject a New Zealand White rabbit as described in 2.6. To verify reactivity of the antiserum, purified protein was transferred from polyacrylamide gels onto polyvinylidene difluoride membrane (PVDF) as described in 2.9. The membrane was then subjected to western blotting as described in 2.9 which included incubation with primary antibody (pre-immune sera diluted 1:200, or anti-rpL7/L12 sera diluted 1:200-1:500 in wash solution), followed by sheep anti-rabbit HRP conjugated secondary antibody (Silenus) at 1:1000 and developed in a DAB solution.

5.2.6 Mass spectrometry analysis of recombinant rpL7L12

A sample of rpL7L12 purified protein in PBS (from 5.2.5) was reduced and electrophoresed on a 15% SDS-PAGE gel as described in 2.7. The resulting band of rpL7/L12 was excised from the gel and subjected to MALDI-TOF mass spectrometry

analysis, as described in 2.8. This technique was used to confirm the identity of the protein.

5.2.7 Expression patterns of rpL7/L12 by *M. hyopneumoniae* J and 232

Samples from *in vitro* grown cultures of *M. hyopneumoniae* strains 232 and J were prepared as in 2.1, separated by electrophoresis through 15% SDS PAGE gels and transferred to PVDF, as described in 2.9. Blots were exposed to anti-rpL7/L12 rabbit sera diluted 1:200, followed by anti-rabbit HRP conjugated antibody (Silenus) at 1:1000 and developed in a DAB solution as outlined in 2.9.

5.2.8 FACScan analysis of *M. hyopneumoniae* with anti-rpL7/L12 sera

The location of rpL7/L12 protein in *M. hyopneumoniae* was explored using fluorescent techniques and flow cytometry as follows. The cell surface assay involved growing a 6 ml culture of *M. hyopneumoniae* strain 232. The absorbance of the culture at 600 nm was determined to ensure that the same numbers of bacterial cells were used in all experiments. The culture was divided into 1 ml aliquots which were centrifuged at 8,000 g for 3 min at 4^{o}C and washed once in 1 ml of PBS. The bacterial pellets were resuspended in PBS with 0.1% BSA and based on the absorbance values an aliquot of cells (e.g. 100 µl of a culture with an OD of 0.1) was added to sterile microcentrifuge tubes (this was based on initial experiments optimising the number of cells necessary for the assay). Volumes of 50 µl of the primary antibodies at a concentration of 1:20 (diluted in PBS with 0.1% BSA) were added to an aliquot of cells. These antibodies were the anti-rpL7/L12 rabbit serum and normal rabbit serum (Zymed). A control tube with no primary antibody was also prepared. The tubes were incubated on ice for 30 min after which the pellets were washed twice with chilled PBS by centrifugation as above. The pellets were

resuspended in 50 µl of the secondary antibody, (FITC conjugated sheep anti-rabbit [Silenus] diluted at 1:50 in PBS with 0.1% BSA) and incubated on ice for 30 min. The pellets were washed twice in PBS and resuspended in 0.5 ml of chilled 1% paraformaldehyde in PBS. The samples were then transferred to flow cytometry tubes and analysed on a Becton Dickinson FACScan, counting at least 10,000 events per sample.

The assay to determine whether the rpL7/L12 protein was located intracellularly involved the same strategy although saponin was added to introduce holes in the cell membrane to allow the antibodies to reach any internal proteins. The method used was as follows. The culture was washed twice with PBS before being fixed with 4% paraformaldehyde in PBS and being placed on ice for 2 h. The cells were washed twice with 1 ml of 0.1% saponin containing 1% FCS in PBS. The primary antibodies were the same as for the cell-surface assay although they were diluted in 0.3% saponin with 1% FCS in PBS and the cells were incubated at RT for 2 h. The cells were then washed twice as before and the secondary antibody added as in the cell-surface assay but diluted in 0.3% saponin with 1% FCS in PBS and incubated at RT for 1 h. Lastly the cells were washed once, resuspended in 1 ml PBS, transferred to flow cytometry tubes and subjected to FACScan analysis (Becton Dickinson).

5.2.9 Convalescent pig sera ELISA

To test the immunogenicity of rpL7/L12 this protein was reacted with convalescent pig sera as follows: wells of a 96 well ELISA plate (Nunc) were coated with 100 µl of a 10 µg/ml solution of recombinant rpL7/L12 protein (in PBS from section 5.2.5) in carbonate coating buffer. The plate was then incubated overnight at RT in a humidifying chamber for the protein to coat to the plate, washed and blocked as described previously (2.10). A

total of 16 different pig sera were chosen from a collection held at EMAI. Sera from pigs that had been tested for *M. hyopneumoniae* (using the *M. hyopneumoniae* ELISA diagnostic test used at EMAI) were selected. Pigs with various ELISA ratios (which indicate a positive or negative reaction; Djordjevic *et al*., 1994), ranging from 0-3 (negative), 5-10, 10-15 and 15 or above were chosen. These sera were diluted 1:100 with 1% w/v skim milk in PBS after which 100 µl of each was added to the wells of the ELISA plate. Wells not coated with rpL7/L12 were also incubated with each pig serum to ensure that serum antibodies were not non-specifically binding to the plate. After washing, goat anti-swine HRP conjugated antibody diluted 1:1000 in 1% w/v skim milk in PBS was then added to the ELISA plate. Wells with no rpL7/L12 or pig serum were also incubated with the goat anti-swine sera to check that these antibodies were not binding to the plate. Reactivity was detected with an ABTS solution as described previously (section 2.10).

Chapter 5: Characterization of *M. hyopneumoniae* ribosomal protein L7/L12

5.3 Results

5.3.1 Sequence similarity of L7/L12 between bacterial species

A similarity matrix generated from a ClustalW alignment showed that the *M. hyopneumoniae* L7/L12 protein sequence has greatest homology to those from other *Mycoplasma* species. The *M. hyopneumoniae* L7/L12 protein sequence displayed 57%, 43% and 45% identity and 76%, 65% and 65% similarity to sequences from *M. pulmonis*, *M. genitalium* and *M. pneumoniae*, respectively.

Ribosomal proteins belonging to the L7/L12 family of bacteria share strong amino acid sequence identity (Kolberg *et al*., 1997). Alignment of the complete amino acid sequences available for L7/L12 ribosomal proteins from 27 different bacterial species is shown in Fig. 5.3. The C-terminus contains the highly conserved regions, whereas there is less sequence conservation at the N-terminus. A consensus tree containing 27 sequences from pylogenetically diverse bacteria was also constructed from this data using Phylip (Fig. 5.4).

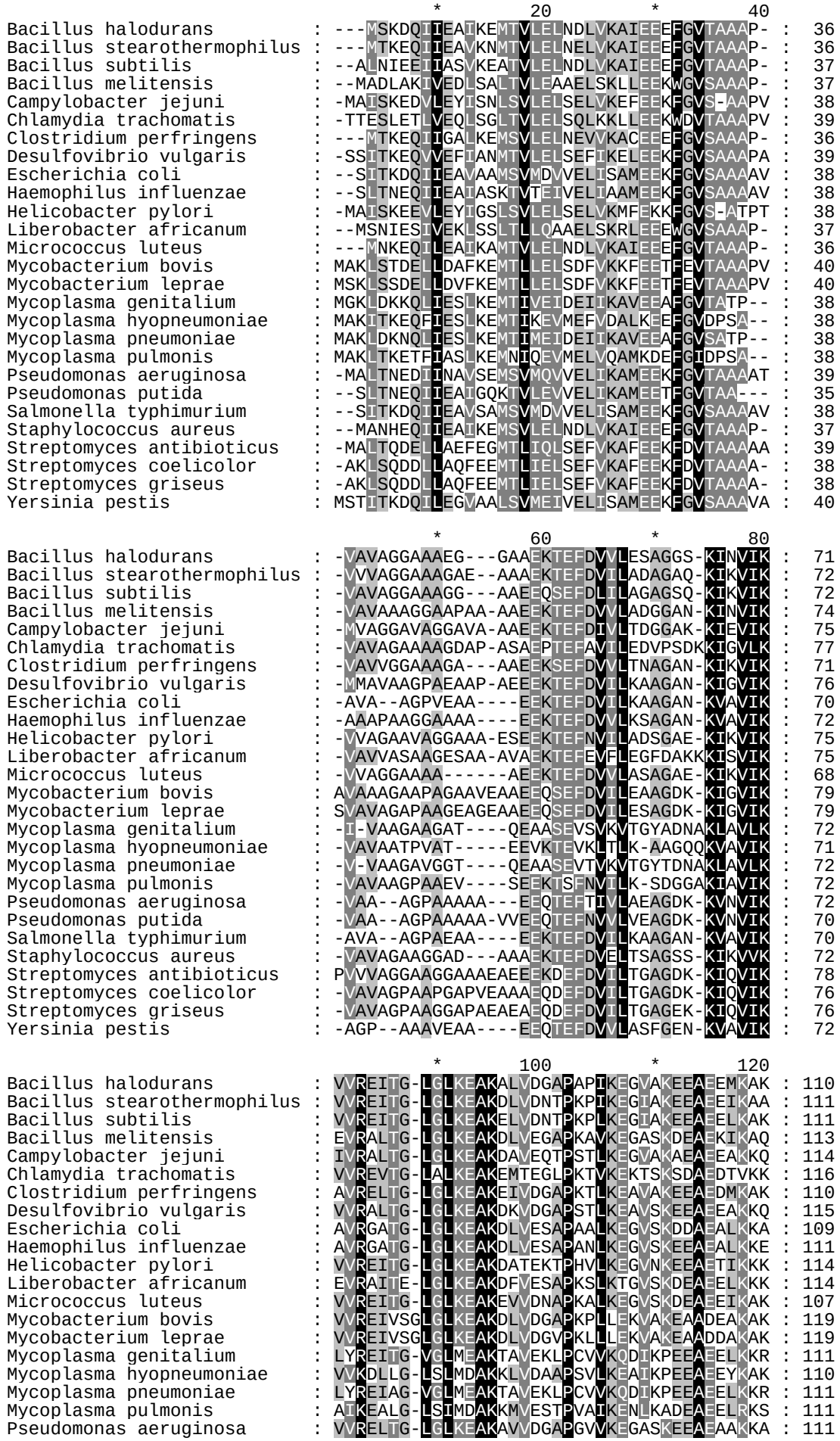
Bacillus halodurans
Bacillus stearothermophilus
Bacillus subtilis
Bacillus melitensis
Campylobacter jejuni
Chlamydia trachomatis
Clostridium perfringens
Desulfovibrio vulgaris
Escherichia coli
Haemophilus influenzae
Helicobacter pylori
Liberobacter africanum
Micrococcus luteus
Mycobacterium bovis
Mycobacterium leprae
Mycoplasma genitalium
Mycoplasma hyopneumoniae
Mycoplasma pneumoniae
Mycoplasma pulmonis
Pseudomonas aeruginosa
Pseudomonas putida
Salmonella typhimurium
Staphylococcus aureus
Streptomyces antibioticus
Streptomyces coelicolor
Streptomyces griseus
Yersinia pestis

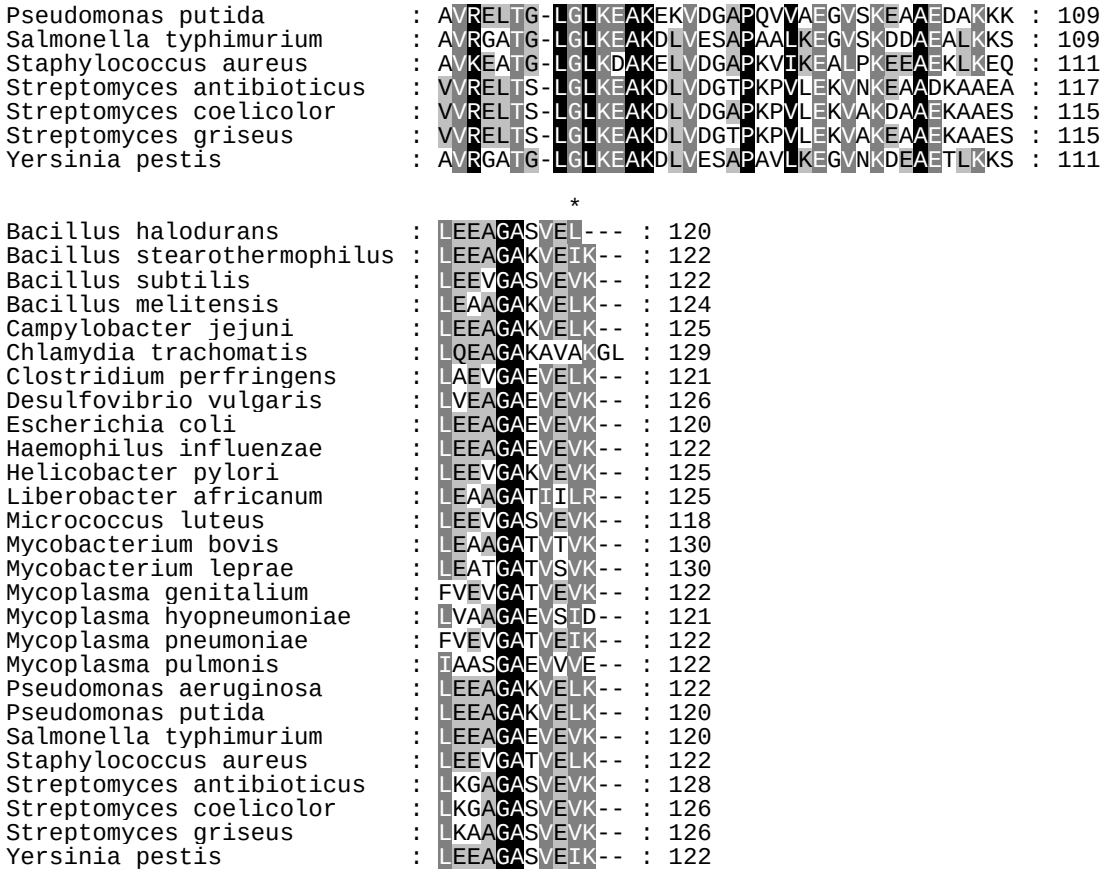

Fig. 5.3. ClustalW alignment of the complete amino acid sequences available for L7/L12 ribosomal proteins from 27 diverse bacterial species. Black shading indicates areas where all (100%) species show conservation, dark grey highlights the areas that are 80% conserved among species and light grey shading shows the areas where 60% of all bacterial species show conservation.

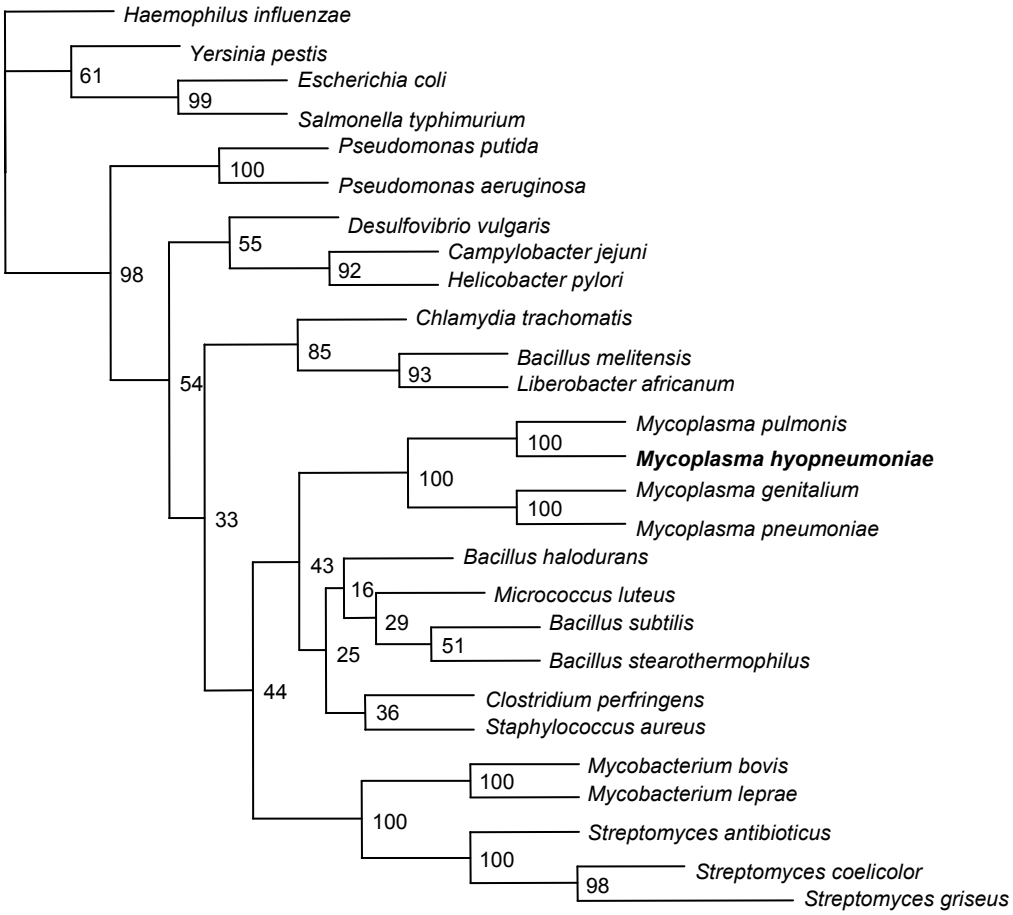

Fig. 5.4. A phylogenetic tree showing the relationship between rpL7/L12 proteins of various bacterial species. The numbers on the nodes represent bootstrap values from 100 replicates.

5.3.2 Cloning and expression of rpL7/L12 in *Escherichia coli*

The *rpL7/L12* gene of *M. hyopneumoniae* strain 232 was cloned into *E. coli* strain M15, the gene contains 363 nucleotides encoding a protein of 121 amino acids and the sequence of the gene is displayed in Fig. 5.5.

```
    M  A  K  I  T  K  E  Q  F  I  E  S  L  K  E  M  T  I  K  E   -

    ATGGCTAAAATTACAAAAGAACAATTTATTGAATCATTAAAAGAAATGACCATTAAAGAA
1   ---------+---------+---------+---------+---------+---------+  60
    TACCGATTTTAATGTTTTCTTGTTAAATAACTTAGTAATTTTCTTTACTGGTAATTTCTT

    V  M  E  F  V  D  A  L  K  E  E  F  G  V  D  P  S  A  V  A   -

    GTAATGGAATTTGTTGATGCACTTAAAGAAGAATTTGGAGTTGATCCATCAGCAGTTGCA
61  ---------+---------+---------+---------+---------+---------+ 120
    CATTACCTTAAACAACTACGTGAATTTCTTCTTAAACCTCAACTAGGTAGTCGTCAACGT

    V  A  A  T  P  V  A  T  E  E  V  K  T  E  V  K  L  T  L  K    -

    GTAGCTGCAACTCCAGTTGCTACCGAAGAGGTAAAAACCGAAGTAAAATTAACACTCAAA
121 ---------+---------+---------+---------+---------+---------+ 180
    CATCGACGTTGAGGTCAACGATGGCTTCTCCATTTTTGGCTTCATTTTAATTGTGAGTTT

    A  A  G  Q  Q  K  V  A  V  I  K  V  V  K  D  L  L  G  L  S   -
    GCTGCCGGACAACAAAAAGTTGCTGTAATTAAAGTAGTAAAAGATCTTTTAGGTCTAAGT
181 ---------+---------+---------+---------+---------+---------+ 240
    CGACGGCCTGTTGTTTTTCAACGACATTAATTTCATCATTTTCTAGAAAATCCAGATTCA

    L  M  D  A  K  K  L  V  D  A  A  P  S  V  L  K  E  A  I  K   -
    CTAATGGATGCAAAAAAACTTGTTGATGCAGCCCCTTCAGTTCTCAAAGAGGCAATAAAA
241 ---------+---------+---------+---------+---------+---------+ 300
    GATTACCTACGTTTTTTTGAACAACTACGTCGGGGAAGTCAAGAGTTTCTCCGTTATTTT

    P  E  E  A  E  E  Y  K  A  K  L  V  A  A  G  A  E  V  S  I   -
    CCTGAAGAAGCTGAAGAATATAAAGCAAAATTAGTCGCAGCGGGAGCAGAAGTTTCGATT
301 ---------+---------+---------+---------+---------+---------+ 360
    GGACTTCTTCGACTTCTTATATTTCGTTTTAATCAGCGTCGCCCTCGTCTTCAAAGCTAA

    D   -
    GAC
361 --- 363
    CTG
```

Fig. 5.5. The sequence of the *rpL7/L12* gene from *M. hyopneumoniae*. The primer sequences (rpL7/L12 forward and rpL7/L12 reverse) used for PCR amplification are shaded in grey.

Following PCR, the 363 bp product and the pQE-9 vector were digested with the restriction enzymes *Bam*H1 and *Hin*DIII and then ligated together. The construct is shown in Fig. 5.6. The ligated vector was then transformed into competent *E. coli* M15 [pREP4] cells which were plated onto selective media and the colonies screened for recombinants. Positive clones contained both the pQE-9 and *rpL7/L12* bands following restriction enzyme digestion (Fig. 5.6B).

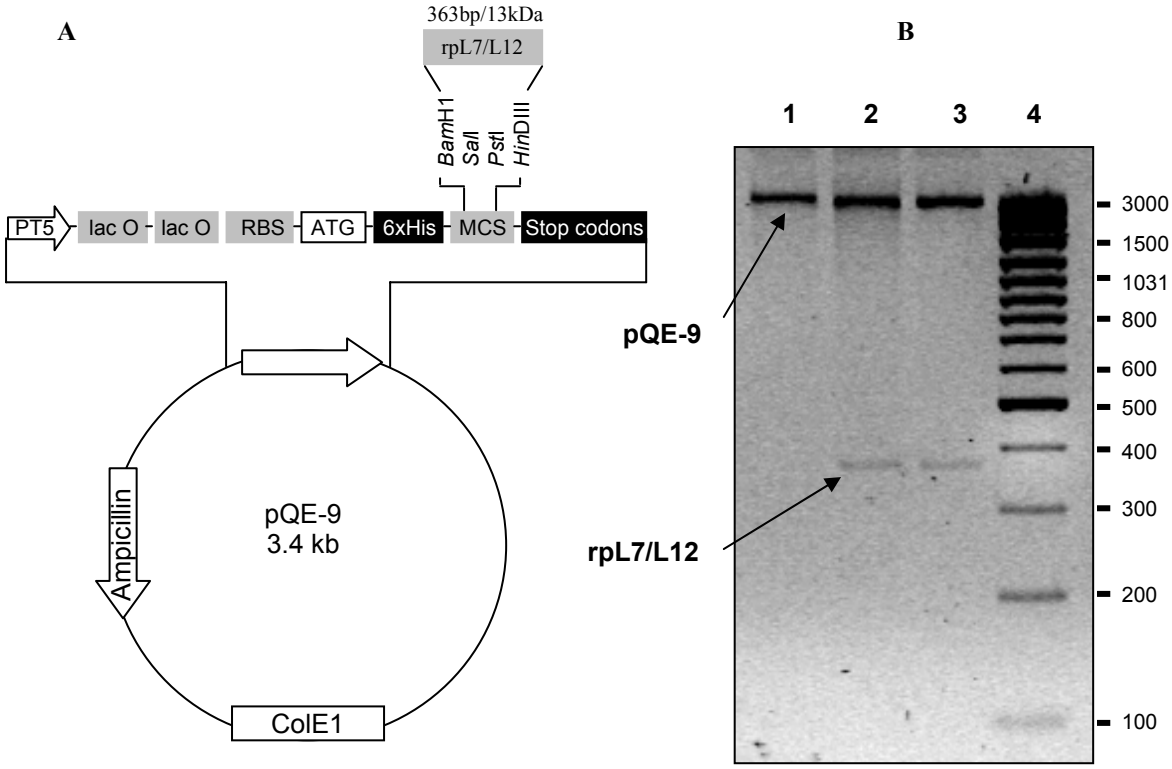

Fig. 5.6. (A) pQE-9 cloning vector showing the multiple cloning site (MCS) and the *rpL7/L12* gene inserted between the *Bam*H1 and *Hin*DIII sites. Also depicted is the ColE1origin of replication, an ampicillin resistance gene (*bla*, to aid in screening for recombinants), the phage T5 promoter (PT5), two *lac* operator sequences which increase *lac* repressor binding, ribosome binding site (RBS) for high translation rates, ATG translation start codon, the 6x Histidine-tag, the multiple cloning site (MCS) and a cluster of translational stop codons in all reading frames. (B) B*am*H1 and *Hin*DIII restriction digest of *M. hyopneumoniae* 232 rpL7/L12 pQE-9 clones on an agarose gel. Lane 1 shows a vector only control, whereas lanes 2 and 3 contain the rpL7/L12 insert and are designated pTB1 and pTB2. The 100 bp DNA ladder plus marker is included in lane 4 and the values of bands in bp are given.

5.3.3 Verifying recombinant rpL7/L12 expression and the production of rabbit polyclonal antiserum

DNA sequence analysis confirmed the identity and integrity of the *rpL7/L12* gene within the pTB1 plasmid. PCR amplification of the *rpL7/L12* gene from *M. hyopneumoniae* strain J using primers rpL7/L12 forward and reverse generated a 363 bp fragment as expected. DNA sequence analysis confirmed that *rpL7/L12* from both strains were identical (results not shown).

Fig. 5.7 shows the purified rpL7/L12 as it appears on a reducing 15% SDS-PAGE gel, and after western analysis with the anti-rpL7/L12 rabbit serum that was raised using the purified rpL7/L12 protein. The antiserum also reacts with two higher molecular weight bands. These bands may represent multimers of the rpL7/L12 molecule although this would need further verification. The identity of the protein expressed from pTB1 was examined using MALDI-TOF mass-spectrometry. Fig. 5.8 below shows the results of the peptide matches obtained in this analysis after excision of the rpL7/L12 band in Fig. 5.7 (circled).

5.3.4 Expression pattern of *M. hyopneumoniae* rpL7/L12 in strains 232 and J

Whole cell protein samples from *in vitro* cultures of the pathogenic *M. hyopneumoniae* strain 232 and non-pathogenic J strain were analyzed for the expression of rpL7/L12. RpL7/L12 is expressed by both strains at an apparent molecular weight of 14 kDa, Fig. 5.9. The higher band of approximately 30 kDa detected by the antiserum is expressed by both strains although to a greater extent in strain J and may possibly represent a multimeric form of rpL7/L12.

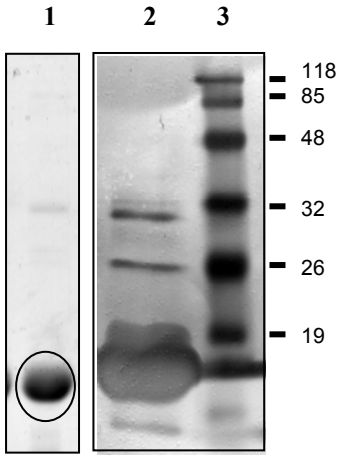

Fig. 5.7. SDS-PAGE and immunoblot analyses of rpL7/L12. 15% polyacrylamide gel containing purified rpL7/L12 (lane 1), and purified rpL7/L12 reacted with rabbit antisera to rpL7/L12 (lane 2). Lane 3 contains the molecular weight marker.

1 MAKITKEQFIESLKEMTIKEVMEFVDALKEEFGVDPSAVAVAATPVATEEVKTEVKLTLKAA
GQQKVAVIKVVKDLLGLSLMDAKKLVDAAPSVLKEAIKPEEAEEYKAKLVAAGAEVSID 121

Fig. 5.8. Peptide matches (underlined) as they align on the entire sequence of rpL7/L12 from MALDI-TOF mass-spectrometry analysis of the recombinant rpL7/L12 expression product from *E. coli*, circled in Fig. 5.7.

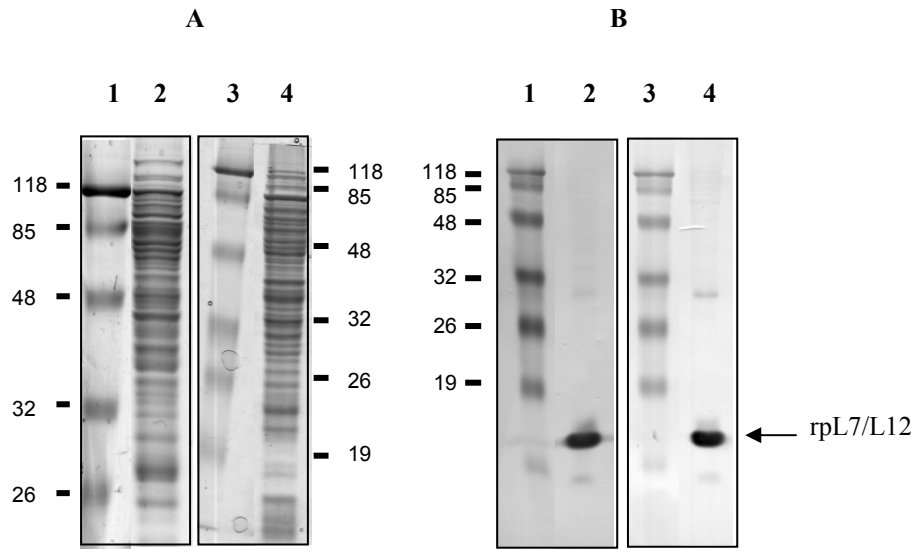

Fig. 5.9. Western blot images of whole cell protein preparations of *M. hyopneumoniae* 232 and *M. hyopneumoniae* J reacted with anti-rpL7/L12 rabbit sera. (A) Whole cell lysate protein preparations of *M. hyopneumoniae* strains 232 (lane 2) and J (lane 4) on SDS-PAGE gels stained in Coomassie. (B) Western blot images of whole cell protein preparations of *M. hyopneumoniae* 232 (lane 2) and *M. hyopneumoniae* J (lane 4) reacted with anti-rpL7/L12 rabbit sera. The markers are the same for all images and the sizes are as indicated, in kilodaltons.

5.3.5 rpL7/L12 is expressed inside the *M. hyopneumoniae* cell

Figure 5.10 displays the results of FACScan analysis with anti-rpL7/L12 rabbit serum. After analyzing the external surface of *M. hyopneumoniae* using intact cells and being unable to detect the presence of rpL7/L12 (Fig. 5.10A), an assay using saponin treated cells was conducted which perforated the *M. hyopneumoniae* cells. Saponin treated cells were found to react with the antisera resulting in a shift in fluorescence intensity of the peak, indicating rpL7/L12 is expressed inside the *M. hyopneumoniae* cell (Fig. 5.10B). Purified normal rabbit serum (Zymed) failed to react with *M. hyopneumoniae* cells, either without (Fig. 5.10C) or with (Fig. 5.10D) saponin treatment.

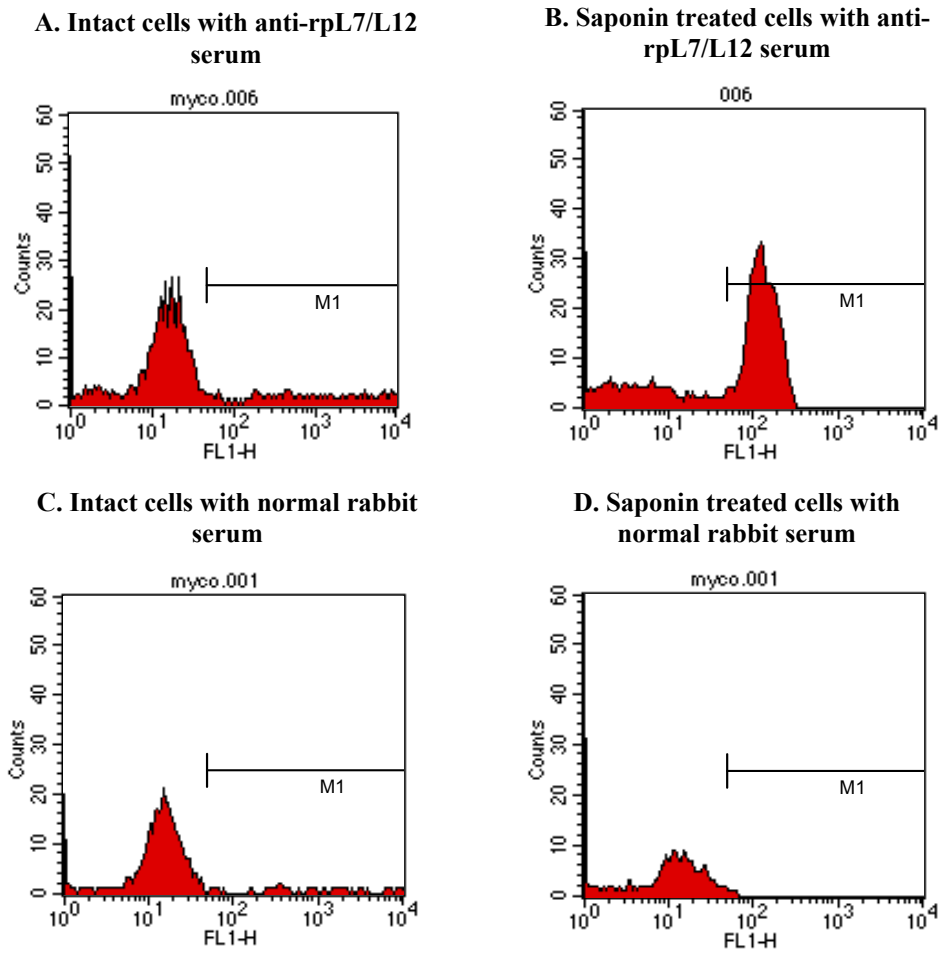

Fig. 5.10. FACScan analysis with anti-rpL7/L12 rabbit serum and normal rabbit serum. A and C represent intact *M. hyopneumoniae* cells whereas B and D represent saponin treated cells. A and B were reacted with anti-rpL7/L12 serum whilst C and D were reacted with commercial normal rabbit serum. Highlighted with a bar is the area of interest (M1) in the histograms with a peak present in B but not in A, C or D. The x-axis is a logarithmic scale while the y-axis is a numerical scale of fluorescent counts.

The data generated from the FACScan histograms are presented in Table 5.2. From this table we see a distinct positive reaction with the anti-rpL7/L12 sera, when analyzing saponin treated *M. hyopneumoniae* cells (highlighted).

Table 5.2. FACScan analysis of *M. hyopneumoniae* intact cells and saponin-treated cells with anti-rpL7/L12 serum and normal rabbit serum. Positive results are highlighted.

Intact *M. hyopneumoniae* cells		
	Normal rabbit serum	Anti-rpL7/L12 serum
% Gated[a]	10.05	12.44
Median of M1 region[b]	850.53	809.47

Saponin treated *M. hyopneumoniae* cells		
	Normal rabbit serum	Anti-rpL7/L12 serum
% Gated[a]	1.58	60.94
Median of M1 region[b]	61.53	120.79

[a] represents the percentage that the M1 region represents of the entire histogram. The higher the value indicates a more positive result due to the presence of a peak in the M1 region.
[b] the middle fluorescent value for the M1 region only, once again the higher the value the more positive the result.
These results are based on comparison with the normal rabbit serum control as this represents the fluorescence detected when normal serum from rabbits is incubated with *M. hyopneumoniae* cells.

5.3.6 rpL7/L12 is recognized by convalescent pig sera

A selection of porcine sera previously tested using an accredited enzyme-linked immunosorbent assay (Djordjevic *et al*., 1994) were used to determine if swine with a history of exposure to *M. hyopneumoniae* generate antibodies to rpL7/L12. The pig sera were separated into four groups based on their ELISA ratios. Negative samples are those with an ELISA ratio below 3, sera with ratios between 5 and 10, 10 and 15, and 15 or above were also tested. Table 5.4 shows the ELISA ratio obtained in the *M. hyopneumoniae* ELISA (conducted by J. Gonsalves, EMAI). The pig sera showing significant OD's (above an arbitrary 0.2 cut-off) when reacted with rpL7/L12 are highlighted.

Table 5.3. *M. hyopneumoniae* (EMAI) ELISA ratios for each of the 16 pig sera used in the rpL7/L12 ELISA. The ELISA grouping of each is also shown based on these ratios. Highlighted are those pig sera that gave significant OD values (above 0.2) when reacted with rpL7/L12.

Pig	Actual ELISA ratio	ELISA status
Pig 1	Less than 3	negative
Pig 2	Less than 3	negative
Pig 3	Less than 3	negative
Pig 4	9.12	5-10
Pig 5	7.77	5-10
Pig 6	8.39	5-10
Pig 7	8.79	5-10
Pig 8	13.53	10-15
Pig 9	12.22	10-15
Pig 10	10.65	10-15
Pig 11	13.75	10-15
Pig 12	22.77	≥15
Pig 13	19.02	≥15
Pig 14	15.14	≥15
Pig 15	18.17	≥15
Pig 16	17.66	≥15

Fig. 5.11 below shows the results when recombinant rpL7/L12 was reacted with each of the 16 pig sera from table 5.3 above. Six serum samples reacted (OD $\geq$ 0.2) with rpL7/L12, these were sera 5, 6, 8, 10, 11 and 15.

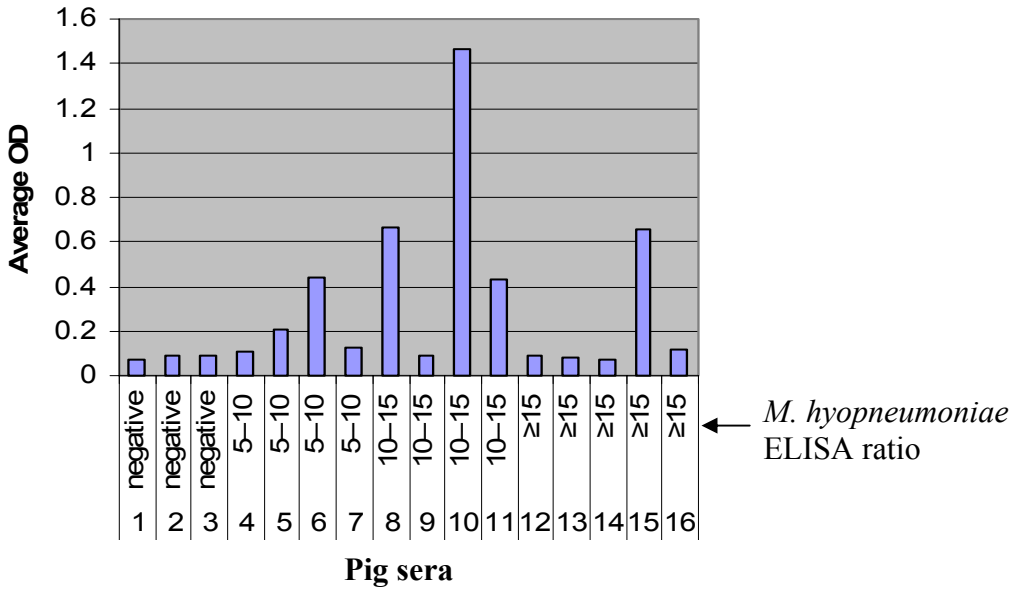

Fig. 5.11. Reactivity of rpL7/L12 with 16 different convalescent pig sera. These are the average OD values obtained from duplicate samples.

5.4 Discussion

Ribosomal protein L7/L12 has been shown to play a role in the pathogenesis of a number of bacterial pathogens *in vitro*. For example in *Neisseria gonorrhoeae*, rpL12 plays a role in the invasion of human reproductive cells (human endometrial cell line, Hec1B). The observation that the rpL7/L12 protein of *M. hyopneumoniae* did react with a subset of convalescent pig sera indicates that this protein is immunogenic and expressed during the course of infection. Flow cytometry experiments did not detect rpL7/L12 expression on the surface of intact *M. hyopneumoniae* cells as had been previously described for *N. gonorrhoeae* (Spence and Clarke, 2000).

The consensus tree constructed from rpL7/L12 protein sequences from 27 phylogenetically diverse bacteria showed *M. hyopneumoniae* clustered together with the other *Mycoplasma* species. The *Mycoplasma* species were found to be most closely related to other members of the firmicutes, such as the *Bacillus* species, *Clostridium perfringens* and *Staphylococcus aureus*.

The fact that both strains of *Mycoplasma hyopneumoniae* (232 and J) expressed the rpL7/L12 molecule is likely attributed to its important function in the translocation step of translation and was not unexpected. A sequence alignment and phylogenetic tree from these sequences demonstrate the highly conserved nature of this protein. DNA sequencing data demonstrated this molecule to be identical in both *M. hyopneumoniae* strains. The 14 kDa rpL7/L12 band was detected in both strains of *M. hyopneumoniae* when reacted with anti-rpL7/L12 serum, representing the monomer of this protein. However, a second band

of approximately 30 kDa was also detected which might represent a SDS-stable dimer of rpL7/L12. The polyhistidine fusion protein expressed in *E. coli* also showed the possibility of multimer formation due to the production of extra bands at approximately 26 kDa and 30 kDa during the purification process. These bands remained even after the protein sample was reduced in a buffer containing β-mercaptoethanol and SDS and heat treatment at 100^{o}C for 5 min. The samples from the purification and in the *M. hyopneumoniae* whole cell extracts were not produced in sufficient quantities to allow identification by MALDI-TOF mass spectrometry. However identification of these protein bands is required to verify the hypothesis that these higher molecular weight bands consist of rpL7/L12.

Bachrach *et al.* (1997) showed that the ribosomal protein L7/L12 isolated from *Brucella melitensis* induces a DTH reaction in Brucella-sensitised guinea pigs. Surprisingly, the recombinant Brucella L7/L12 protein expressed in *E. coli* as a fusion protein with a six-Histidine tag cannot elicit such a reaction. The histidine tag on the recombinant L7/L12 protein was removed enzymatically, but the resulting protein did not induce a DTH reaction in sensitized animals (Bachrach *et al*., 1997). Incubation of the recombinant L7/L12 fusion protein in a *B. melitensis* lysate endowed the recombinant protein with a DTH activity, suggesting that the recombinant protein was modified by this treatment. It was shown that acetylation of the *Brucella* L7/L12 protein is crucial for the proteins recognition by the host cells that trigger the DTH reaction (Bachrach *et al*., 1997). This could also be true for the *M. hyopneumoniae* L7/L12 protein, where post-translational modification that might occur in *M. hyopneumoniae* may not occur in the *E. coli* expression strain.

In conclusion, rpL7/L12 is recognised by a subset of convalescent pig sera and this protein appears to be highly conserved within *M. hyopneumoniae* strains. Further work is required to examine the immunological status of swine to this antigen, however this recombinant poly-histidine fusion protein represents an excellent negative control of a *M. hyopneumoniae* derived protein for ligand binding studies.

Chapter 6: General Discussion and Future Studies

M. hyopneumoniae is the etiological agent of porcine enzootic pneumonia and significantly impacts swine production (Ross, 1992). *M. hyopneumoniae* adheres exclusively to ciliated cells of the respiratory tract and this colonization disrupts the normal function of the mucociliary escalator through ciliostasis, loss of cilia and acute inflammation. The disease can be resolved after a long period but *M. hyopneumoniae* colonization predisposes the host to secondary infections and more severe and longer lasting diseases (Frey *et al*., 1994; Ross, 1992). Current vaccines are unsatisfactory as they do not protect against colonization and vaccinated herds can still develop disease (Thacker *et al*., 1998).

For cilial damage to occur, *M. hyopneumoniae* must attach to the swine respiratory epithelial cells (Zielinski and Ross, 1990; DeBey and Ross 1994). Non-pathogenic *M. hyopneumoniae* and excessively *in vitro* passaged *M. hyopneumoniae* do not adhere to ciliated cells (Zielinski and Ross, 1990), and are therefore unable to colonize the respiratory epithelium and establish infection. It is therefore important to identify the adhesins associated with attachment of pathogenic *M. hyopneumoniae in vivo* for production of vaccines that prevent infection in the pig (DeBey and Ross, 1994).

Ribosomal protein L7/L12 has been shown to play a role in the pathogenesis of a number of bacterial pathogens *in vitro* and has been identified as one of the dominant immunoreactive proteins in pathogens such as *Chlamydia trachomatis* (Sanchez-Campillo *et al*., 1999), *Brucella abortus* (Oliveira and Splitter, 1996) and *Brucella melitensis* (Bachrach *et al*., 1997). This protein has been found to be expressed on the cell surface of some pathogenic bacteria, including *Neisseria gonorrhoeae* (Spence and Clarke, 2000).

Further work has shown this molecule to be internally expressed in *M. hyopneumoniae* and that this protein has immunogenic properties due to its reactivity with convalescent pig serum. This protein may be a good target for antimicrobial therapy and vaccine development because of its immunogenic properties and has been useful in this study as an *E. coli* expressed His-tagged protein control for adherence assays, including radioactive experiments and ELISAs (results not shown), due to its inability to adhere to the ECM components analysed.

Pre-incubation of *M. hyopneumoniae* cells with periodate and trypsin abolished attachment of *M. hyopneumoniae* to ciliated respiratory tract cells (Zielinski and Ross, 1993), indicating that adherence is mediated by carbohydrates and proteins on the surface of the organism. A 97 kDa surface protein of *M. hyopneumoniae*, P97, has been implicated as playing a role in host cell adhesion. However, monoclonal antibodies F1B6 and F2G5, which recognise P97 in immunoblots, reduce adherence of *M. hyopneumoniae* (*in vitro*) to purified cilia and to ciliated cells by only 67% (Zhang *et al*., 1995). These authors proposed that other molecules must be involved in adherence.

Analysis of the *M. hyopneumoniae* genome for paralogs of the gene for the P97 cilium adhesin and the adjacent locus *p102*, revealed the presence of six adhesin parolog operons. The *p159* gene is found in one of these operons adjacent to a *p97* paralog but shows no resemblance to *p97* or *p102*. Two-dimensional gel electrophoresis revealed that P159 is cleaved into distinct fragments. Cleavage of surface proteins has been reported for other *Mycoplasma* species (Davis and Wise, 2002) and for the P97 cilium adhesin of *M. hyopneumoniae* (Djordjevic *et al.*, 2004). The protease(s) involved in the cleavage of P159 and P97 remain to be determined and is the focus of further research.

This study has shown that at least regions of P159 are surface expressed *in vitro* and that this molecule is highly immunogenic. P159 may therefore be a candidate for antimicrobial therapy against *M. hyopneumoniae*, such as in a multi-subunit vaccine. The C-terminal half of the P159 molecule was shown to bind to heparin which may play a role in the adherence of *M. hyopneumoniae* to swine respiratory cilia. Some pathogenic bacteria have been shown to bind heparin which can then bind to further components on the surface of cells, thereby acting as a bridging molecule (Duensing *et al*., 1999; Ljungh *et al*., 1996; Van Putten *et al*., 1998). Future work will aim at determining whether, through molecules such as P159 and P97 (also a heparin binding protein, Djordjevic *et al*., 2004 IOM), *M. hyopneumoniae* may be binding directly to heparin on the swine ciliated cells or to heparin as a bridging molecule.

Portions of the P159 molecule were shown to have the ability to adhere to a porcine kidney epithelial cell line (PK15). Whole *M. hyopneumoniae* cells also showed the ability to adhere to these cells and it is possible that the surface exposed P159 molecules are involved in the adherence of the bacteria to the PK15 cells. Parts of the P159 protein also showed the ability to cross the PK15 cell membrane, although the mechanism utilized for this is unknown. As whole *Mycoplasma* cells were not able to invade PK15 cells it could be that P159 molecules are released from the bacteria and are able to invade the PK15 cells, although this remains to be determined. The accumulation of flask or omega-shape like structures in the PK15 cell membrane in the near vicinity to attached bacteria which resemble caveolae may represent a mode for entry of the secreted proteins. Caveolae (which are found in a variety of mammalian cells; Anderson, 1998) represent an entry port for pathogenic agents such as viruses, bacteria and parasites (Couet *et al*., 2001; Norkin, 2001; Marjomäki *et al*., 2002; Shin and Abraham, 2001a,b,c,d; Shin *et al*., 2000). For example, caveolae have been shown to act as an entry port for group A streptococci

into epithelial and endothelial cells (Rohde *et al*., 2003). Incubation of cells with SfbI protein also triggered accumulation of caveolae showing that SfbI is the triggering factor that activates the caveolae-mediated endocytic pathway (Rohde *et al*., 2003). Future work will be aimed at determining whether these structures are caveolae and whether or not proteins, including P159, secreted from *M. hyopneumoniae* cells utilize these caveolae to enter PK15 cells.

P159 can bind heparin; whether this ability is utilized in the adherence to PK15 cells remains to be determined. That is, heparin molecules may be produced by PK15 cells or supplied by the media. *M. hyopneumoniae* may bind to these heparin molecules on the PK15 cells through the P159 molecule or other heparin binding proteins on the surface of *M. hyopneumoniae*.

P159 cleavage fragments are found on the surface of *M. hyopneumoniae* however, it is not clear from these studies how P159 cleavage fragments that lack a putative transmembrane domain(s) remain associated with the cell surface after cells are harvested from culture and washed several times with PBS. The N-terminal protein P27 is the only cleavage fragment that possesses a hydrophobic stretch of amino acids that would be predicted to span the cell membrane. It is possible that this transmembrane domain allows transfer of the entire P159 molecule to the surface of the *M. hyopneumoniae* cell where it is further processed and cleaved. Similar to P159, the cilium adhesin P97 only possesses a single putative N-terminal leader peptide that is capable of spanning the cell membrane (Djordjevic *et al*., 2004). Recently Djordjevic and colleagues have demonstrated that the C-terminal third of P97, the region that contains the cilium binding domain R1 (Minion *et al*., 2000) is found associated with the cell surface (Djordjevic *et al*., 2004). This portion of the molecule binds strongly to porcine and human fibronectin and like P159, to the

glycosaminoglycan heparin (Djordjevic *et al*., 2004 IOM). P159 fragments possess the ability to remain attached to the cell surface either by protein-protein interactions with other surface anchored membrane proteins or sequestering ECM and other medium components to the surface, such as heparin. ECM components can be found on epithelial surfaces, including those that line the respiratory tract and we propose that the ability to sequester ECM components to the surface of the *M. hyopneumoniae* cell may play a role in facilitating adherence and colonisation and possibly immune evasion in the porcine respiratory tract.

In conclusion, the P159 protein of *M. hyopneumoniae* was shown to be post-translationally cleaved and parts of this molecule were found to be expressed on the surface of *M. hyopneumoniae*. P159 also reacted with convalescent pig serum and the C-terminal half of the molecule bound to the glycosaminoglycan heparin. Parts of the molecule were also shown to bind to and cross the cell membrane of porcine epithelial (PK15) cells. This data collectively indicates the potential of P159 as a *M. hyopneumoniae* adhesin and future work will aim at verifying this hypothesis and determining the adhesive mechanism utilised to further understand the pathogenic mechanisms of *M. hyopneumoniae* and to control infections in swine.

References

Alvarez-Dominguez, C., Vazquez-Boland, J.A., Carrasco-Marin, E., Lopez-Mato, P., and Leyva-Cobian, F. (1997) Host cell heparan sulfate proteoglycans mediate attachment and entry of *Listeria monocytogenes*, and the listerial surface protein ActA is involved in heparan sulfate receptor recognition. *Infect Immun* **65**: 78-88.

Anderson, R.G. (1998) The caveolae membrane system. *Annu Rev Biochem* **67**: 199-225.

Aoki, K., Matsumoto, S., Hirayama, Y., Wada, T., Ozeki, Y., Niki, M., Domenech, P., Umemori, K., Yamamoto, S., Mineda, A., Matsumoto, M., and Kobayashi, K. (2004) Extracellular mycobacterial DNA-binding protein 1 participates in mycobacterium-lung epithelial cell interaction through hyaluronic acid. *J Biol Chem* **279**: 39798-39806.

Arumugham, R.G., Hsieh, T.C., Tanzer, M.L., and Laine, R.A. (1986) Structures of the asparagine-linked sugar chains of laminin. *Biochim Biophys Acta* **883**: 112-126.

Bachrach, G., Banai, M., Bardenstein, S., Hoida, G., Genizi, A., and Bercovier, H. (1994) Brucella ribosomal protein L7/L12 is a major component in the antigenicity of brucellin INRA for delayed-type hypersensitivity in brucella-sensitized guinea pigs. *Infect Immun* **62**: 5361-5366.

Bachrach, G., Banai, M., Fishman, Y., and Bercovier, H. (1997) Delayed-type hypersensitivity activity of the Brucella L7/L12 ribosomal protein depends on posttranslational modification. *Infect Immun* **65**: 267-271.

Baker, R.E., Hill, W.E., and Larson, C.L. (1973) Ribosomes of acid-fast bacilli: immunogenicity, serology, and *in vitro* correlates of delayed hypersensitivity. *Infect Immun* **8**: 236-244.

Barrow, R.T., Parker, E.T., Krishnaswamy, S., and Lollar, P. (1994) Inhibition by heparin of the human blood coagulation intrinsic pathway factor X activator. *J Biol Chem* **269**: 26796-26800.

Baseggio, N., Glew, M.D., Markham, P.F., Whithear, K.G., and Browning, G.F. (1996) Size and genomic location of the pMGA multigene family of *Mycoplasma gallisepticum*. *Microbiology* **142 (Pt 6)**: 1429-1435.

Baseman, J.B., Cole, R.M., Krause, D.C., and Leith, D.K. (1982) Molecular basis for cytadsorption of *Mycoplasma pneumoniae*. *J Bacteriol* **151**: 1514-1522.

Baseman, J.B., Lange, M., Criscimagna, N.L., Giron, J.A., and Thomas, C.A. (1995) Interplay between mycoplasmas and host target cells. *Microb Pathog* **19**: 105-116.

Baseman, J.B., and Tully, J.G. (1997) Mycoplasmas: sophisticated, reemerging, and burdened by their notoriety. *Emerg Infect Dis* **3**: 21-32.

Bauer, M.E., and Spinola, S.M. (1999) Binding of *Haemophilus ducreyi* to extracellular matrix proteins. *Infect Immun* **67**: 2649-2652.

Beck, K., Hunter, I., and Engel, J. (1990) Structure and function of laminin: anatomy of a multidomain glycoprotein. *FASEB J* **4**: 148-160.

Bernfield, M., Gotte, M., Park, P.W., Reizes, O., Fitzgerald, M.L., Lincecum, J., and Zako, M. (1999) Functions of cell surface heparan sulfate proteoglycans. *Annu Rev Biochem* **68**: 729-777.

Blanchard, B., Vena, M.M., Cavalier, A., Le Lannic, J., Gouranton, J., and Kobisch, M. (1992) Electron microscopic observation of the respiratory tract of SPF piglets inoculated with *Mycoplasma hyopneumoniae*. *Vet Microbiol* **30**: 329-341.

Blaser, M.J., and Parsonnet, J. (1994) Parasitism by the "slow" bacterium *Helicobacter pylori* leads to altered gastric homeostasis and neoplasia. *J Clin Invest* **94**: 4-8.

Bocharov, E.V., Gudkov, A.T., and Arseniev, A.S. (1996) Topology of the secondary structure elements of ribosomal protein L7/L12 from *E. coli* in solution. *FEBS Lett* **379**: 291-294.

Boden, M.K., and Flock, J.I. (1989) Fibrinogen-binding protein/clumping factor from *Staphylococcus aureus*. *Infect Immun* **57**: 2358-2363.

Bove, J.M. (1993) Molecular features of mollicutes. *Clin Infect Dis* **17**: S10-31.

Bower, K., Djordjevic, S.P., Andronicos, N.M., and Ranson, M. (2003) Cell surface antigens of Mycoplasma species bovine group 7 bind to and activate plasminogen. *Infect Immun* **71**: 4823-4827.

Brooks-Worrell, B.M., and Splitter, G.A. (1992) Antigens of *Brucella abortus* S19 immunodominant for bovine lymphocytes as identified by one- and two-dimensional cellular immunoblotting. *Infect Immun* **60**: 2459-2464.

Burnette, W.N. (1981) "Western blotting": electrophoretic transfer of proteins from sodium dodecyl sulfate--polyacrylamide gels to unmodified nitrocellulose and radiographic detection with antibody and radioiodinated protein A. *Anal Biochem* **112**: 195-203.

Burns, D.L. (1999) Biochemistry of type IV secretion. *Curr Opin Microbiol* **2**: 25-29.

Buttenschon, J., Friis, N.F., Aalbaek, B., Jensen, T.K., Iburg, T., and Mousing, J. (1997) Microbiology and pathology of fibrinous pericarditis in Danish slaughter pigs. *Zentralbl Veterinarmed A* **44**: 271-280.

Caparon, M.G., Stephens, D.S., Olsen, A., and Scott, J.R. (1991) Role of M protein in adherence of group A streptococci. *Infect Immun* **59**: 1811-1817.

Cardin, A.D., and Weintraub, H.J. (1989) Molecular modeling of protein-glycosaminoglycan interactions. *Arteriosclerosis* **9**: 21-32.

Carle, P., Laigret, F., Tully, J.G., and Bove, J.M. (1995) Heterogeneity of genome sizes within the genus Spiroplasma. *Int J Syst Bacteriol* **45**: 178-181.

Carson, S.E. (1989) The structure and function of fibronectin. In *Fibronectin in health and disease*. Carson, S.E. (ed). Boca Raton, Fla.: CRC Press, Inc., pp. 1-21.

Chen, T., Belland, R.J., Wilson, J., and Swanson, J. (1995a) Adherence of pilus- Opa+ gonococci to epithelial cells *in vitro* involves heparan sulfate. *J Exp Med* **182**: 511-517.

Chen, T., Swanson, J., Wilson, J., and Belland, R.J. (1995b) Heparin protects Opa+ *Neisseria gonorrhoeae* from the bactericidal action of normal human serum. *Infect Immun* **63**: 1790-1795.

Chmiela, M., Czkwianianc, E., Wadstrom, T., and Rudnicka, W. (1997) Role of *Helicobacter pylori* surface structures in bacterial interaction with macrophages. *Gut* **40**: 20-24.

Cho, S.H., Strickland, I., Boguniewicz, M., and Leung, D.Y. (2001) Fibronectin and fibrinogen contribute to the enhanced binding of *Staphylococcus aureus* to atopic skin. *J. Allergy. Clin. Immunol.* **108**: 269-274.

Clarke, L.K., Armstrong, C.H., Freeman, M.J., Scheidt, A.B., Sands-Freman, L., and Knocks, K. (1991) Investigating the herd with enzootic pneumonia. *Vet. Med.* **43**: 543-550.

Conrad, H. (1998) *Heparin-binding proteins.* San Diego: Academic Press.

Corbel, M.J. (1976) The immunogenic activity of ribosomal fractions derived from *Brucella abortus*. *J Hyg (Lond)* **76**: 65-74.

Cordwell, S.J., Basseal, D.J., Bjellqvist, B., Shaw, D.C., and Humphery-Smith, I. (1997) Characterisation of basic proteins from *Spiroplasma melliferum* using novel immobilised pH gradients. *Electrophoresis* **18**: 1393-1398.

Couet, J., Belanger, M.M., Roussel, E., and Drolet, M.C. (2001) Cell biology of caveolae and caveolin. *Adv Drug Deliv Rev* **49**: 223-235.

Courtney, H.S., Li, Y., Dale, J.B., and Hasty, D.L. (1994) Cloning, sequencing, and expression of a fibronectin/fibrinogen-binding protein from group A streptococci. *Infect Immun* **62**: 3937-3946.

Cue, D., Dombek, P.E., Lam, H., and Cleary, P.P. (1998) *Streptococcus pyogenes* serotype M1 encodes multiple pathways for entry into human epithelial cells. *Infect Immun* **66**: 4593-4601.

Dallo, S.F., and Baseman, J.B. (1991) Adhesin gene of *Mycoplasma genitalium* exists as multiple copies. *Microb Pathog* **10**: 475-480.

Daniels, C., and Morona, R. (1999) Analysis of *Shigella flexneri* wzz (Rol) function by mutagenesis and cross-linking: wzz is able to oligomerize. *Mol Microbiol* **34**: 181-194.

Davis, K.L., and Wise, K.S. (2002) Site-specific proteolysis of the MALP-404 lipoprotein determines the release of a soluble selective lipoprotein-associated motif-containing fragment and alteration of the surface phenotype of *Mycoplasma fermentans*. *Infect Immun* **70**: 1129-1135.

de Bentzmann, S., Plotkowski, C., and Puchelle, E. (1996) Receptors in the *Pseudomonas aeruginosa* adherence to injured and repairing airway epithelium. *Am J Respir Crit Care Med* **154**: S155-162.

Dean, J.W., 3rd, Chandrasekaran, S., and Tanzer, M.L. (1988) Lectins inhibit cell binding and spreading on a laminin substrate. *Biochem Biophys Res Commun* **156**: 411-416.

DeBey, M.C., Jacobson, C.D., and Ross, R.F. (1992) Histochemical and morphologic changes of porcine airway epithelial cells in response to infection with *Mycoplasma hyopneumoniae*. *Am J Vet Res* **53**: 1705-1710.

DeBey, M.C., and Ross, R.F. (1994) Ciliostasis and loss of cilia induced by *Mycoplasma hyopneumoniae* in porcine tracheal organ cultures. *Infect Immun* **62**: 5312-5318.

Dennis, J.W., Waller, C.A., and Schirrmacher, V. (1984) Identification of asparagine-linked oligosaccharides involved in tumor cell adhesion to laminin and type IV collagen. *J Cell Biol* **99**: 1416-1423.

Dinkla, K., Rohde, M., Jansen, W.T., Kaplan, E.L., Chhatwal, G.S., and Talay, S.R. (2003) Rheumatic fever-associated *Streptococcus pyogenes* isolates aggregate collagen. *J Clin Invest* **111**: 1905-1912.

Djordjevic, S.P., Eamens, G.J., Romalis, L.F., and Saunders, M.M. (1994) An improved enzyme linked immunosorbent assay (ELISA) for the detection of porcine serum antibodies against *Mycoplasma hyopneumoniae*. *Vet Microbiol* **39**: 261-273.

Djordjevic, S.P., Eamens, G.J., Romalis, L.F., Nicholls, P.J., Taylor, V., and Chin, J. (1997) Serum and mucosal antibody responses and protection in pigs vaccinated against *Mycoplasma hyopneumoniae* with vaccines containing a denatured membrane antigen pool and adjuvant. *Aust Vet J* **75**: 504-511.

Djordjevic, S.P., Cordwell, S.J., Djordjevic, M.A., Wilton, J., and Minion, F.C. (2004) Proteolytic processing of the *Mycoplasma hyopneumoniae* cilium adhesin. *Infect Immun* **72**: 2791-2802.

Djordjevic, S.P., Wilton, J., Stewart, K., Minion, F.C., Young, P., Collins, A., and Walker, M.F. (2004 IOM) Domains in the carboxy-terminal region of the cilium adhesin of *Mycoplasma hyopneumoniae* bind fibronectin and heparin. *International Organization for Mycoplasmology conference abstract number 257*. Presented in Athens, Georgia.

Dombek, P.E., Cue, D., Sedgewick, J., Lam, H., Ruschkowski, S., Finlay, B.B., and Cleary, P.P. (1999) High-frequency intracellular invasion of epithelial cells by serotype M1 group A streptococci: M1 protein-mediated invasion and cytoskeletal rearrangements. *Mol Microbiol* **31**: 859-870.

Dubreuil, J.D., Giudice, G.D., and Rappuoli, R. (2002) *Helicobacter pylori* interactions with host serum and extracellular matrix proteins: potential role in the infectious process. *Microbiol Mol Biol Rev* **66**: 617-629.

Duensing, T.D., Wing, J.S., and van Putten, J.P. (1999) Sulfated polysaccharide-directed recruitment of mammalian host proteins: a novel strategy in microbial pathogenesis. *Infect Immun* **67**: 4463-4468.

Dybvig, K., and Voelker, L.L. (1996) Molecular biology of mycoplasmas. *Annu Rev Microbiol* **50**: 25-57.

Eberhard, T., Virkola, R., Korhonen, T., Kronvall, G., and Ullberg, M. (1998) Binding to human extracellular matrix by *Neisseria meningitidis*. *Infect Immun* **66**: 1791-1794.

Elm, C., Braathen, R., Bergmann, S., Frank, R., Vaerman, J.P., Kaetzel, C.S., Chhatwal, G.S., Johansen, F.E., and Hammerschmidt, S. (2004) Ectodomains 3 and 4 of human polymeric Immunoglobulin receptor (hpIgR) mediate invasion of *Streptococcus pneumonia*e into the epithelium. *J Biol Chem* **279**: 6296-6304.

Emody, L., Heesemann, J., Wolf-Watz, H., Skurnik, M., Kapperud, G., O'Toole, P., and Wadstrom, T. (1989) Binding to collagen by *Yersinia enterocolitica* and *Yersinia pseudotuberculosis*: evidence for yopA-mediated and chromosomally encoded mechanisms. *J Bacteriol* **171**: 6674-6679.

Fath, M.J., and Kolter, R. (1993) ABC transporters: bacterial exporters. *Microbiol Rev* **57**: 995-1017.

Fenno, J.C., Tamura, M., Hannam, P.M., Wong, G.W., Chan, R.A., and McBride, B.C. (2000) Identification of a *Treponema denticola* OppA homologue that binds host proteins present in the subgingival environment. *Infect Immun* **68**: 1884-1892.

Flugel, A., Schulze-Koops, H., Heesemann, J., Kuhn, K., Sorokin, L., Burkhardt, H., von der Mark, K., and Emmrich, F. (1994) Interaction of enteropathogenic *Yersinia enterocolitica* with complex basement membranes and the extracellular matrix proteins collagen type IV, laminin-1 and -2, and nidogen/entactin. *J Biol Chem* **269**: 29732-29738.

Fraser, C.M., Gocayne, J.D., White, O., Adams, M.D., Clayton, R.A., Fleischmann, R.D., Bult, C.J., Kerlavage, A.R., Sutton, G., Kelley, J.M., and *et al*. (1995) The minimal gene complement of *Mycoplasma genitalium*. *Science* **270**: 397-403.

Frey, J., Haldimann, A., Kobisch, M., and Nicolet, J. (1994) Immune response against the L-lactate dehydrogenase of *Mycoplasma hyopneumoniae* in enzootic pneumonia of swine. *Microb Pathog* **17**: 313-322.

Frick, I.M., Schmidtchen, A., and Sjobring, U. (2003) Interactions between M proteins of *Streptococcus pyogenes* and glycosaminoglycans promote bacterial adhesion to host cells. *Eur J Biochem* **270**: 2303-2311.

Fujiwara, S., Shinkai, H., Deutzmann, R., Paulsson, M., and Timpl, R. (1988) Structure and distribution of N-linked oligosaccharide chains on various domains of mouse tumour laminin. *Biochem J* **252**: 453-461.

Gehlsen, K.R., Dillner, L., Engvall, E., and Ruoslahti, E. (1988) The human laminin receptor is a member of the integrin family of cell adhesion receptors. *Science* **241**: 1228-1229.

Gigli, M., Consonni, A., Ghiselli, G., Rizzo, V., Naggi, A., and Torri, G. (1992) Heparin binding to human plasma low-density lipoproteins: dependence on heparin sulfation degree and chain length. *Biochemistry* **31**: 5996-6003.

Graham, D.Y., Lew, G.M., Klein, P.D., Evans, D.G., Evans, D.J., Jr., Saeed, Z.A., and Malaty, H.M. (1992) Effect of treatment of *Helicobacter pylori* infection on the long-term recurrence of gastric or duodenal ulcer. A randomized, controlled study. *Ann Intern Med* **116**: 705-708.

Gregory, R.L. (1986) Microbial ribosomal vaccines. *Rev Infect Dis* **8**: 208-217.

Haapasalo, M., Muller, K.H., Uitto, V.J., Leung, W.K., and McBride, B.C. (1992) Characterization, cloning, and binding properties of the major 53-kilodalton *Treponema denticola* surface antigen. *Infect Immun* **60**: 2058-2065.

Hamawy, M.M., Mergenhagen, S.E., and Siraganian, R.P. (1994) Adhesion molecules as regulators of mast-cell and basophil function. *Immunol Today* **15**: 62-66.

Hasan, M., Najjam, S., Gordon, M.Y., Gibbs, R.V., and Rider, C.C. (1999) IL-12 is a heparin-binding cytokine. *J Immunol* **162**: 1064-1070.

Himmelreich, R., Hilbert, H., Plagens, H., Pirkl, E., Li, B.C., and Herrmann, R. (1996) Complete sequence analysis of the genome of the bacterium *Mycoplasma pneumoniae*. *Nucleic Acids Res* **24**: 4420-4449.

Hook, M., Switalski, L.M., Wadstrom, T., and Lindberg, M. (1989) Interactions of pthogenic microorganisms with fibronectin. In *Fibronectin*. Mosher, D.F. (ed). San Diego: Academic Press, pp. 295-308.

Hsu, T., Artiushin, S., and Minion, F.C. (1997) Cloning and functional analysis of the P97 swine cilium adhesin gene of *Mycoplasma hyopneumoniae*. *J Bacteriol* **179**: 1317-1323.

Hsu, T., and Minion, F.C. (1998a) Identification of the cilium binding epitope of the *Mycoplasma hyopneumoniae* P97 adhesin. *Infect Immun* **66**: 4762-4766.

Hsu, T., and Minion, F.C. (1998b) Molecular analysis of the P97 cilium adhesin operon of *Mycoplasma hyopneumoniae*. *Gene* **214**: 13-23.

Hueck, C.J. (1998) Type III protein secretion systems in bacterial pathogens of animals and plants. *Microbiol Mol Biol Rev* **62**: 379-433.

Humphery-Smith, I., Cordwell, S.J., and Blackstock, W.P. (1997) Proteome research: complementarity and limitations with respect to the RNA and DNA worlds. *Electrophoresis* **18**: 1217-1242.

Inamine, J.M., Loechel, S., and Hu, P.C. (1988) Analysis of the nucleotide sequence of the P1 operon of *Mycoplasma pneumoniae*. *Gene* **73**: 175-183.

Jensen, J.S., Blom, J., and Lind, K. (1994) Intracellular location of *Mycoplasma genitalium* in cultured Vero cells as demonstrated by electron microscopy. *Int J Exp Pathol* **75**: 91-98.

Joh, D., Wann, E.R., Kreikemeyer, B., Speziale, P., and Hook, M. (1999) Role of fibronectin-binding MSCRAMMs in bacterial adherence and entry into mammalian cells. *Matrix Biol* **18**: 211-223.

Jonsson, K., Signas, C., Muller, H.P., and Lindberg, M. (1991) Two different genes encode fibronectin binding proteins in *Staphylococcus aureus*. The complete nucleotide sequence and characterization of the second gene. *Eur J Biochem* **202**: 1041-1048.

Jordan, J.L., Berry, K.M., Balish, M.F., and Krause, D.C. (2001) Stability and subcellular localization of cytadherence-associated protein P65 in *Mycoplasma pneumoniae*. *J Bacteriol* **183**: 7387-7391.

Kapral, F.A., Godwin, J.R., and Dye, E.S. (1980) Formation of intraperitoneal abscesses by *Staphylococcus aureus*. *Infect Immun* **30**: 204-211.

Katerov, V., Andreev, A., Schalen, C., and Totolian, A.A. (1998) Protein F, a fibronectin-binding protein of *Streptococcus pyogenes*, also binds human fibrinogen: isolation of the protein and mapping of the binding region. *Microbiology* **144 (Pt 1)**: 119-126.

Knibbs, R.N., Perini, F., and Goldstein, I.J. (1989) Structure of the major concanavalin A reactive oligosaccharides of the extracellular matrix component laminin. *Biochemistry* **28**: 6379-6392.

Kobisch, M., Blanchard, B., and Le Potier, M.F. (1993) *Mycoplasma hyopneumoniae* infection in pigs: duration of the disease and resistance to reinfection. *Vet Res* **24**: 67-77.

Kobisch, M., and Friis, N.F. (1996) Swine mycoplasmoses. *Rev Sci Tech* **15**: 1569-1605.

Kolberg, J., Hoiby, E.A., Lopez, R., and Sletten, K. (1997) Monoclonal antibodies against *Streptococcus pneumoniae* detect epitopes on eubacterial ribosomal proteins L7/L12 and on streptococcal elongation factor Ts. *Microbiology* **143 (Pt 1)**: 55-61.

Krause, D.C., Leith, D.K., Wilson, R.M., and Baseman, J.B. (1982) Identification of *Mycoplasma pneumoniae* proteins associated with hemadsorption and virulence. *Infect Immun* **35**: 809-817.

Krause, D.C. (1996) *Mycoplasma pneumoniae* cytadherence: unravelling the tie that binds. *Mol Microbiol* **20**: 247-253.

Krause, D.C. (1998) *Mycoplasma pneumoniae* cytadherence: organization and assembly of the attachment organelle. *Trends Microbiol* **6**: 15-18.

Krause, D.C., and Balish, M.F. (2001) Structure, function, and assembly of the terminal organelle of *Mycoplasma pneumoniae*. *FEMS Microbiol Lett* **198**: 1-7.

Krause, D.C., and Balish, M.F. (2004) Cellular engineering in a minimal microbe: structure and assembly of the terminal organelle of *Mycoplasma pneumoniae*. *Mol Microbiol* **51**: 917-924.

Kreis, T., and Vale, R. (1993) *Guidebook to the Extracellular Matrix and Adhesion Proteins.* Oxford: Oxford University Press.

Kuusela, P. (1978) Fibronectin binds to *Staphylococcus aureus*. *Nature* **276**: 718-720.

Kuypers, J.M., and Proctor, R.A. (1989) Reduced adherence to traumatized rat heart valves by a low-fibronectin-binding mutant of *Staphylococcus aureus*. *Infect Immun* **57**: 2306-2312.

Ladefoged, S.A., and Christiansen, G. (1994) Sequencing analysis reveals a unique gene organization in the gyrB region of *Mycoplasma hominis*. *J Bacteriol* **176**: 5835-5842.

Laemmli, U.K. (1970) Cleavage of structural proteins during the assembly of the head of bacteriophage T4. *Nature* **227**: 680-685.

Layh-Schmitt, G., Podtelejnikov, A., and Mann, M. (2000) Proteins complexed to the P1 adhesin of *Mycoplasma pneumoniae*. *Microbiology* **146 (Pt 3)**: 741-747.

Liotta, L.A., Rao, C.N., and Wewer, U.M. (1986) Biochemical interactions of tumor cells with the basement membrane. *Annu Rev Biochem* **55**: 1037-1057.

Livingston, C.W., Jr., Stair, E.L., Underdahl, N.R., and Mebus, C.A. (1972) Pathogenesis of mycoplasmal pneumonia in swine. *Am J Vet Res* **33**: 2249-2258.

Ljungh, A., and Wadstrom, T. (1995) Binding of extracellular matrix proteins by microbes. *Methods Enzymol* **253**: 501-514.

Ljungh, A., Moran, A.P., and Wadstrom, T. (1996) Interactions of bacterial adhesins with extracellular matrix and plasma proteins: pathogenic implications and therapeutic possibilities. *FEMS Immunol Med Microbiol* **16**: 117-126.

Lo, S.C., Hayes, M.M., Kotani, H., Pierce, P.F., Wear, D.J., Newton, P.B., 3rd, Tully, J.G., and Shih, J.W. (1993) Adhesion onto and invasion into mammalian cells by *Mycoplasma penetrans*: a newly isolated mycoplasma from patients with AIDS. *Mod Pathol* **6**: 276-280.

Lodish, H., Berk, A., Zipursky, S.L., Matsudaira, P., Baltimore, P., and Darnell, J. (2000) Integrating cells into tissues. In *Molecular Cell Biology*. New York: W.H. Freeman and Co., pp. 969-993.

Loge, R.V., Hill, W.E., Baker, R.E., and Larson, C.L. (1974) Delayed hypersensitivity reactions provoked by ribosomes from acid-fast bacilli: physical characteristics and immunological aspects of core ribosomal proteins from *Mycobacterium smegmatis*. *Infect Immun* **9**: 489-496.

Luirink, J., and Dobberstein, B. (1994) Mammalian and *Escherichia coli* signal recognition particles. *Mol Microbiol* **11**: 9-13.

Machner, M.P., Frese, S., Schubert, W.D., Orian-Rousseau, V., Gherardi, E., Wehland, J., Niemann, H.H., and Heinz, D.W. (2003) Aromatic amino acids at the surface of InlB are essential for host cell invasion by *Listeria monocytogenes*. *Mol Microbiol* **48**: 1525-1536.

Maes, D., Verdonck, M., Deluyker, H., and de Kruif, A. (1996) Enzootic pneumonia in pigs. *Vet Q* **18**: 104-109.

Marjomaki, V., Pietiainen, V., Matilainen, H., Upla, P., Ivaska, J., Nissinen, L., Reunanen, H., Huttunen, P., Hyypia, T., and Heino, J. (2002) Internalization of echovirus 1 in caveolae. *J Virol* **76**: 1856-1865.

Markham, P.F., Glew, M.D., Sykes, J.E., Bowden, T.R., Pollocks, T.D., Browning, G.F., Whithear, K.G., and Walker, I.D. (1994) The organisation of the multigene family which encodes the major cell surface protein, pMGA, of *Mycoplasma gallisepticum*. *FEBS Lett* **352**: 347-352.

Marshall, A.J., Miles, R.J., and Richards, L. (1995) The phagocytosis of mycoplasmas. *J Med Microbiol* **43**: 239-250.

Marshall, B.J., and Warren, J.R. (1984) Unidentified curved bacilli in the stomach of patients with gastritis and peptic ulceration. *Lancet* **1**: 1311-1315.

McDevitt, D., Francois, P., Vaudaux, P., and Foster, T.J. (1994) Molecular characterization of the clumping factor (fibrinogen receptor) of *Staphylococcus aureus*. *Mol Microbiol* **11**: 237-248.

McGavin, M.H., Krajewska-Pietrasik, D., Ryden, C., and Hook, M. (1993) Identification of a *Staphylococcus aureus* extracellular matrix-binding protein with broad specificity. *Infect Immun* **61**: 2479-2485.

Mebus, C.A., and Underdahl, N.R. (1977) Scanning electron microscopy of trachea and bronchi from gnotobiotic pigs inoculated with *Mycoplasma hyopneumoniae*. *Am J Vet Res* **38**: 1249-1254.

Menozzi, F.D., Boucher, P.E., Riveau, G., Gantiez, C., and Locht, C. (1994) Surface-associated filamentous hemagglutinin induces autoagglutination of *Bordetella pertussis*. *Infect Immun* **62**: 4261-4269.

Mernaugh, G.R., Dallo, S.F., Holt, S.C., and Baseman, J.B. (1993) Properties of adhering and nonadhering populations of *Mycoplasma genitalium*. *Clin Infect Dis* **17**: S69-78.

Minion, F.C., Adams, C., and Hsu, T. (2000) R1 region of P97 mediates adherence of *Mycoplasma hyopneumoniae* to swine cilia. *Infect Immun* **68**: 3056-3060.

Minion, F.C., Lefkowitz, E.J., Madsen, M.L., Cleary, B.J., Swartzell, S.M., and Mahairas, G.G. (2004) The genome sequence of *Mycoplasma hyopneumoniae* strain 232, the agent of swine mycoplasmosis. *J Bacteriol* **186**: 7123-7133.

Molinari, G., Talay, S.R., Valentin-Weigand, P., Rohde, M., and Chhatwal, G.S. (1997) The fibronectin-binding protein of *Streptococcus pyogenes*, SfbI, is involved in the internalization of group A streptococci by epithelial cells. *Infect Immun* **65**: 1357-1363.

Moller, W., and Castleman, H. (1967) Primary structure heterogeneity in ribosomal proteins from *Escherichia coli*. *Nature* **215**: 1293-1295.

Morrissey, J.J., Cupp, L.E., Weissbach, H., and Brot, N. (1976) Synthesis of ribosomal proteins L7L12 in relaxed and stringent strains of *Escherichia coli*. *J Biol Chem* **251**: 5516-5521.

Morrissey, J.J., Weissbach, H., and Brot, N. (1975) The identification and characterization of proteins similar to L7, L12 in ribosome-free extracts of *Escherichia coli*. *Biochem Biophys Res Commun* **65**: 293-302.

Multhaup, G., Mechler, H., and Masters, C.L. (1995) Characterization of the high affinity heparin binding site of the Alzheimer's disease beta A4 amyloid precursor protein (APP) and its enhancement by zinc(II). *J Mol Recognit* **8**: 247-257.

Naito, M., Fukuda, T., Sekiguchi, K., and Yamada, T. (2000) The domains of human fibronectin mediating the binding of alpha antigen, the most immunopotent antigen of mycobacteria that induces protective immunity against mycobacterial infection. *Biochem J* **347**: 725-731.

Najjam, S., Gibbs, R.V., Gordon, M.Y., and Rider, C.C. (1997) Characterization of human recombinant interleukin 2 binding to heparin and heparan sulfate using an ELISA approach. *Cytokine* **9**: 1013-1022.

Norkin, L.C. (1995) Virus receptors: implications for pathogenesis and the design of antiviral agents. *Clin Microbiol Rev* **8**: 293-315.

Norkin, L.C. (2001) Caveolae in the uptake and targeting of infectious agents and secreted toxins. *Adv Drug Deliv Rev* **49**: 301-315.

Nouwens, A.S., Cordwell, S.J., Larsen, M.R., Molloy, M.P., Gillings, M., Willcox, M.D., and Walsh, B.J. (2000) Complementing genomics with proteomics: the membrane subproteome of *Pseudomonas aeruginosa* PAO1. *Electrophoresis* **21**: 3797-3809.

Oehmcke, S., Podbielski, A., and Kreikemeyer, B. (2004) Function of the fibronectin-binding serum opacity factor of *Streptococcus pyogenes* in adherence to epithelial cells. *Infect Immun* **72**: 4302-4308.

Oliveira, S.C., and Splitter, G.A. (1996) Immunization of mice with recombinant L7/L12 ribosomal protein confers protection against *Brucella abortus* infection. *Vaccine* **14**: 959-962.

Olsen, G.J., Woese, C.R., and Overbeek, R. (1994) The winds of (evolutionary) change: breathing new life into microbiology. *J Bacteriol* **176**: 1-6.

Ortiz-Ortiz, L., Solarolo, E.B., and Bojalil, L.F. (1971) Delayed hypersensitivity to ribosomal protein from BCG. *J Immunol* **107**: 1022-1026.

Pankhurst, G.J., Bennett, C.A., and Easterbrook-Smith, S.B. (1998) Characterization of the heparin-binding properties of human clusterin. *Biochemistry* **37**: 4823-4830.

Papazisi, L., Frasca, S., Jr., Gladd, M., Liao, X., Yogev, D., and Geary, S.J. (2002) GapA and CrmA coexpression is essential for *Mycoplasma gallisepticum* cytadherence and virulence. *Infect Immun* **70**: 6839-6845.

Park, S.C., Yibchok-Anun, S., Cheng, H., Young, T.F., Thacker, E.L., Minion, F.C., Ross, R.F., and Hsu, W.H. (2002) *Mycoplasma hyopneumoniae* increases intracellular calcium release in porcine ciliated tracheal cells. *Infect Immun* **70**: 2502-2506.

Patankar, M.S., Oehninger, S., Barnett, T., Williams, R.L., and Clark, G.F. (1993) A revised structure for fucoidan may explain some of its biological activities. *J Biol Chem* **268**: 21770-21776.

Patti, J.M., Allen, B.L., McGavin, M.J., and Hook, M. (1994a) MSCRAMM-mediated adherence of microorganisms to host tissues. *Annu Rev Microbiol* **48**: 585-617.

Patti, J.M., Bremell, T., Krajewska-Pietrasik, D., Abdelnour, A., Tarkowski, A., Ryden, C., and Hook, M. (1994b) The *Staphylococcus aureus* collagen adhesin is a virulence determinant in experimental septic arthritis. *Infect Immun* **62**: 152-161.

Peterson, T.E., Skorstengaard, K., and Vide-Pederson, K. (1989) Primary structure of fibronectin. In *Biology of extracellular matrix: series A. Fibronectin*. Mosher, D.F. (ed). San Diego, Calif.: Academic Press, Inc., pp. 1-24.

Pethe, K., Aumercier, M., Fort, E., Gatot, C., Locht, C., and Menozzi, F.D. (2000) Characterization of the heparin-binding site of the mycobacterial heparin-binding hemagglutinin adhesin. *J Biol Chem* **275**: 14273-14280.

Popham, P.L., Hahn, T.W., Krebes, K.A., and Krause, D.C. (1997) Loss of HMW1 and HMW3 in noncytadhering mutants of *Mycoplasma pneumoniae* occurs post-translationally. *Proc Natl Acad Sci U S A* **94**: 13979-13984.

Powers, T., and Walter, P. (1997) Co-translational protein targeting catalyzed by the *Escherichia coli* signal recognition particle and its receptor. *Embo J* **16**: 4880-4886.

Rauws, E.A., and Tytgat, G.N. (1990) Cure of duodenal ulcer associated with eradication of *Helicobacter pylori*. *Lancet* **335**: 1233-1235.

Razin, S. (1978) The mycoplasmas. *Microbiol Rev* **42**: 414-470.

Razin, S. (1985) Mycoplasma adherence. In *The mycoplasmas*. Vol. IV. Razin, S. and Barile, M.F. (eds). Orlando Fla: Academic Press, pp. 161-202.

Razin, S. (1992) Mycoplasma taxonomy and ecology. In *Mycoplasmas: molecular biology and pathogenesis*. Maniloff, J., McElhaney, R.N., Finch, L.R. and Baseman, J.B. (eds). Washington, D.C.: American Society for Microbiology, pp. 3-22.

Razin, S., and Jacobs, E. (1992) Mycoplasma adhesion. *J Gen Microbiol* **138**: 407-422.

Razin, S., Yogev, D., and Naot, Y. (1998) Molecular biology and pathogenicity of mycoplasmas. *Microbiol Mol Biol Rev* **62**: 1094-1156.

Reddy, S.P., Rasmussen, W.G., and Baseman, J.B. (1995) Molecular cloning and characterization of an adherence-related operon of *Mycoplasma genitalium*. *J Bacteriol* **177**: 5943-5951.

Ringner, M., Paulsson, M., and Wadstrom, T. (1992) Vitronectin binding by *Helicobacter pylori*. *FEMS Microbiol Immunol* **5**: 219-224.

Robertson, J.A., Pyle, L.E., Stemke, G.W., and Finch, L.R. (1990) Human ureaplasmas show diverse genome sizes by pulsed-field electrophoresis. *Nucleic Acids Res* **18**: 1451-1455.

Rohde, M., Muller, E., Chhatwal, G.S., and Talay, S.R. (2003) Host cell caveolae act as an entry port for Group A streptococci. *Cell Microbiol* **5**: 323-342.

Ross, R.F. (1992) Mycoplasma diseases. In *Diseases of swine*. Leman, A.D., Straw, B.E., Mengeling, W.L., D' Allaire, S. and Taylor, D.J. (eds). Ames, Iowa: Iowa State University Press, pp. 537-551.

Rostand, K.S., and Esko, J.D. (1997) Microbial adherence to and invasion through proteoglycans. *Infect Immun* **65**: 1-8.

Ruoslahti, E., and Pierschbacher, M.D. (1987) New perspectives in cell adhesion: RGD and integrins. *Science* **238**: 491-497.

Ruoslahti, E. (1988) Fibronectin and its receptors. *Annu Rev Biochem* **57**: 375-413.

Sanchez-Campillo, M., Bini, L., Comanducci, M., Raggiaschi, R., Marzocchi, B., Pallini, V., and Ratti, G. (1999) Identification of immunoreactive proteins of *Chlamydia trachomatis* by Western blot analysis of a two-dimensional electrophoresis map with patient sera. *Electrophoresis* **20**: 2269-2279.

Sandkvist, M. (2001) Type II secretion and pathogenesis. *Infect Immun* **69**: 3523-3535.

Schulze-Koops, H., Burkhardt, H., Heesemann, J., Kirsch, T., Swoboda, B., Bull, C., Goodman, S., and Emmrich, F. (1993) Outer membrane protein YadA of enteropathogenic yersiniae mediates specific binding to cellular but not plasma fibronectin. *Infect Immun* **61**: 2513-2519.

Schwarzbauer, J.E. (1991) Alternative splicing of fibronectin: three variants, three functions. *Bioessays* **13**: 527-533.

Seto, S., Layh-Schmitt, G., Kenri, T., and Miyata, M. (2001) Visualization of the attachment organelle and cytadherence proteins of *Mycoplasma pneumoniae* by immunofluorescence microscopy. *J Bacteriol* **183**: 1621-1630.

Seto, S., and Miyata, M. (2003) Attachment organelle formation represented by localization of cytadherence proteins and formation of the electron-dense core in wild-type and mutant strains of *Mycoplasma pneumoniae*. *J Bacteriol* **185**: 1082-1091.

Shin, J.S., Gao, Z., and Abraham, S.N. (2000) Involvement of cellular caveolae in bacterial entry into mast cells. *Science* **289**: 785-788.

Shin, J.S., and Abraham, S.N. (2001a) Caveolae as portals of entry for microbes. *Microbes Infect* **3**: 755-761.

Shin, J.S., and Abraham, S.N. (2001b) Cell biology. Caveolae-not just craters in the cellular landscape. *Science* **293**: 1447-1448.

Shin, J.S., and Abraham, S.N. (2001c) Co-option of endocytic functions of cellular caveolae by pathogens. *Immunology* **102**: 2-7.

Shin, J.S., and Abraham, S.N. (2001d) Glycosylphosphatidylinositol-anchored receptor-mediated bacterial endocytosis. *FEMS Microbiol Lett* **197**: 131-138.

Skurnik, M., el Tahir, Y., Saarinen, M., Jalkanen, S., and Toivanen, P. (1994) YadA mediates specific binding of enteropathogenic *Yersinia enterocolitica* to human intestinal submucosa. *Infect Immun* **62**: 1252-1261.

Slomiany, B.L., Piotrowski, J., Sengupta, S., and Slomiany, A. (1991) Inhibition of gastric mucosal laminin receptor by *Helicobacter pylori* lipopolysaccharide. *Biochem Biophys Res Commun* **175**: 963-970.

Spence, J.M., and Clark, V.L. (2000) Role of ribosomal protein L12 in gonococcal invasion of Hec1B cells. *Infect Immun* **68**: 5002-5010.

Sperker, B., Hu, P., and Herrmann, R. (1991) Identification of gene products of the P1 operon of *Mycoplasma pneumoniae*. *Mol Microbiol* **5**: 299-306.

Strycharz, W.A., Nomura, M., and Lake, J.A. (1978) Ribosomal proteins L7/L12 localized at a single region of the large subunit by immune electron microscopy. *J Mol Biol* **126**: 123-140.

Su, C.J., Chavoya, A., and Baseman, J.B. (1988) Regions of *Mycoplasma pneumoniae* cytadhesin P1 structural gene exist as multiple copies. *Infect Immun* **56**: 3157-3161.

Switalski, L.M., Speziale, P., and Hook, M. (1989) Isolation and characterization of a putative collagen receptor from *Staphylococcus aureus* strain Cowan 1. *J Biol Chem* **264**: 21080-21086.

Switalski, L.M., Patti, J.M., Butcher, W., Gristina, A.G., Speziale, P., and Hook, M. (1993) A collagen receptor on *Staphylococcus aureus* strains isolated from patients with septic arthritis mediates adhesion to cartilage. *Mol Microbiol* **7**: 99-107.

Tajima, M., and Yagihashi, T. (1982) Interaction of *Mycoplasma hyopneumoniae* with the porcine respiratory epithelium as observed by electron microscopy. *Infect Immun* **37**: 1162-1169.

Tantimavanich, S., Nagai, S., Nomaguchi, H., Kinomoto, M., Ohara, N., and Yamada, T. (1993) Immunological properties of ribosomal proteins from *Mycobacterium bovis* BCG. *Infect Immun* **61**: 4005-4007.

Taylor-Robinson, D., Davies, H.A., Sarathchandra, P., and Furr, P.M. (1991) Intracellular location of mycoplasmas in cultured cells demonstrated by immunocytochemistry and electron microscopy. *Int J Exp Pathol* **72**: 705-714.

Tertti, R., Skurnik, M., Vartio, T., and Kuusela, P. (1992) Adhesion protein YadA of Yersinia species mediates binding of bacteria to fibronectin. *Infect Immun* **60**: 3021-3024.

Thacker, E.L., Thacker, B.J., Boettcher, T.B., and Jayappa, H. (1998) Comparison of antibody production, lymphocyte stimulation and production induced by four commercial *Mycoplasma hyopneumoniae* bacterins. *Swine Health and Production* **6**: 107-112.

Thacker, E.L., Thacker, B.J., Young, T.F., and Halbur, P.G. (2000) Effect of vaccination on the potentiation of porcine reproductive and respiratory syndrome virus (PRRSV)-induced pneumonia by *Mycoplasma hyopneumoniae*. *Vaccine* **18**: 1244-1252.

Tham, T.N., Ferris, S., Bahraoui, E., Canarelli, S., Montagnier, L., and Blanchard, A. (1994) Molecular characterization of the P1-like adhesin gene from *Mycoplasma pirum*. *J Bacteriol* **176**: 781-788.

Thompson, H.C., and Snyder, I.S. (1971) Protection against pneumococcal infection by a ribosomal preparation. *Infect. Immun.* **3**: 16-23.

Timpl, R. (1989) Structure and biological activity of basement membrane proteins. *Eur J Biochem* **180**: 487-502.

Trust, T.J., Doig, P., Emody, L., Kienle, Z., Wadstrom, T., and O'Toole, P. (1991) High-affinity binding of the basement membrane proteins collagen type IV and laminin to the gastric pathogen *Helicobacter pylori*. *Infect Immun* **59**: 4398-4404.

Ullberg, M., Kuusela, P., Kristiansen, B.E., and Kronvall, G. (1992) Binding of plasminogen to *Neisseria meningitidis* and *Neisseria gonorrhoeae* and formation of surface-associated plasmin. *J Infect Dis* **166**: 1329-1334.

Umemoto, T., Nakatani, Y., Nakamura, Y., and Namikawa, I. (1993) Fibronectin-binding proteins of a human oral spirochete *Treponema denticola*. *Microbiol Immunol* **37**: 75-78.

Valent, Q.A., Scotti, P.A., High, S., de Gier, J.W., von Heijne, G., Lentzen, G., Wintermeyer, W., Oudega, B., and Luirink, J. (1998) The *Escherichia coli* SRP and SecB targeting pathways converge at the translocon. *Embo J* **17**: 2504-2512.

Valkonen, K.H., Ringner, M., Ljungh, A., and Wadstrom, T. (1993) High-affinity binding of laminin by *Helicobacter pylori*: evidence for a lectin-like interaction. *FEMS Immunol Med Microbiol* **7**: 29-37.

Valkonen, K.H., Wadstrom, T., and Moran, A.P. (1994) Interaction of lipopolysaccharides of *Helicobacter pylori* with basement membrane protein laminin. *Infect Immun* **62**: 3640-3648.

van der Flier, M., Chhun, N., Wizemann, T.M., Min, J., McCarthy, J.B., and Tuomanen, E.I. (1995) Adherence of *Streptococcus pneumoniae* to immobilized fibronectin. *Infect Immun* **63**: 4317-4322.

van Putten, J.P., Duensing, T.D., and Cole, R.L. (1998) Entry of OpaA+ gonococci into HEp-2 cells requires concerted action of glycosaminoglycans, fibronectin and integrin receptors. *Mol Microbiol* **29**: 369-379.

Venneman, M.R., and Bigley, N.J. (1969) Isolation and partial characterization of an immunogenic moiety obtained from *Salmonella typhimurium*. *J Bacteriol* **100**: 140-148.

Virkola, R., Lahteenmaki, K., Eberhard, T., Kuusela, P., van Alphen, L., Ullberg, M., and Korhonen, T.K. (1996) Interaction of *Haemophilus influenzae* with the mammalian extracellular matrix. *J Infect Dis* **173**: 1137-1147.

Wadstrom, T., Hirmo, S., and Boren, T. (1996) Biochemical aspects of *Helicobacter pylori* colonization of the human gastric mucosa. *Aliment Pharmacol Ther* **10**: 17-27.

Wadstrom, T., and Ljungh, A. (1999) Glycosaminoglycan-binding microbial proteins in tissue adhesion and invasion: key events in microbial pathogenicity. *J Med Microbiol* **48**: 223-233.

Warren, J.R., and Marshall, B. (1983) Unidentified curved bacilli on gastric epithelium in active chronic gastritis. *Lancet* **1**: 1273-1275.

Westerlund, B., van Die, I., Kramer, C., Kuusela, P., Holthofer, H., Tarkkanen, A.M., Virkola, R., Riegman, N., Bergmans, H., Hoekstra, W., and et al. (1991) Multifunctional nature of P fimbriae of uropathogenic *Escherichia coli*: mutations in fsoE and fsoF influence fimbrial binding to renal tubuli and immobilized fibronectin. *Mol Microbiol* **5**: 2965-2975.

Williams, R.J., Henderson, B., and Nair, S.P. (2002) *Staphylococcus aureus* fibronectin binding proteins A and B possess a second fibronectin binding region that may have biological relevance to bone tissues. *Calcif Tissue Int* **70**: 416-421.

Wilton, J.L., Scarman, A.L., Walker, M.J., and Djordjevic, S.P. (1998) Reiterated repeat region variability in the ciliary adhesin gene of *Mycoplasma hyopneumoniae*. *Microbiology* **144 (Pt 7)**: 1931-1943.

Winram, S.B., and Lottenberg, R. (1996) The plasmin-binding protein Plr of group A streptococci is identified as glyceraldehyde-3-phosphate dehydrogenase. *Microbiology* **142 (Pt 8)**: 2311-2320.

Xiao, J., Hook, M., Weinstock, G.M., and Murray, B.E. (1998) Conditional adherence of *Enterococcus faecalis* to extracellular matrix proteins. *FEMS Immunol Med Microbiol* **21**: 287-295.

Yamada, K.M. (1989) Fibronectins: structure, functions and receptors. *Curr Opin Cell Biol* **1**: 956-963.

Yavlovich, A., Higazi, A.A., and Rottem, S. (2001) Plasminogen binding and activation by *Mycoplasma fermentans*. *Infect Immun* **69**: 1977-1982.

Yurchenco, P.D., and Schittny, J.C. (1990) Molecular architecture of basement membranes. *FASEB J* **4**: 1577-1590.

Zhang, Q., Young, T.F., and Ross, R.F. (1994a) Glycolipid receptors for attachment of *Mycoplasma hyopneumoniae* to porcine respiratory ciliated cells. *Infect Immun* **62**: 4367-4373.

Zhang, Q., Young, T.F., and Ross, R.F. (1994b) Microtiter plate adherence assay and receptor analogs for *Mycoplasma hyopneumoniae*. *Infect Immun* **62**: 1616-1622.

Zhang, Q., Young, T.F., and Ross, R.F. (1995) Identification and characterization of a *Mycoplasma hyopneumoniae* adhesin. *Infect Immun* **63**: 1013-1019.

Zhou, Q., and Cummings, R.D. (1990) The S-type lectin from calf heart tissue binds selectively to the carbohydrate chains of laminin. *Arch Biochem Biophys* **281**: 27-35.

Zielinski, G.C., and Ross, R.F. (1990) Effect of growth in cell cultures and strain on virulence of *Mycoplasma hyopneumoniae* for swine. *Am J Vet Res* **51**: 344-348.

Zielinski, G.C., and Ross, R.F. (1993) Adherence of *Mycoplasma hyopneumoniae* to porcine ciliated respiratory tract cells. *Am J Vet Res* **54**: 1262-1269.

Appendix A: General Buffers and Reagents

Commonly used buffer solutions

1X Phosphate buffered saline (PBS) pH 7.2

0.5 M K_2HPO_4	71.7 ml/l
0.5 M KH_2PO_4	28.3 ml/l
NaCl	8.57 g/l

Phosphate buffer (PB) pH 7.2

0.5 M K_2HPO_4	71.7 ml/l
0.5 M KH_2PO_4	28.3 ml/l

1.5 M Tris pH 8.8

Tris	181.71g/l

1 M Tris pH 6.8

Tris	121.14 g/l

1% Triton X-114 buffer

Triton X-114	0.5 ml/50 ml
Tris	0.0606 g/50 ml
NaCl	0.438 g/50 ml
0.5M EDTA	0.1 ml/50 ml

TE buffer pH 7.5

Tris	1.21 g/l
EDTA	0.37 g/l

1-D SDS-PAGE gels/4 gels

	12% resolving gel	**15% resolving gel**	**4% stacking gel**
MilliQ water	13.2 ml	9.2 ml	10.8 ml
30% acrylamide	16 ml	20 ml	1.95 ml
1.5 M Tris pH 8.8	10 ml	10 ml	
1.0 M Tris pH 6.8			1.95 ml
10% w/v SDS	0.4 ml	0.4 ml	0.15 ml
APS	45 mg	45 mg	10 mg
TEMED	16 µl	16 µl	11 µl

2-D SDS-PAGE gels/ 6 gels

	12.5% resolving gel
40% 37.5:1 Acrylamide	156 ml/500 ml
1.5 M Tris pH 8.8	125 ml/500 ml
MilliQ water	208 ml/500 ml
10% w/v SDS	6 ml/500 ml
10% APS (0.6g in 6 ml MilliQ)	6 ml/500 ml
TEMED	100 µl/500 ml

Electrophoresis reagents

1X SDS-PAGE buffer

Tris	3.03 g/l
Glycine	14.33 g/l
SDS	1.0 g/l

Reducing solution/cracking buffer

Tris pH 6.8	0.73 g/100 ml
SDS	1 g/100 ml
β-mercaptoethanol	1 g/100 ml
Glycerol	10 g/100 ml
Bromophenol Blue	0.01 g/100 ml

Coomassie stain 1-D

Coomassie R250	1.25 g/500 ml
Methanol	225 ml/500 ml
Acetic Acid	50 ml/500 ml

Coomassie de-stain 1-D

Acetic acid	100 ml/l
Methanol	450 ml/l

0.5X TBE for agarose gels

Boric acid	2.75 g/l
Tris	5.4 g/l
0.5 M EDTA	2 ml/l

1X TAE for agarose gels

Tris	4.84 g/l
Acetic Acid	1.14 ml/l
0.5 M EDTA	2 ml/l

Agarose gel loading buffer (bromophenol blue loading dye)

bromophenol blue	0.25 g/100 ml
ficoll	15 g/100 ml

2-D Gel Electrophoresis Reagents

5X Tris buffer pH 8.8

Tris	227 g/l

Equilibration buffer

Urea	21.6 g/60 ml
SDS	1.2 g/60 ml
5X Tris buffer pH 8.8	12 ml/60 ml
Glycerol	12 ml/60 ml
DTT	1.2 g/60 ml
40% Acrylamide	3.75 ml/60 ml

Lysis buffer

Urea	0.54 g/100 ml
DTT	1 g/100 ml
CHAPS	4 g/100 ml
Ampholytes pH 3-10	0.8 ml/100 ml
Tris	0.42 g/100 ml
PMSF	10 µl/ml
EDTA 0.5 M	9 µl/ml

Standard solubilisation solution (SSS)

Urea	9.6 g/20 ml
DTT	0.308 g/20 ml
CHAPS	0.8 g/20 ml
Ampholytes pH 3-10	0.4 ml/20 ml
Tris	0.097 g/20 ml

Multiple surfactant solution (MSS)

Urea	6.0 g/20 ml
Thiourea	3.04 g/20 ml
DTT	0.2 g/20 ml
CHAPS	0.4 g/20 ml
Sulfobetaine	0.4 g/20 ml
0.8% Ampholytes 3-10	0.4 ml/20 ml
Tris	0.1 g/20 ml

Colloidal Coomassie 2-D

Ammonium sulfate	170 g/l
Phosphoric acid	36 ml/l
Coomassie G250	1 g/l
Methanol	340 ml/l

Colloidal Coomassie de-stain 2-D

Acetic acid	10 ml/l

Western Transfer Reagents

1X western transfer buffer

Tris	3.03 g/l
Glycine	14.33 g/l
Methanol	200 ml/l

1X Tris-saline

Tris	1.21 g/l
NaCl	9 g/l

100 mM Tris pH 7.6

Tris	12.1 g/l

DAB solution

DAB	25 mg
100 mM Tris pH 7.6	50 ml
Hydrogen peroxide	15 µl

ELISA Reagents

Carbonate coating buffer pH 9.5

$NaHCO_3$	0.75 g/500 ml
Na_2CO_3	1.45 g/500 ml

Wash solution

Tween20 in PBS	0.05% v/v

ABTS solution, per plate

0.1 M citric acid	4.41 ml
0.2 M Na_2HPO_4	3.09 ml
MilliQ water	7.5 ml

pH to 4.2 and add 8.25 mg ABTS and 4.5 µl hydrogen peroxide

Midi/Maxi Prep Kit (Qiagen) Reagents

P1 pH 8.0

Tris	6.06 g/l
EDTA	3.72 g/l
RNase A	100 mg/l

P2

NaOH	8 g/l
20% SDS solution	50 ml/l

P3 pH 5.5

Potassium acetate	294.5 g/l

QBT pH 7.0

NaCl	43.83 g/l
MOPS	10.46 g/l
Isopropanol	150 ml/l
10% Triton X-100 Solution	15 ml/l

QC pH 7.0

NaCl	58.44 g/l
MOPS	10.46 g/l
Isopropanol	150 ml

QF pH 8.5

NaCl	73.05 g/l
Tris	6.06 g/l
Isopropanol	150 ml/l

Southern Reagents

Denaturation solution

NaOH	20 g/l
NaCl	87.66 g/l

Neutralisation solution

Tris	121.14 g/l

1.5M NaCl

NaCl	87.66 g/l

20X SSC buffer pH 7.0

NaCl	175.3 g/l
Sodium citrate	88.2 g/l

Culture Reagents

LB media

Tryptone	10 g/l
Yeast	5 g/l
NaCl	5 g/l

LB agar

Tryptone	10 g/l
Yeast	5 g/l
NaCl	5 g/l
Agar	15 g/l

NZY+ broth pH 7.6

NZ Amine	10 g/l
Yeast Extract	5 g/l
NaCl	5 g/l
$MgCl_2$	203.4 g/l
$MgSO_4$	246.4 g/l
Glucose	146 ml/l

SOCS medium

Tryptone	2 g/100 ml
Yeast Extract	0.5 g/100 ml
NaCl	0.06 g/100 ml
KCl	0.02 g/100 ml
$MgCl_2$	0.1 g/100 ml
$MgSO_4$	0.12 g/100 ml
Glucose	0.36 g/100 ml

Hank's buffered salt solution for Friis media

Hanks A

NaCl	80 g/500 ml
KCl	4 g/500 ml
$MgSO_4$	1 g/500 ml
$MgCl_2$	1 g/500 ml
$CaCl_2$	1.4 g/500 ml

Hanks B

Na_2HPO_4	1.5 g/500 ml
KH_2PO_4	0.6 g/500 ml

Friis Base Media for Mycoplasma culturing pH 7.4

Hanks A	30.4 ml/2 l
Hanks B	30.4 ml/2 l
Difco Brain Heart Infusion (BHI)	9.8 g/2 l
Difco PPLO	10.5 g/2 l
0.5% Phenol Red	5.2 ml/2 l
Sterile MilliQ water	1654 ml/2 l

Friis components added to base media before use

Bacitracin	0.288 g/11.4 ml
Methicillin (or Ampicillin)	0.288 g/11.4 ml
Yeast Extract	68 ml
Horse Serum	100 ml
Pig Serum	100 ml

PK15 culture growth media

Dulbecco's Modified Eagle Medium (DMEM, Gibco) with 10% FCS and glutamine

PK15 culture infection media

DMEM/Hepes 25 mM (Gibco) with 1% FCS

Trypsin solution
Trypsin-EDTA (1X) in HBSS without Ca and Mg (Gibco)

Cacodylate Buffer pH 6.9

Cacodylate	21.4 g/l
$MgCl_2$	0.95 g/l
$CaCl_2$	1.47 g/l
Sucrose	308.1 g/l

Bradford's Reagent for protein concentration

Coomassie G250	50 mg/500 ml
95% Ethanol	25 ml/500 ml
Orthophosphoric Acid	50 ml/500 ml

Ni-NTA purification buffer for His-tag clones

Urea	480.48 g/l
NaH_2PO_4 0.1 M	15.6 g/l
Tris 0.01 M	1.21 g/l

Same buffer used but lysis buffer B at pH 8.0, wash buffer C at pH 6.3, elution buffers D and E at pH 5.9 and pH 4.5, respectively.

Sequencing Reagents

PEG_{8000} solution

PEG_{8000}	26.7 ml/100 ml
NaOAc	4.92 g/100 ml
$MgCl_2$	0.062 g/100 ml

Stop Solution

3 M NaOAc pH 5.2	30 µl
100 mM EDTA pH 8.0	30 µl
Glycogen (from DTCS kit)	15 µl

Appendix B: Source of ECM compounds and their antibodies

In Australia:

Laminin	mouse	(Sigma L2020)
rabbit anti-laminin		(Sigma L9393)
Fibronectin	human	(Sigma F3648 and Calbiochem 341635)
rabbit anti-fibronectin		(ICN/CAPPEL)
Biotinylated heparin	porcine	(Sigma B9806)
streptavidin-peroxidase		(Roche)
Fibrinogen	human	(Sigma F3879)
goat anti-fibrinogen		(Sigma F8152)
Chondroitin sulphate A	bovine	(Sigma C8529)
mAb against chondroitin sulphate	mouse	(Sigma C8035)
Chondroitin sulphate B	porcine	(Sigma C3788) no antibody used
Heparan sulphate	porcine	(Sigma H9902) no antibody used
Fucoidan	*Fucus vesiculosus*	(Sigma F5631) no antibody used

In Germany (no antibodies used):

Laminin (Calbiochem); Fibronectin: whole (ICN), alpha-chymotryptic 120kDa fragment (Chemicon), proteolytic fragments 70, 45 and 30 kDa (Sigma); Type IV Collagen (Sigma); Keratin (Sigma); Fibrinogen (Calbiochem).

Appendix C: Commercial kits used in this study

QIAquick PCR Purification Kit	QIAGEN
Midi/Maxi Plasmid Purification Kit	QIAGEN
Mini Plasmid Purification Kit	QIAGEN
GenElute Gel Extraction Kit	Sigma
FlexiPrep Plasmid Purification Kit	Amersham Pharmacia Biotech.
pPCR-Script Amp SK(+) Cloning Kit	Stratagene
DIG Wash and Block Buffer Set	Roche

Appendix D: Cell lines used in this study

- *Escherichia coli* JM109 containing the pQE-9 plasmid from Qiagen (University of Wollongong, Australia).
- *Escherichia coli* M15 containing the pREP4 plasmid from Qiagen (University of Wollongong, Australia).
- XL10-Gold Kan ultra competent cells from pPCR-Script cloning kit (Stratagene).
- pPCR2.1 plasmid in *E. coli* TOP_{10} cells containing entire *p159* gene inserted in this plasmid after mutagenesis of all TGA codons to TGG, supplied by S. Geary (University of Connecticut, USA).
- *M. hyopneumoniae* strains:
    - J strain used in Germany supplied by the Microbiology Institute (Hannover, Germany).
    - J strain (NCTC 10110) supplied by A. Pointon (South Australian Research and Development Institute, Australia).
    - 232 strain isolated from a porcine lung homogenate suspension containing *M. hyopneumoniae* strain 11 supplied by T.F. Young (Veterinary Medical Research Institute, Iowa State University, USA) (Bereiter *et al*., 1990).

Appendix E: Vector maps

Positions of elements in bases	
Vector size (bp)	3439
Start of numbering at XhoI	1-6
T5 promoter/lac operator element	7-87
T5 transcription start	61
6x His-tag coding sequence	127-144
Multiple cloning site	145-170
Lambda t_o transcriptional termination region	186-280
rrnB T1 transcriptional termination region	1042-1140
ColE1 origin of replication	1616
β-lactamase coding sequence	3243-2374

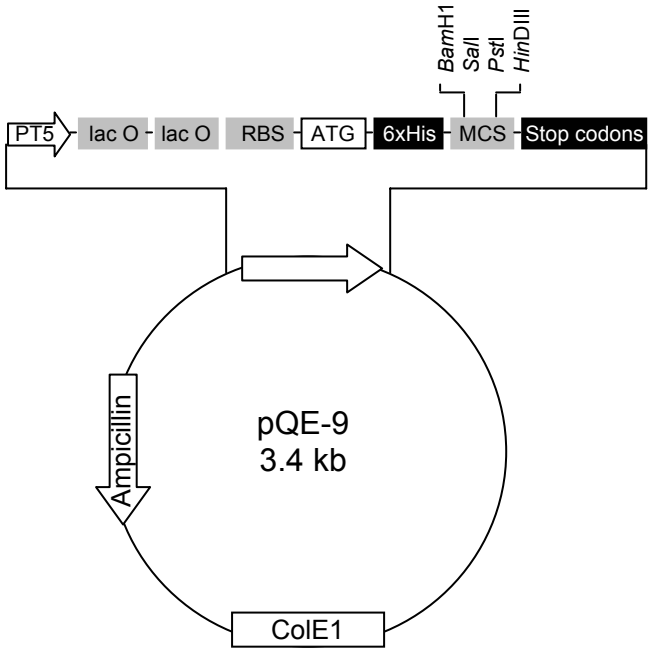

Fig. A1. Map of the prokaryotic expression vector pQE-9 (Qiagen) used to express rpL7/L12 and P159 proteins in this study. For further information including the complete vector sequence please see this website: www1.qiagen.com/literature/vectors_pqe.aspx.

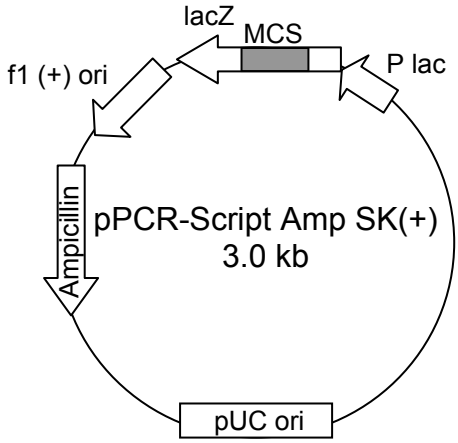

Positions of elements in bases

Vector size (bp)	2961
f1 (+) origin	135-441
β-galactosidase α-fragment	460-816
multiple cloning site	653-760
lac promoter	817-938
pUC origin	1158-1825
ampicillin resistance (*bla*) ORF	1978-2833

MCS contains restriction enzyme sites for:
Kpn I, Apa I/Eco01091/Dra II, Xho I, Acc I/Hinc II/Sal I, Bsp 106 I/Cla I, Hind III, EcoR V, EcoR I, Pst I, Sma I, BamH I, Srf I, Sma I, Not I, Eag I, BstX I, Sac II, Sac I, BssH II.

Fig. A2. Map of the prokaryotic cloning vector pPCR-Script Amp SK(+) (Stratagene) used to clone P159 proteins in this study before being further cloned into the pQE-9 expression vector. For further information including the complete vector sequence please see this website: www.stratagene.com/lit/vector.aspx.

Appendix F: Presentation of Results at Conferences

Poster presentations

Burnett, T.A., Cordwell, S., Geary, S., Minion, C., Walker, M. and Djordjevic, S.P. Analysis of a novel surface exposed protein of *Mycoplasma hyopneumoniae*. Presented at the 14th International Congress of the International Organization for Mycoplasmology, Vienna, Austria, July, 2002.

Burnett, T.A., Cordwell, S., Geary, S., Minion, F.C., Walker, M. and Djordjevic, S.P. Analysis of a novel surface exposed protein of *Mycoplasma hyopneumoniae*. Presented at the Australian Society for Microbiology Conference in Melbourne, Australia, October, 2002.

Oral presentations

Burnett, T.A., Cordwell, S., Geary, S., Minion, F.C., Walker, M. and Djordjevic, S.P Molecular characterization of P159, a major surface antigen of *Mycoplasma hyopneumoniae*. Presented at the Biannual Bacterial Pathogenesis Meeting (Branch of the Australian Society for Microbiology), Jamberoo, Australia, May, 2003.

Burnett, T.A., Cordwell, S., Geary, S., Minion, F.C., Walker, M. and Djordjevic, S.P Molecular characterization of P159, a major surface antigen of *Mycoplasma hyopneumoniae* and an ECM binding protein. Presented at the Elizabeth Macarthur Agricultural Institute in August 2003.

Burnett, T.A., Dinkla, K., Rohde, M., Chhatwal, G.S., Cordwell, S., Geary, S., Minion, F.C., Walker, M. and Djordjevic, S.P. Domains within the surface antigen P159 of *Mycoplasma hyopneumoniae* promote adhesion to and invasion of eukaryote cells and bind the glycosaminoglycan, heparin. Presented at the 15th International Congress of the International Organization for Mycoplasmology, Athens, U.S.A., July, 2004.